Regional and seasonal variability in the vertical distribution of mesozooplankton in the Greenland Sea

Claudio Richter

Ber. Polarforsch. 154 (1994)
ISSN 0176 - 5027

Claudio Richter
Institut für Polarökologie, Christian-Albrechts-Universität zu Kiel
Wischhofstraße 1-3, Gebäude 12
D-24148 Kiel

Druckfassung einer Dissertation, die der Mathematisch-Naturwissenschaftlichen Fakultät der Christian-Albrechts-Universität zu Kiel vorgelegt wurde.
Printed version of a Ph. D. thesis submitted to the Faculty of Mathematics and Natural Sciences of the University of Kiel.

Table of contents page

Summary

A large-scale regional and seasonal zooplankton investigation was carried out in the Greenland Sea covering the entire water column down to 3000 m depth. It focussed on the composition and vertical distribution of zooplankton in relation to the hydrographic régime (i) and in course of time (ii). Sampling was carried out with vertical Multinet hauls (150 µm mesh) in nine depth strata: 3000 (or sea floor)-2000-1500-1000-500-400-300-200-100-0 m.

(i) The regional study comprised a transect along 75°N in November 1988, occupying one station in the Atlantic domain of the West Spitsbergen Current (WSC) and three stations in the arctic domain of the Greenland Sea Gyre (GSG). The WSC station showed a low number of individuals and species and a relatively even distribution of individuals among species. *Calanus finmarchicus* (Calanoida, Copepoda) dominated in abundance (40%) and biomass (55%). Within the GSG, *Oithona* (Cyclopoida, Copepoda) was numerically dominant (38%-58%) and *Calanus hyperboreus* in terms of biomass (35%). Biomass varied only little along the transect (13±1 g DW$*$m^{-2}). Highest numbers of individuals were found in the upper 500 m, while a large fraction of the biomass was located below.

(ii) The seasonal study encompassed six stations in the GSG, revisited in late fall, winter, early and late summer of 1988/89 and spring of 1993. Species composition remained fairly constant throughout the investigation period, around 48 species, with *Oithona* dominating in abundance (53%) and *C. hyperboreus* in biomass (32%). Integrated abundance varied by a factor of 2.5, with maximum values in June (7.4$*$10^5 n$*$m^{-2}). Integrated biomass was high (14 g DW m^{-2}) and remarkably constant, varying by a factor of 1.5 between the winter minimum and the late summer maximum.

Abundance was maximal at the surface throughout the light season, whereas the biomass maximum occurred only briefly at the surface in early summer and prevailed in the subsurface for most of the year.

Depth was the main factor shaping the community, revealing distinct assemblages of

(1) widely distributed and abundant species *(Oithona* spp., *Oncaea* spp., *Calanus* spp., *Pseudocalanus minutus)*

(2) mesopelagic resident species of restricted range (Aetideidae, Ostracoda, Chaetognatha) and

(3) bathypelagic resident species of restricted range (Cnidaria).

Distribution patterns of (1) and (2) were highlighted and discussed with regard to potential food requirements and storage capacities (body size). Seasonal vertical migrations were marked for herbivorous calanoid copepods. Their extent and timing appeared to be related to body size, both inter- and intraspecifically. *Calanus hyperboreus* carried out extensive vertical migrations exceeding 1500 m with a brief surface period for the larger stages. The smaller *Pseudocalanus minutus* remained longer at the surface hibernating at intermediate depths. *Calanus finmarchicus* performed shallower seasonal migrations, but no pattern was obvious for the omnivorous *Metridia longa*. The ubiquitous cyclopoid copepods occurred in high numbers throughout the year, with *Oithona* occupying the epi- and *Oncaea* the meso- and bathypelagial, both reproducing at the surface in early summer.

A rich mesopelagic community of omni- and carnivorous copepods, ostracods and chaetognaths was encountered, showing a seasonally stable vertical partitioning of the water column. It is estimated that a considerable portion of the secondary production goes into the mesopelagic food web, while the bathypelagic zone might serve as a refuge for overwintering herbivore stocks. High overall biomass and low seasonal variability characterize the Greenland Sea Gyre as a remarkably stable system, in spite of marked seasonal variations in food availability.

1 Introduction

Little is known of the plankton fauna of the central Greenland Sea, let alone its quantitative composition and vertical distribution. Seasonal investigations including the deep sea are limited to the detailed investigations carried out on the weather ships of the station 'M' in the Norwegian Sea (66°N, 2°E), where regular plankton collections were made from 1948 to 1951 down to 2000 m (Wiborg 1954, Østvedt 1955). Less systematic investigations were conducted on the numerous drifting ice islands (T3, Arlis II, NP-22, NP-23) in the Arctic Ocean to a maximum depth of 3000 m (Hopkins 1969, Kosobokova 1982). Comparable investigations down to 2000-3000 m from other high latitude oceanic regions are restricted to the Bering Sea (Vinogradov 1970), the station 'P' in the North Pacific (McAllister 1961), the Subantarctic and Antarctic (Foxton 1956).

The present study thus fills a geographic gap between the investigations carried out in the polar (ice islands) and Atlantic (weather ship 'M') domains of the Arctic-Atlantic continuum. The Greenland Sea Project (GSP), a joint oceanographic research program of eleven nations investigating the processes of water mass transformation and transport in the Greenland Sea (GSP Group 1990), offered a unique possibility for biologists to collect samples at all seasons and to combine their results with a good hydrographical data set. Based on the available zooplankton material from the 1988/89 field phase of the GSP, which was supplemented with a station occupied in spring 1993, the present investigation addresses the large-scale vertical distribution of mesozooplankton in the Greenland Sea. It identifies the main contributors to abundance and biomass and follows their seasonal and regional changes over the entire water column down to 3000 m. Adverse meteorological conditions and logistical constraints limited the number of observations to a minimum: Repeated sampling at all seasons at one central station in the Greenland Sea Gyre and a zonal transect of four stations across the Greenland Sea in late fall. However, the resulting data set is exceptional in covering all seasons in this remote ocean area and in spanning the entire vertical range down to the deep sea.

Previous investigations in the Fram Strait and Nansen Basin mostly were restricted to the upper 500 m. They had already indicated that a potentially large fraction of the ostracod and chaetognath community was likely to be missed below (Haberstroh 1985, Mumm 1991). Late-summer investigations from the Greenland Sea (cf. Smith and Schnack-Schiel 1990) as well as Østvedt's (1955) seasonal study in the Norwegian Sea left little doubt that the main biomass carriers, *Calanus* spp. descended beyond this horizon to overwinter. Hirche (1991) was the first to show that the fall descent of *Calanus* spp. in the Greenland Sea exceeded 1000 m, while in the Arctic Ocean the bulk of the wintering population remained within the upper 500 m (Dawson 1978, Rudyakov 1983). The present study extends Hirche's (1991) observations to the whole zooplankton community over all seasons, highlighting the following questions:

- What is the species composition, abundance and biomass in this high latitude oceanic system? How does it vary in the course of time?
- What are the main factors shaping the zooplankton communities?
- Which are the dominant taxa and how does their distribution vary with depth and time?
- What are their life cycles and how are they geared to the seasonal production cycle?
- Are there general conclusions to be drawn? E.g.
  - between the distribution patterns of herbivores, omnivores and carnivores?

- between different sizes? Does size-dependent storage capacity affect the timing and magnitude of the seasonal vertical migrations?

On the basis of the vertically almost homogenous water column (Budéus et al. 1993) and the very low horizontal current velocities in the Greenland Sea Gyre (Visbeck 1993) it was assumed that biological changes outweigh physical variability within the gyre. The large-scale cyclonic circulation (e.g. Swift 1986) was further assumed to retain the plankton in the area assuring repeated sampling of essentially the same population over time. To assess the effect of circulation and water masses on the vertical distribution and quantitative composition of the zooplankton a regional transect was carried out across the Atlantic and arctic[1] domains of the Greenland Sea in late fall 1988.

Overall results are compared with other high latitude ocean areas. Species numbers and diversity are discussed with respect to hydrography and selection of cold-adapted species (Vinogradov 1970), biomass with respect to circulation and the seasonal production cycle and the vertical transport of biomass. Its level and variability is considered an indicator for efficient resource-partitioning in this highly food-limited system (Smith and Sakshaug 1990).

The investigation is a contribution to ongoing and planned research in the area, namely the international Greenland Sea Project (GSP), the joint research project at Kiel University (SFB 313) and MARE COGNITUM/GLOBEC (Norway).

[1] minuscule/majuscule notation adopted from Swift (1986)

2 Study area

The Greenland Sea can be delimited by hydrographical and topographical features, for bottom topography strongly affects the circulation and the distribution of water masses in the Nordic Seas (Johannessen 1986).

Bathymetry

Surrounded by the Arctic Ocean, the Barents, Norwegian and Iceland Seas, the Greenland Sea is bounded by the Fram Strait in the north, Spitsbergen and the Barents Sea slope in the east, Mohns ridge in the southeast, the Jan Mayen fracture zone in the south, and the Greenland coast in the west (Fig. 2.1). According to bathymetry, the Greenland Sea can be further divided into a shelf area and two deep basins. The east Greenland shelf is narrow in the south (50 km), but progressively broadens towards the north. It reaches halfway through the Fram Strait at its maximum zonal extension (280 km, Perry 1986), breaking away rather precipitously into the abyssal plains of the Greenland Sea. The Greenland fracture zone separates the larger and deeper (3400-3600 m) Greenland Basin from the Boreas Basin (3200 m) to the north. The mid-ocean ridge demarcates the southern and eastern borders of these basins along Mohns and Knipovich ridge. Anchored above these bottom features are hydrographic fronts which separate water masses of widely disparate origin, indicating strong topographic steering of the wind-driven current system (Quadfasel and Meincke 1987, van Aken et al. 1991).

Circulation

The most conspicuous feature of the Greenland Sea circulation is the meridional flow of two opposing boundary currents. They carry large amounts of heat and salt from the North Atlantic into high latitudes along the eastern side, and ice and fresh water from the Arctic Ocean towards lower latitudes along the western side (Fig. 2.1). Zonal branching of this meridional flow occurs along topographic barriers and gives rise to a counter-clockwise circulation pattern in the Greenland Sea. Thus, an eastward deflection of part of the southbound East Greenland Current (EGC) occurs along the Jan Mayen fracture zone, known as the Jan Mayen Current. The westward deflection of part of the West Spitsbergen Current (WSC) has been found associated with the Molloy seamounts and the Hovgaard fracture zone in the Fram Strait (Quadfasel et al. 1987). The latter recirculating branches are termed Return Atlantic Current (RAC). Owing to the topographic steering of the mainly barotropic flow, cyclonic gyres are formed over each of the subbasins (Quadfasel and Meincke 1987, not shown in Figure 2.1).

Water masses

Swift (1986) distinguishes the Atlantic and polar domains of the Greenland Sea periphery from the „arctic waters" of the central basins (Helland-Hansen and Nansen 1909). These domains are separated by meridional hydrographic fronts: the East Greenland Polar Front (EGPF) to the west and the Arctic Front to the east. Swift (1986) points to the fact that

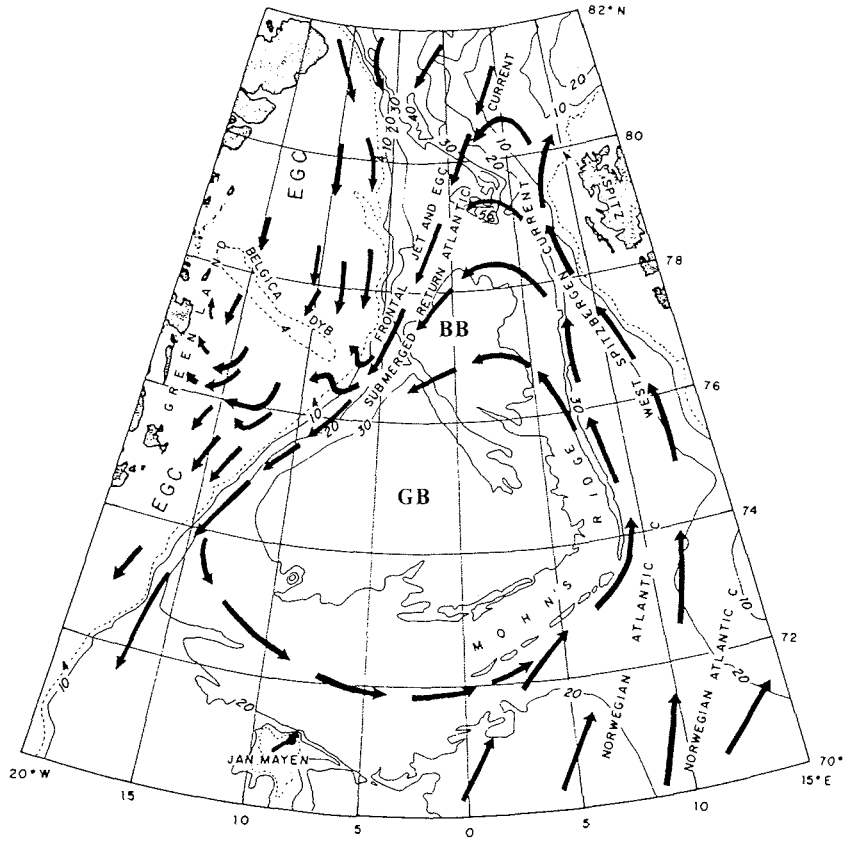

Fig. 2.1: Bathymetry and currents in the Greenland Sea. Depth labels are in hundreds of meters (BB= Boreas Basin, EGC= East Greenland Currrent, GB= Greenland Basin, modified from Paquette et al. 1985).

the arctic waters are not simply the product of mixing between the Polar and Atlantic Water (PW, AW), since they are much denser than any of the source waters and concludes that extensive modification must occur to account for the observed changes. Relatively high salinities and low Tritium concentrations in the Greenland Sea Gyre (GSG) indicate that PW contributes only little to the arctic waters (Swift and Aagard 1981). On the other hand, the steep horizontal gradients constituting the Arctic Front preclude extensive mixing of AW into the central gyre. This is taken as further evidence for AW having to undergo modification (cooling and sinking) before entering the arctic domain (Swift 1986). However, cross-frontal mixing of AW has been proposed by van Aken (1989) and van Aken et al. (1991), based on the occurrence of warm core eddies to the west of the front.

Within the arctic domain, the cyclonic circulation leads to a doming of the isopycnals and a reduced density stratification in the center of the gyre. A 20 to 40 m thick seasonally warmed layer with temperatures of about 4.5°C marks the surface of the GSG. This is Arctic Surface Water (ASW), with temperatures above 2°C and salinities ranging between 34.7 and 34.9 (Swift 1986). Below the seasonal pycnocline a second water mass is associated with the upper temperature minimum located between 75 and 150 m. This

upper Arctic Intermediate Water (UAIW) forms in fall and winter. Its salinity is determined by the depth of wintertime mixing. Lower Arctic Intermediate Water (LAIW) is associated with a marked temperature and salinity maximum located between 250 and ≥400 m. The temperatures are in the range of 0 to 3°C, and salinity is greater than 34.9 (Swift 1986). The property maxima are clear signs that this water mass is produced by the cooling and sinking of AW. Below these intermediate waters we find the Greenland Sea Deep Water (GSDW) which comprises about 85% of the volume of the Greenland Sea water masses (Carmack and Aagard 1973). It is the coldest and densest water in the Greenland Sea, with salinities typically between 34.88 and 34.90 and potential temperatures between -1.1 and -1.3°C (Swift 1986). It is believed to be formed by winter cooling and deep convection in the center of the GSG, resulting in a homogeneous water column from the surface to the bottom (Nansen 1906). However, such conditions have not (yet) been observed and other possible mechanisms of deep water formation have therefore been proposed (Metcalf 1955, Carmack and Aagard 1973, Clarke et al. 1990).

Water exchange

There have been several attempts to quantify the volume transport of the exchange flow between the Arctic Ocean and the North Atlantic, but the estimates are based on a variety of methods, many of which are not considered reliable in the oceanographic literature. A recent summary of estimates for the overflow into the North Atlantic across the sills in the Denmark Strait (620 m) and the Faroe Bank Channel (840 m) indicates a transport of 5.6 Sv[2] (Dickson et al. 1990). The main overflow occurs across the Denmark Strait (2.9 Sv) and is principally supplied by UAIW (Swift et al. 1980), whereas the overflow across the Faroe Bank Channel (1.7 Sv) consists primarily of Norwegian Sea Deep Water. Net outflow from the Arctic Ocean into the Greenland Sea (sill depth 2650 m) is estimated some 1.7 Sv (Rudels and Quadfasel 1991), of which a considerable portion (0.5 Sv) is Arctic Ocean Deep Water. Deep water can circulate freely within the Norwegian, Greenland and Eurasian basins, but it is confined by the shallow sills of the Greenland-Scotland ridge.

Ice cover

Permanent ice cover in the Greenland Sea is restricted to the polar waters west of the East Greenland Polar Front and consists mainly of multi-year ice originating from the Arctic Ocean (e.g. Wadhams 1986). Within the GSG, sea ice cover is seasonal and shows high interannual variability (Vinje 1977). A recurring feature, however, appears to be a tongue of pack extending into the area from the southwest and curling around the center of the GSG. This is the 'is odden' named by the Norwegian seal hunters, leaving an ice-free 'nordbukta' in its center. A plausible mechanism for the formation of this phenomenon has been recently proposed by Visbeck (1993).

Summary

The most important features of the physical setting relevant to the biological oceanography of the Greenland Sea can be summarized as follows:

[2] $1\ Sv = 10^6\ m^3 * s^{-1}$

- the surface connection to both, the Arctic Ocean and North Atlantic,
- the deep connection to the Arctic Ocean and Norwegian Sea,
- the vicinity of water masses of disparate origin and the hydrographic separation of polar, arctic and Atlantic domains,
- the slow and circular current regime within the arctic domain,
- the doming of isopycnals and vertical instability in the GSG,
- the recurrence of an ice-free 'nordbukta' in the center of the GSG.

3 Material and Methods

Sampling and sample processing

Large-scale regional and seasonal sampling was carried out during the 1988/89 field phase of the international Greenland Sea Project (GSP) and during spring of 1993 (Table 3.1).

Material for the regional study was collected during cruise Nr. 8 of RV „Meteor" in November 1988, occupying four stations on a zonal transect from Bear Island to the East Greenland Polar Front (Fig. 3.1, Table 3.1). All stations were ice-free at that time. The Arctic Front separated the Bear Island station 609 (12°57'E) in the West Spitsbergen Current (WSC) from the arctic stations in the gyre. Later sections will refer to the ensemble of stations of this cruise as *„regional"* or „zonal" transect across the *Greenland Sea* in *late fall*, to station 609 as „WSC" or simply „13°E".

Fig. 3.2 shows conspicuously different temperature and salinity profiles between 13°E and the arctic stations. In the arctic domain, cold low salinity Arctic Surface Water overlies a warm saline layer of Arctic Intermediate Water between 50 and 200 m (data are missing for the upper 50 m at station 616). The water column is nearly homogenous below (Greenland Sea Deep Water). The WSC (13°E) displays a complicated hydrographic structure with warm saline Atlantic water at the surface, and a series of cold and warm intrusions below, not giving way to a homogenous water column until about 1200 m.

For the seasonal study, the center of the Greenland Sea Gyre (GSG) was revisited on board RVs „Meteor", „Valdivia" and „Polarstern" in late fall, winter, early and late summer of 1988/89 and again in spring 1993 (Table 3.1). Later sections will address the ensemble of stations, excluding 609 and 616, as *„seasonal"* or „temporal" investigation in the *GSG*. For definition of seasons see Table 3.1. Stations 613, 653 and 8 are collectively referred to as „dark season" (November-February), stations 61, 91 and 177 as „light season" (April-

Table 3.1: Station data for deep Multinet hauls in the Greenland Sea, sampling the depth strata 3000 (or bottom)-2000-1500-1000-500-400-300-200-100-0 m (WSC= West Spitsbergen Current, GSG= Greenland Sea Gyre, EGPF= East Greenland Polar Front).

Station	RV	Cruise	Region	Position		Season	Date	Time range [h UTC]	Depth [m]
609	Meteor	8/1	WSC	74°45'N	12°57'E	late fall	06 Nov 88	22-02	2284
613	"	"	GSG	74°45'N	01°04'E	"	08 Nov 88	13-18	3777
616	"	"	EGPF	74°42'N	08°33'W	"	10 Nov 88	10-15	3352
653	"	8/2	GSG	74°06'N	03°02'W	"	27 Nov 88	18-22	3655
8	Valdivia	78/1	"	74°45'N	08°01'W	winter	07 Feb 89	22-05	3400
91	Polarstern	ARK VI/3	"	74°45'N	01°02'E	early summer	15 Jun 89	07-12	3770
177	Valdivia	86	"	74°45'N	01°04'E	late summer	18 Aug 89	14-18	3780
61	Polarstern	ARK IX/1b	"	75°00'N	02°38'W	spring	09 Apr 93	13-22	3688

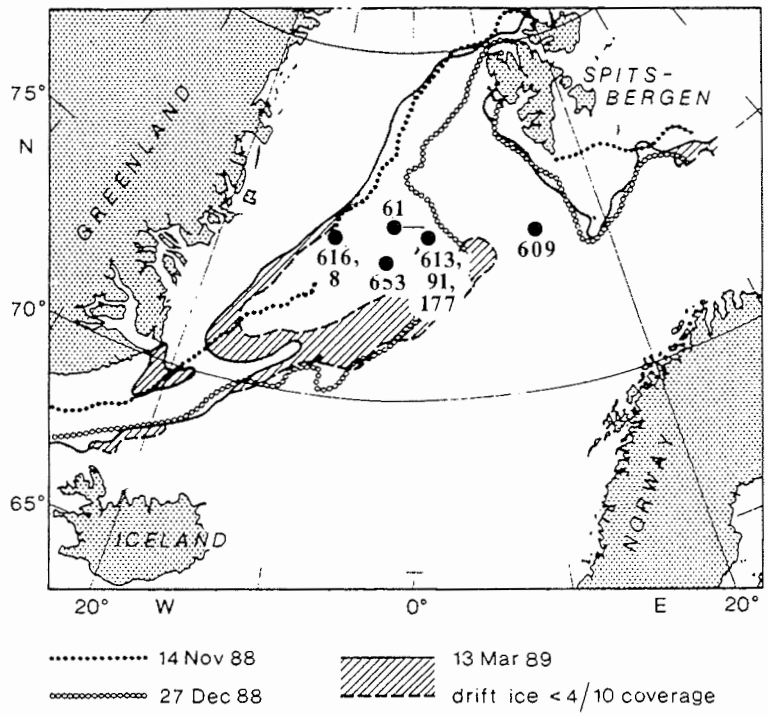

Fig. 3.1: Sampling locations and extent of ice-cover during the sampling period (modified from Fischer and Visbeck 1993).

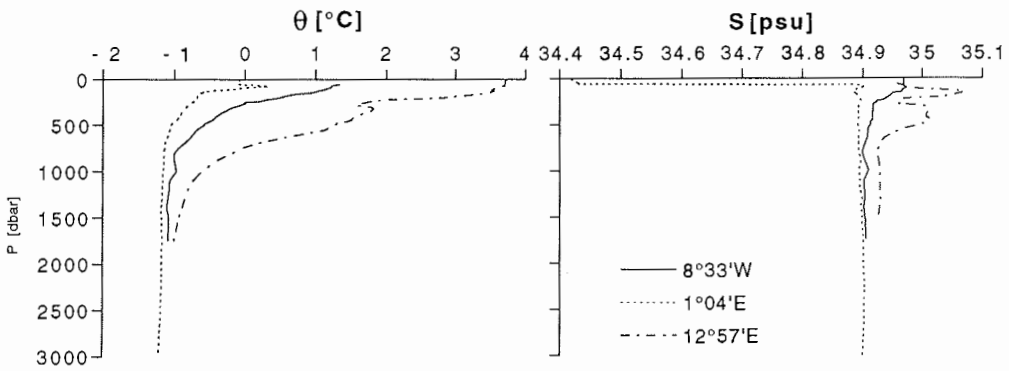

Fig. 3.2: Profiles of potential temperature (θ) and salinity (S) along the regional transect across the Greenland Sea in November 1988, at 8°33'W, 1°04'E (arctic domain) and 12°57'E (Atlantic domain), (uncalibrated data, courtesy of D. Quadfasel, IfM Hamburg).

August). Results are presented in chronological order, i.e. beginning with late fall of 1988 (station 613) and ending with late summer of 1989 (station 177). The only exception is spring (station 61) which is from a different year (1993). Temperature and salinity profiles for the 1988/89 period in the GSG are given in Fig. 3.3. They show pronounced modifications of ASW and AIW in course of the year which may extend down to about 1800 m.

Sampling equipment and design was identical throughout the entire investigation. Zooplankton was sampled from 3000 m (or sea bed, 13°E) to the surface, deploying a Kiel Multinet equipped with five nets (150 µm mesh) in two successive vertical hauls from 3000 m (or bottom) and 500 m to the surface. Sampling intervals were 3000 (or bottom)-2000-1500-1000-500-0 m for the deep hauls, and 500-400-300-200-100-0 m for the shallow casts. Clogging never was a problem and filtered volume was calculated from wire length and Multinet mouth area (0.25 m^2), assuming 100% filtering efficiency at 0.3-0.5 $m*s^{-1}$ hauling velocity. Samples were preserved in 4% borax-buffered formaldehyde.

Part of the material was shared with other investigators, who kindly made available their data and samples to this study (Table 3.2).

For species identification, specimens were dissected under a stereo microscope and determined under high magnification (up to 400*) in the microscope. Reference was made to the extensive taxonomic literature cited in Mumm (1991, pp. 22-25), furthermore to Sars (1903), Heptner (1971), Park (1978), Brodskii et al. (1983), Nishida (1985), Frost (1989), and Koszteyn and Kwasniewski (1991) for copepods; to Weslawski (1991) for amphipods, and to Herman and Andersen (1989) for pteropods.

Samples were sorted in a Bogorov plate under a stereo microscope with dark and bright field illumination. As a rule, the entire sample was enumerated for the larger plankton (>1 mm), and only occasionally the sample was split with a Folsom splitter (1:2) for quantification of very abundant species or stages. Routine identification was usually to the

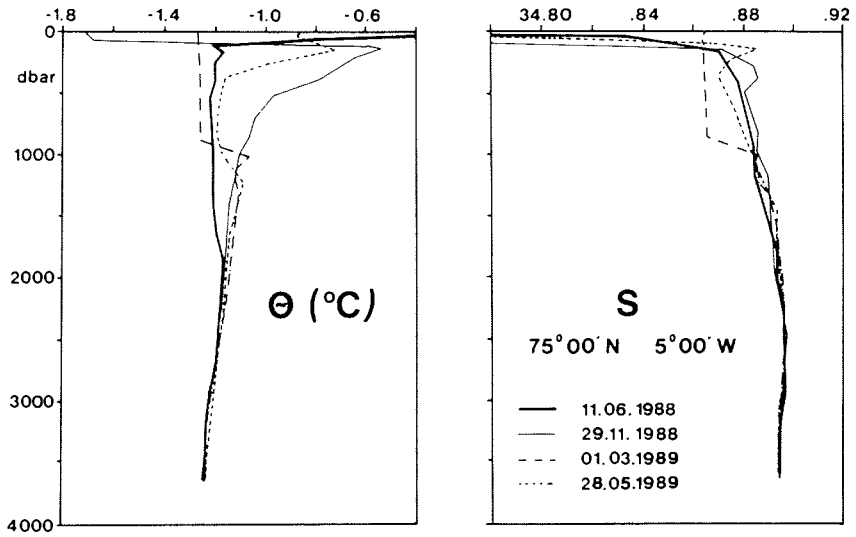

Fig. 3.3: Profiles of potential temperature (θ) and salinity (S) in the central Greenland Basin in early summer 1988, late fall 1988, winter 1989 and early summer 1989 (from GSP Group 1990).

Table 3.2: Stations and taxa and for which abundance data were provided, courtesy of H.-J. Hirche, T. Scherzinger and R. Weigmann-Haass.

St.	*Calanus* spp.	*Metridia longa*	Ostracoda	Hyperiidae	Euphausiacea	Chaetognatha
609	*Hirche 1991	†Hirche 1991	Haass unpubl.	Haass unpubl.	Haass unpubl.	**Hirche unpubl.
613	"	Scherzinger 1994	"	"	"	"
616	"	†Hirche 1991	"	"	"	"
653	"	Scherzinger 1994	"	"	"	"
8	*‡Hirche unpubl.	†Hirche unpubl.				
91	"	"				**Hirche unpubl.
177	"	"				"

* and † denote missing values for copepodite stages CI-CII and CI-CIII, respectively; ‡= no separation between *Calanus finmarchicus* and *C. glacialis* for all stages; **= including length data

species level and most of the larger calanoid copepods were further separated into copepodite stages. For the small plankton (<1 mm), an aliquot (1:2, 1:4, 1:10, exceptionally 1:100) of the sample was counted after fractionation with a Folsom or Wiborg splitter. Only metazoans were counted. Cyclopoid copepods were sorted to the genus. Taxonomic identification of the smallest calanoids (*Microcalanus pygmaeus, M. pusillus, Spinocalanus* spp.) and of calanoid nauplii was not attempted on a routine basis. The latter were recorded as „small calanoids" and „nauplii", respectively. Subsequent length measurements via digital image analysis allowed to delimit *a posteriori* taxonomic entities from the occurrence of multiple modes in the length-frequency distributions. This was verified microscopically for *Oithona* and *Oncaea* at the species level and for *Pseudocalanus* and *Boroecia* at the stage level, as will be shown later.

Image analysis

Computer analysis of digitized video images was performed with an unpublished image analysis software ('BILD') developed by W. Hukriede (IfM, Kiel) on a NeXT workstation. Specimens were placed in calibrated measuring vials and videotaped with a S-VHS camera equipped with a macro lens. The processing involved digitizing, scaling and measuring of the image on the computer screen by means of a 'mouse'. The procedure is semi-automatic and fast, allowing for several hundred measurements per hour. Damaged specimens as well as those which were off-axis or out of focus were excluded. Repeated measurements of 25 individuals of *Oncaea* (0.6 mm total length) yielded a precision of 3.4% of the mean. This is probably a 'worst case scenario', since usually tens to hundreds of animals were measured per sample. Furthermore, precision increases with organism size. Prosome lengths (i.e. from the tip of the rostrum to the median articulation between prosome and urosome) were measured for calanoid copepods and total lengths (i.e. largest extension excluding projections) for all other taxa. Line measurements were performed in most cases, but polygones or curves were applied on bent animals [*Oncaea*, amphipods and (often) chaetognaths]. Data were stored in spreadsheet files for subsequent length-frequency analysis.

Length-frequency histograms were plotted to visualize vertical and seasonal shifts in the length distribution of the assemblage. Lower mode distributions were the rule, and modes were traced by eye to follow vertical or seasonal increments in length.

Biomass calculation

Plankton material for direct biomass determinations was not available for this investigation. Biomass was therefore calculated from published and unpublished taxon-specific weight-length relationships, individual dry weights (DW_i), stage- and length composition and numbers of individuals in the samples (APPENDIX 1). The compiled DW_i are from fresh or frozen GSG material, ideally, and from formaline samples outside the area, at the worst. They are given as somewhat bold averages but standard deviations are provided as a measure of variance within the source data.

Statistical analysis

The regional, seasonal and vertical centers of distribution were calculated according to Mumm (1991). Species were ranked depending on their centers of distribution in order to display the distribution patterns in the tabular fashion introduced by Mumm (1991, 'Mumm-plot', Figs. 4.16-18).

To display the seasonal changes in the vertical distribution of abundance and biomass, the z_{50} depths were calculated. These are the depths above which 50% of the population is distributed (cf. Fig 4.14), assuming a homogeneous distribution within each sampling interval. For the biomass-dominating taxa, the z_{05}, z_{25}, z_{75} and z_{95} depths were calculated accordingly. The vertical biomass distribution of these taxa is depicted in box plots, each box encompassing 50% of the population, in terms of biomass (cf. Figs. 4.37, 4.55 and 4.59).

The similarities between the samples in terms of faunistic composition were examined by the ANOSIM permutation test (Clarke and Warwick 1994) as well as classification and ordination techniques as proposed by Field et al. (1982). These non-parametric multivariate methods were performed on a data matrix of 39 rows (taxa) and 54 columns (samples) comprising the recurring taxa of all samples from the temporal study. All three analyses were based on Bray-Curtis similarities (Bray and Curtis 1957) between sample pairs computed on fourth-root transformed abundances, following the recommendations of Clarke and Green (1988) (transformations) and Faith et al. (1987) (similarity coefficients). The matrix of similarities was used to test for vertical and seasonal differences between the samples. Subsequently, the samples were classified by hierarchical agglomerative clustering with group-average linking (e.g. Clifford and Stephenson 1975) and mapped according to their faunistic similarities in an ordination by non-metric multidimensional scaling (MDS, e.g. Kruskal and Wish 1978). Classification and ordination was repeated after transposing the abundance matrix and computing a similarity matrix between every pair of species, in order to examine the inter-relationships between the species.

While clustering and MDS are explorative statistical methods, Clarke and Warwick (1994) recently introduced a formal test to establish statistical assemblage differences between sites, times, etc. This ANOSIM test (in analogy to ANOVA) covers the case of a two-way crossed layout of samples *without* replication, in which „treatments" (here: depths) are replicated only once within each „block" (here: seasons). The crossed design

arises when e.g. the samples are taken from a set of depth intervals at a number of seasons, the term „crossed" implying that for each season there are observations from the same set of depth intervals. The test yields significance levels for the overall presence of treatment effects (depth), based on a measure of concordance within each block (season). The factors are reversed to obtain a test for block effects. For the purpose of this study the following null hypotheses were tested:

H_{01}: there are no seasonal effects in community patterns among the samples (but allowing for the possibility of depth differences)

H_{02}: there are no depth differences (but allowing for possible seasonal effects).

The average Spearman's correlation ρ_{av} is calculated as a measure of concordance and its significance is examined by a permutation test: if the observed ρ_{av} is greater than e.g. in all 999 of 1000 permutated simulations, the null hypothesis can be rejected at a significance level of 0.1% ($p<0.001$). 5000 permutations were carried out in the present study.

All computations were performed with the PRIMER programs (Plymouth Routines in Multivariate Ecological Research) developed at Plymouth Marine Laboratory.

Standard measures are given for species numbers (S), diversity (H') and evenness (J) of samples (Shannon and Weaver 1963, Pielou 1969).

4 Results

The first part of this section will give an overview of the qualitative and quantitative results from the regional and seasonal investigation, including species composition, total abundance and biomass, before leading over to species distribution and multivariate analyses of community patterns. Finally, dominant species as well as species representing a particular distribution type will be highlighted.

Within each chapter, the integrated values (on a square meter basis) of the regional and seasonal study are presented first, followed by the vertical distributions (on a cubic meter basis) encountered during the regional and seasonal investigation.

4.1 General overview

Species numbers and diversity

A total of 67 taxa belonging to seven phyla are reported for this study (Table 4.1). 61 species were identified, nine of which are recorded at the generic level. Including sexes and developmental stages, a total of 145 categories were enumerated.

Most species are listed for calanoid copepods (28), followed by cyclopoids (6), hydromedusans and siphonophores (each 5).

The regional and seasonal variations in species numbers (S) and diversity (H') are given in Figs. 4.1 and 4.2.

Along the zonal transect across the Greenland Sea in late fall, the highest numbers of species are found in the center of the gyre (1°E and 3°W, S=48-49), while at the East Greenland Polar Front (8°30'W) and in the West Spitsbergen Current (WSC, 13°E) only 41 and 40 are recorded, respectively (Fig. 4.1). The diversity index (H') appears to be rather unrelated to the number of species present and is higher on the two eastern stations. At 13°E the diversity maximum coincides with the species minimum.

Species numbers in the Greenland Sea Gyre (GSG) vary seasonally between 44 and 52 (February, April; Fig. 4.2). Diversity (H')

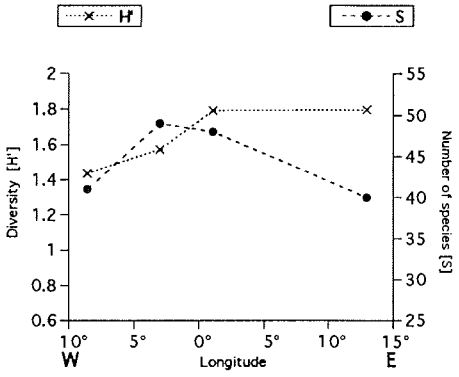

Fig. 4.1: Regional distribution of diversity [H'] and species number [S] across the Greenland Sea (75°N) in November 1988 (cf. Table 3.1 for station data).

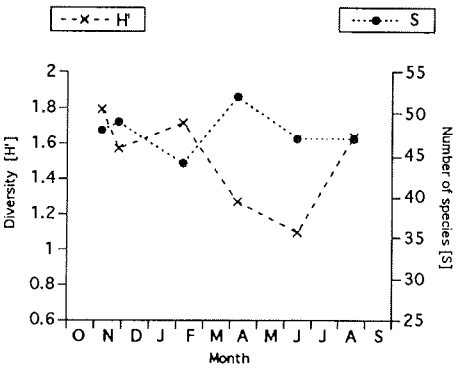

Fig. 4.2: Seasonal distribution of diversity [H'] and species number [S] in the Greenland Sea Gyre.

again follows a different pattern, with a pronounced minimum in spring and early summer. The correlation of Shannon-Wiener diversity (H') versus species numbers for all samples yields a 'shotgun plot' (Fig. 4.3), corroborating the earlier observation that species numbers contribute only little to diversity. Figure 4.4 shows that diversity is rather determined by the evenness (J'), low values representing an uneven distribution of individuals among species, i.e. dominance of a few species.

The vertical distribution of S and H' from 0-3000 m, pooled for all seasons, shows a steady increase of both parameters from the surface to 1000-1500 m, followed by a

Table 4.1a: Species list of copepods in the Greenland Sea (cf. Figs. 4.16-4.18 for regional, seasonal and vertical distributions).

Species	Family	Copepodite stages
Calanoida		
Calanus finmarchicus (Gunnerus)	Calanidae	CIII-CVI
Calanus glacialis Jashnov	"	"
Calanus hyperboreus Krøyer	"	"
Microcalanus pygmaeus (Sars)	Pseudocalanidae	-
Microcalanus pusillus Sars	"	-
Pseudocalanus minutus (Krøyer)	"	-
Spinocalanus horridus Wolfenden	Spinocalanidae	-
Spinocalanus spp.	"	-
Aetideopsis multiserrata Wolfenden	Aetideidae	CI-CVI
Aetideopsis rostrata Sars	"	"
Chiridiella abyssalis Brodskii	"	CVI
Chiridius obtusifrons Sars	"	CI-CVI
Gaidius brevispinus (Sars)	"	"
Gaidius tenuispinus (Sars)	"	"
Undeuchaeta spectabilis Sars	"	CVI
Euchaeta barbata Brady	Euchaetidae	CVI
Euchaeta farrani With	"	"
Euchaeta glacialis Hansen	"	"
Euchaeta norvegica Boeck	"	"
Euchaeta cf. *polaris* (Brodskii)	"	"
Euchaeta spp.	"	CI-CV
Scaphocalanus brevicornis Sars	Scolecithricidae	≤CV, CVI
Scaphocalanus magnus (Scott)	"	"
Scolecithricella minor Brady	"	-
Metridia longa (Lubbock)	Metridiidae	CI-CVI
Heterorhabdus compactus Sars	Heterorhabdidae	≤CV, CVI
Heterorhabdus norvegicus (Boeck)	"	CI-CVI
Lucicutia polaris Brodskii	Lucicutiidae	CVI
Augaptilus glacialis Sars	Augaptilidae	CVI
Haloptilus acutifrons (Giesbrecht)	"	CVI
Cyclopoida		
Mormonilla sp.	Mormonillidae	-
Oithona atlantica Farran	Oithonidae	-
Oithona similis Claus	"	-
Oncaea borealis (Sars)	Oncaeidae	-
Oncaea curta (Sars)	"	-
Oncaea cf. *similis* (Sars)	"	-
Harpacticoidea		
Microsetella norvegica Boeck	Ectinosomidae	-

Table 4.1b: Species list of other zooplankton taxa (cf. Figs. 4.16-4.18 for regional, seasonal and vertical distributions).

Species	Family	
Amphipoda		
Themisto abyssorum (Boeck)	Hyperiidae	
Themisto libellula (Lichtenstein)	"	
Ostracoda		
Boroecia borealis (Sars)	Halocypridae	
Discoconchoecia elegans (Sars)	"	
Isopoda		
isopod larvae	Bopyridae	
Euphausiacea		
Thysanoessa inermis Krøyer)	Euphausiidae	
Thysanoessa longicaudata (Krøyer)	"	
Meganyctiphanes norvegica (Sars)	"	
Decapoda		
Hymenodora glacialis (Buchholz)	Oplophoridae	
Polychaeta		
indet.		
Pteropoda		
Clione limacina (Phillips)	Clionidae	
Limacina helicina (Phillips)	Limacinidae	
Limacina retroversa (Fleming)	"	
Appendicularia		
Oikopleura vanhoeffeni Lohmann	Oikopleuridae	
Chaetognatha		
Eukrohnia bathypelagica Alvariño		
Eukrohnia hamata (Möbius)		
Heterokrohnia mirabilis Ritter-Záhony		
Sagitta maxima (Conant)		
Siphonophora		
Crystallophyes amygdalina Moser	Chuniphyidae	ant./post. nect.
Dimophyes arctica (Chun)	Diphyidae	ant./post. nect., eudoxia
Lensia reticulata Totton	"	eudoxia
Muggiaea bargmannae Totton	"	nect, eudoxia
Marrus orthocanna (Kramp)	Agalmidae	-
Hydromedusae		
Aegina citrea Eschscholtz	Aeginidae	
Aglantha digitale (Müller)	Rhopalonematidae	
Crossota norvegica Vanhoeffen	"	
Botrynema brucei Browne	Halicreatidae	
Botrynema ellinorae Hartlaub	"	
Botrynema sp.	"	
Scyphomedusae		
Atolla wyvillei Haeckel	Atollidae	
Ctenophora		
indet.		

ant.= anterior, post.= posterior, nect.= nectophore

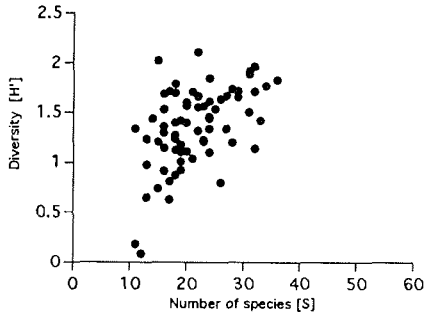

Fig. 4.3: Diversity [H'] versus species number [S] for all samples.

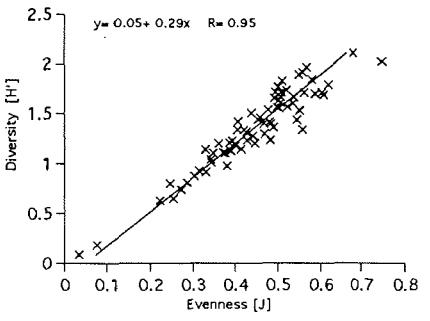

Fig. 4.4: Diversity [H'] versus evenness [J] for all samples.

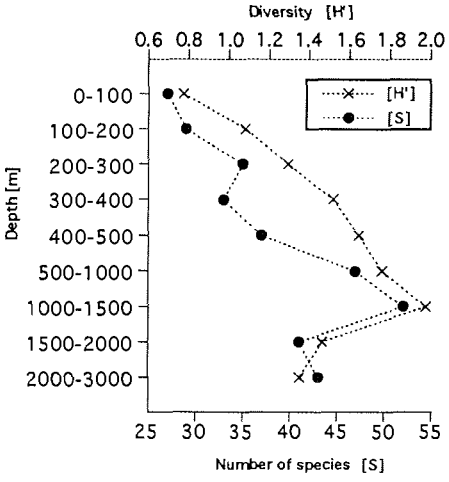

Fig. 4.5: Diversity [H'] and species number [S] versus depth. Species numbers are pooled for each depth stratum over all seasons. Note the scale break at 500 and 2000 m.

marked drop below (Fig. 4.5). Correlation plots show that both, species numbers and evenness contribute to diversity (Figs. 4.6 and 4.7). I.e., few species predominate at the surface, while in the upper bathypelagial high species numbers coincide with an even distribution of individuals among species. It will be a matter of discussion whether the observed vertical pattern, e.g. the intermediate maximum, is spurious (sampling bias) or 'real' (seasonal vertical migrations).

Total zooplankton

Regional and seasonal variations of abundance and biomass, integrated over a

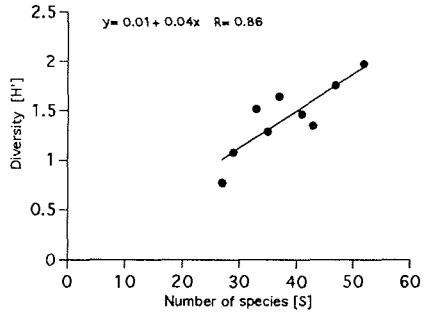

Fig. 4.6: Diversity [H'] versus species number [S] pooled for each depth stratum over all seasons.

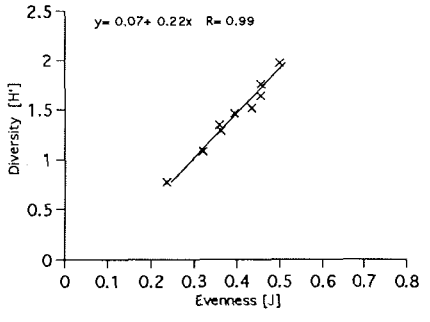

Fig. 4.7: Diversity [H'] versus evenness [J] pooled for each depth stratum over all seasons.

3000 m water column, are shown in Figs. 4.8 and 4.9.

The zonal transect along 74°45'N in late fall shows only moderate changes in both parameters (Fig. 4.8). No pattern emerges for the abundances, except for a drop in the WSC (13°E). The numbers here ($0.7*10^5$ $n*m^{-2}$) are markedly lower than the values in the gyre [$(3\pm1)*10^5$ $n*m^{-2}$]. Biomass, by contrast, is remarkably constant along the section, the standard deviation is only 7% of the mean (13±1 g $DW*m^{-2}$). The apparent disparity between biomass and abundance is due to differences in species and stage/size distributions, as will be shown later.

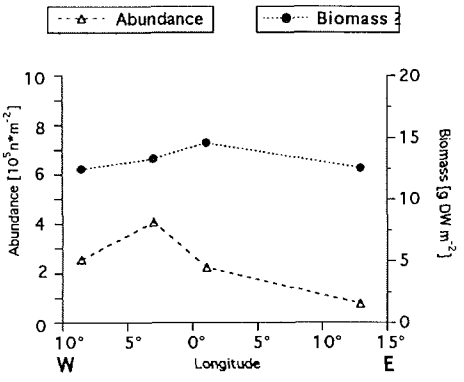

Fig. 4.8: Regional distribution of abundance and biomass in the Greenland Sea (75°N) in November 1988.

Overall variability is greater in the GSG on a seasonal scale (Fig. 4.9). A sharp abundance peak of $7.4*10^5$ $n*m^{-2}$ in June towers above a more or less constant level of $(3.0\pm0.8)*10^5$ $n*m^{-2}$ during the rest of the year. Biomass follows a much smoother curve, describing a sinusoid around 14 $g*m^{-2}$ with a small amplitude of 3 $g*m^{-2}$. The seasonal biomass minimum coincides with the abundance minimum in February. The biomass maximum, however, is out of phase with the abundance peak and occurs later in summer, at a time when abundance values have again dropped to winter levels. It will be shown in the following that different organisms account for the observed abundance and biomass changes in the GSG.

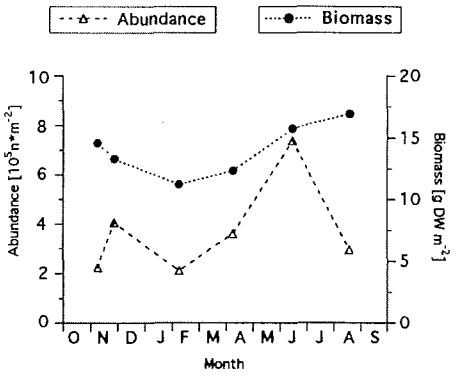

Fig. 4.9: Seasonal distribution of abundance and biomass in the Greenland Sea Gyre.

Mean vertical distributions of abundance and biomass

Vertical distributions of regionally and seasonally averaged zooplankton abundance and biomass are shown in Figs. 4.10 and 4.11.

The regional mean shows a general but moderate decrease of abundance with depth of one order of magnitude from the surface to the deep sea (>1000 m, Fig. 4.10a). However, this decrease is not monotonous, as evidenced by a subsurface peak in the lower epipelagial[3] (200-300 m). A subsurface feature is also apparent in the vertical distribution of biomass, albeit deeper in the water column (400-500 m, Fig. 4.10b). Biomass remains high down to the upper reaches of the bathypelagial (1500 m), at about half the concentration of the surface layer.

Averaged over the whole year, highest densities of both, individuals and dry weights are found at the surface (Fig. 4.11). Variability in this layer is also highest, and the standard

[3] According to the terminology proposed by Omori and Ikeda (1984), the epipelagic zone extends from the surface down to 300 m, the mesopelagic zone from 300 to 1000 m and the bathypelagic from 1000 to 3000 m. The 150 m and 700 m marks separate the upper and the lower epi- and mesopelagial, respectively.

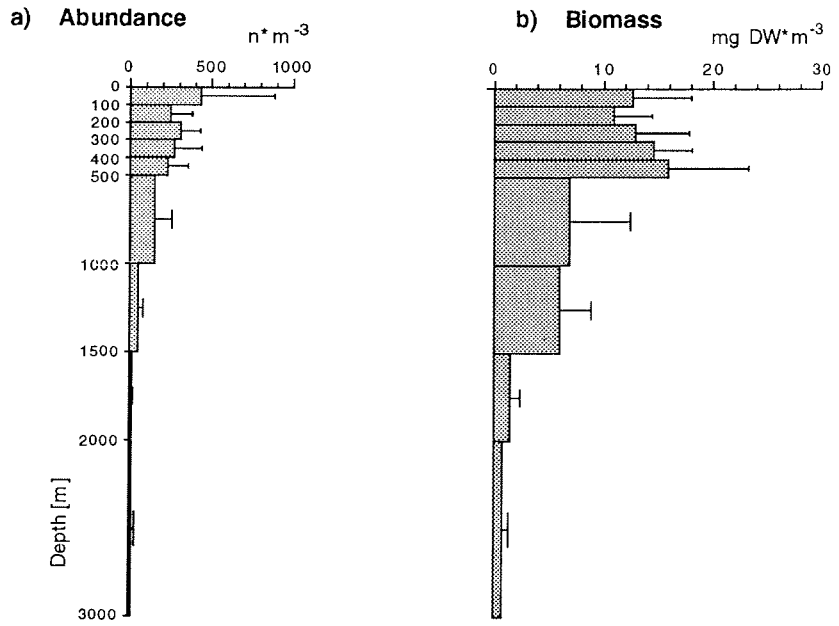

Fig. 4.10: Vertical distribution of abundance (a) and biomass (b), regional average across the Greenland Sea (75°N) in November 1988. Error bars denote standard deviations.

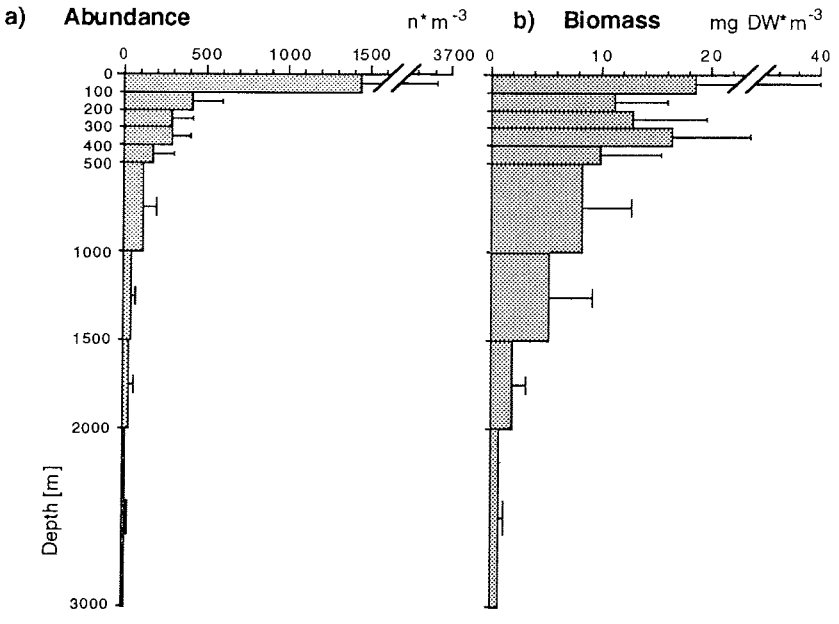

Fig. 4.11: Vertical distribution of abundance (a) and biomass (b), annual mean across the Greenland Sea Gyre. Error bars denote standard deviations. Note the scale breaks for the top 100 m.

deviation of the abundance values exceeds 1.5 times the mean. Abundances plummet along the vertical over two orders of magnitude between the surface and the deep sea.

The decline is less dramatic in terms of biomass (about one order of magnitude, Fig. 4.11b) but appears to be superimposed by a subsurface peak located in the upper mesopelagial (300-400 m). A similar feature has already been described for late fall (see above).

Vertical distributions of abundance and biomass

The vertical distribution of abundance and biomass along the zonal section through the Greenland Sea in late fall is shown in Fig. 4.12. At the westernmost station (08°33'W) abundance is highest in the surface layer and decreases exponentially with depth (Fig. 4.12a). No such pattern is evident for the other stations, where the maxima are located deeper in the water column, between 100 and 500 m.

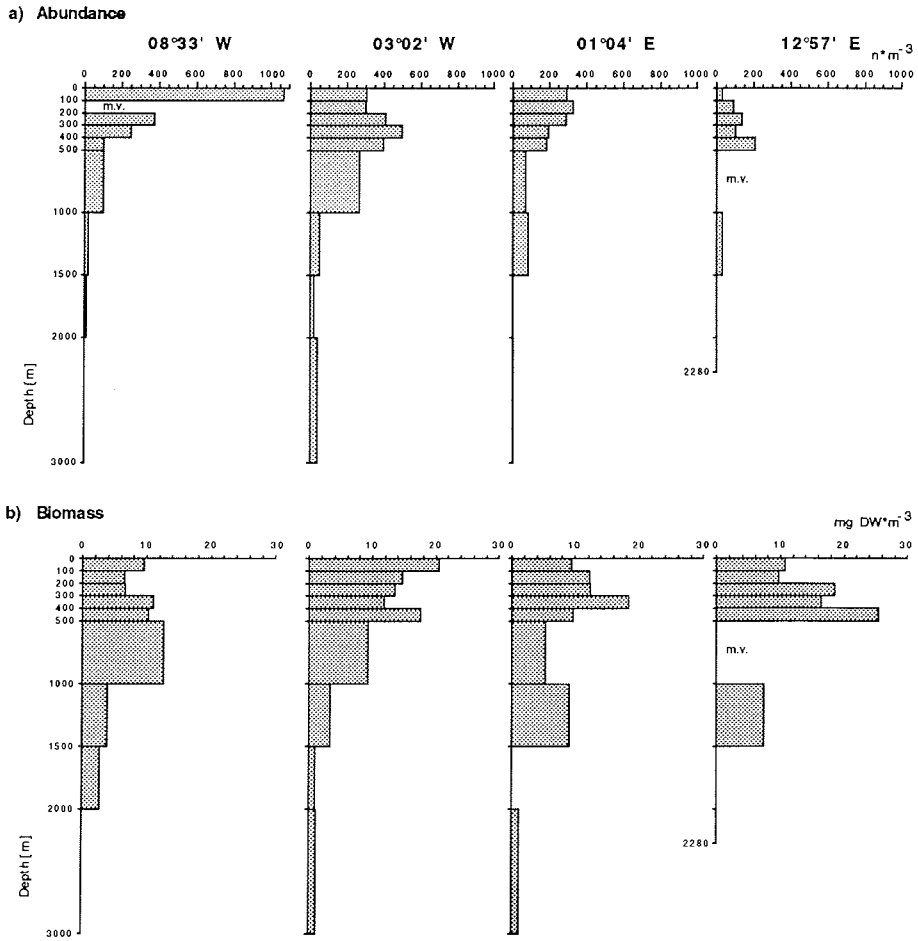

Fig. 4.12: Vertical distributions of abundance (a) and biomass (b) across the Greenland Sea (75°N) in November 1988 (m.v.= missing values for all taxa or those taxa not listed in Table 3.2).

In terms of biomass there is no conspicuous trend (Fig. 4.12b). The highest concentrations are usually found in the upper 1000 m, but no clear vertical pattern is discernible.

The temporal sequence of events underlying the average yearly pattern (presented in the foregoing chapter) reveals considerable changes in the vertical distribution of abundance and biomass in course of the year (Fig. 4.13). The dark season is characterized by only weak vertical gradients of abundance and biomass, leading to a more or less homogeneous distribution of these parameters in early February. The light season, by contrast, shows a surface-biassed vertical structure culminating in a highly aggregated distribution with maximum concentrations in the early summer surface layer (15 June). However, the abundance maximum precedes the biomass maximum and persists longer, whereas the biomass peak seems to be a rather ephemeral surface feature which desintegrates rather early, by the end of the summer season (18 August).

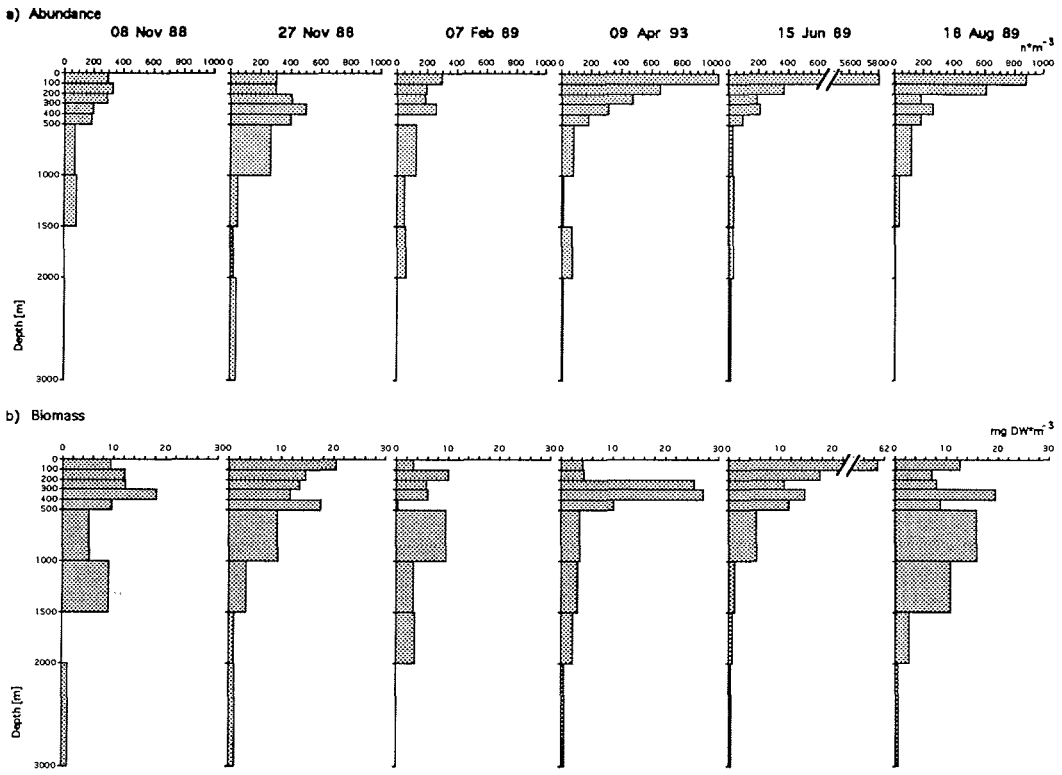

Fig. 4.13: Vertical distributions of abundance (a) and biomass (b) in the Greenland Sea Gyre in the course of the year. Note the scale breaks for 15 June 89.

Figure 4.14 shows the seasonal translocation of the depths of median zooplankton occurrence, in terms of abundance and biomass, where 50% of all specimens or biomass are above, and 50% below that depth. Both curves agree in phase and amplitude with seasonal extremes in February and June and vertical ranges of about 600 m. They are, however, separated in space, as evidenced by the shallower distribution of abundance relative to biomass.

This is a further indication of marked differences in the species and size contributions to zooplankton abundance and biomass in the Greenland Sea.

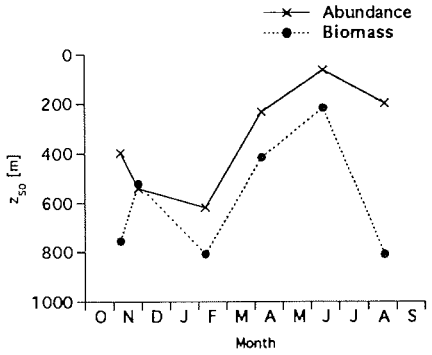

Fig. 4.14: Seasonal translocation of z_{50} depths of total zooplankton abundance and biomass in the Greenland Sea Gyre. These are the depths above which 50% of the population is distributed.

Relative composition of zooplankton abundance and biomass

Table 4.2 lists the „top ten" contributors to abundance and biomass, respectively, in rank order of importance on a regional and and annual basis. Obviously, only few but very different species account for the observed abundance and biomass changes. *Oithona* alone [almost exclusively *O. similis* (Cyclopoida, Copepoda)] accounts for more than half of total numbers, whereas *Calanus hyperboreus* (Calanoida, Copepoda) dominates the biomass, making up about one third of the yearly total biomass. Conversely, *C. hyperboreus* ranks only fifth in abundance (3%) and *O. similis* sixth in biomass (4%). This shows, that total abundance and biomass are largely independent measures of zooplankton stocks in the Greenland Sea. The numerical dominance of copepods is overwhelming. Abundance ranks one to seven on both, a regional and annual basis, are occupied by copepods, accounting for 97% of total numbers. The most numerous taxa are also the smallest, as illustrated by the inverse relationship between the yearly mean abundances and mean individual dry weights of the species set in question (Fig. 4.15).

In terms of biomass, the relative composition is somewhat less dominated by copepods, for the chaetognath *Eukrohnia* (chiefly *E. hamata*) ranks second and the ostracod *Boroecia borealis* third, amounting to roughly one fourth of the share (22% and 6%).

Table 4.3 summarizes the yearly averaged relative importance of the major taxonomic groups in the GSG. Two thirds of total numbers are cyclopoid copepods, slightly less than a third are calanoid copepods, and the remainder (<2%) are other taxa. Calanoids and cyclopoids make up about two thirds of the biomass (58%

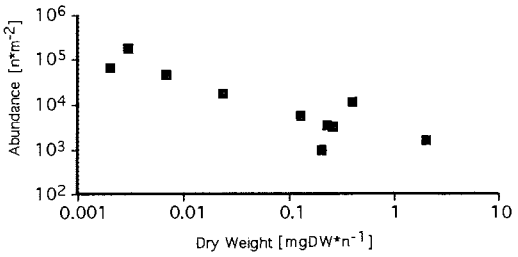

Fig. 4.15: Taxon-specific abundance versus mean individual dry weight, for the 'top ten' contributors to abundance in the Greenland Sea (cf. Table 4.2).

and 5%), other crustaceans add another 18%, chaetognaths 14%, and other taxa the remaining <6%.

Temporal variability in relative composition is below 10% of the mean for the main abundance and biomass constituents. Regional variability is higher (>20% and >10%,

Table 4. 2: 'Top ten' species in terms of total abundance and biomass in the Greenland Sea [incidental large macroplankton (*Atolla*, *Hymenodora*) excluded from biomass].

Abundance

Taxon	regional mean (%)	Taxon	annual mean (%)
Oithona spp.	44.3	*Oithona* spp.	53.3
Oncaea spp.	19.4	*Oncaea* spp.	19.2
small calanoids (*Microcalanus*)	15.7	small calanoids (*Microcalanus*)	13.6
Pseudocalanus minutus	5.9	*Pseudocalanus minutus*	5.0
Calanus finmarchicus	4.8	*Calanus hyperboreus*	3.4
Calanus hyperboreus	4.6	*Metridia longa*	1.6
Metridia longa	1.7	*Calanus finmarchicus*	1.0
Boroecia borealis	0.9	*Boroecia borealis*	0.9
Eukrohnia spp.	0.7	*Eukrohnia* spp.	0.5
Oikopleura vanhoeffeni	0.3	*Oikopleura vanhoeffeni*	0.3
other	1.7	other	1.2

Biomass

Taxon	regional mean (%)		annual mean (%)
Calanus hyperboreus	25.7	*Calanus hyperboreus*	31.8
Eukrohnia spp.	24.5	*Eukrohnia* spp.	21.9
Calanus finmarchicus	17.4	*Boroecia borealis*	5.5
Boroecia borealis	5.5	*Calanus finmarchicus*	5.3
Thysanoessa longicaudata	3.5	*Metridia longa*	4.7
Metridia longa	2.7	*Oithona* spp.	3.7
Pseudocalanus minutus	2.4	*Pseudocalanus minutus*	2.8
Oithona spp.	2.2	small calanoids (*Microcalanus*)	2.2
small calanoids (*Microcalanus*)	1.8	*Thysanoessa inermis*	1.6
Euchaeta spp.	1.6	*Euchaeta* spp.	1.6
other	12.7	other	18.9

respectively), due to a shift in numerical dominance from cyclopoid to calanoid copepods in the WSC, leaving them 59% and 75% of abundance and biomass, respectively (not shown in Table 4.3).

Table 4.3: Relative importance of major taxonomic groups in terms of total abundance and biomass in the Greenland Sea (means ± standard deviations).

Abundance

Taxon	regional mean %	Taxon	annual mean %
Cyclopoida	61.8±13.4	Cyclopoida	67.9±6.6
Calanoida	35.8±11.7	Calanoida	30.5±6.3
Ostracoda	0.9±0.4	Ostracoda	0.8±0.3
Chaetognatha	0.6±0.4	Chaetognatha	0.3±0.2
Pteropoda	0.3±0.8	Appendicularia	0.3±0.3
Appendicularia	0.3±0.2	Amphipoda	0.1±<0.1
Amphipoda	0.1±<0.1	Pteropoda	0.1±0.2
Euphausiacea	0.1±0.1	other	<0.1
other	<0.1		

Biomass

Taxon	regional mean %		annual mean %
Calanoida	61.7±8.6	Calanoida	58.2±5.0
Chaetognatha	16.0±5.9	Chaetognatha	13.6±4.8
Ostracoda	6.3±2.2	Ostracoda	6.1±1.7
Euphausiacea	5.5±2.2	Cyclopoida	5.1±2.6
Cyclopoida	3.1±1.7	Decapoda	4.6±3.7
Amphipoda	2.4±0.5	Euphausiacea	3.8±2.2
Pteropoda	2.0±1.8	Amphipoda	3.0±0.6
Hydromedusae	1.4±0.9	Hydromedusae	3.0±1.1
Appendicularia	1.1±0.9	Appendicularia	1.4±3.0
Siphonophora	0.5±0.2	Pteropoda	0.6±1.1
other	<0.1	Siphonophora	0.5±0.2
		Polychaeta	0.1±<0.1
		Isopoda	<0.1

Horizontal and vertical distribution patterns of abundance

Figure 4.16 displays the regional distribution pattern of copepods and other taxa in late fall, in the tabular fashion introduced by Mumm (1991, 'Mumm-plot', cf. Material and methods, p. 11). Species are ranked according to their zonal centers of distribution: taxa with a westerly distribution are listed in the upper, those with an easterly distribution in the lower part of the panel. The former case is represented by *Oithona*, which thrives west of the prime meridian, the latter by *Calanus finmarchicus* (Fig. 4.16a), the ostracod *Discoconchoecia elegans* and the pteropod *Limacina retroversa* (Fig. 4.16b), which are more

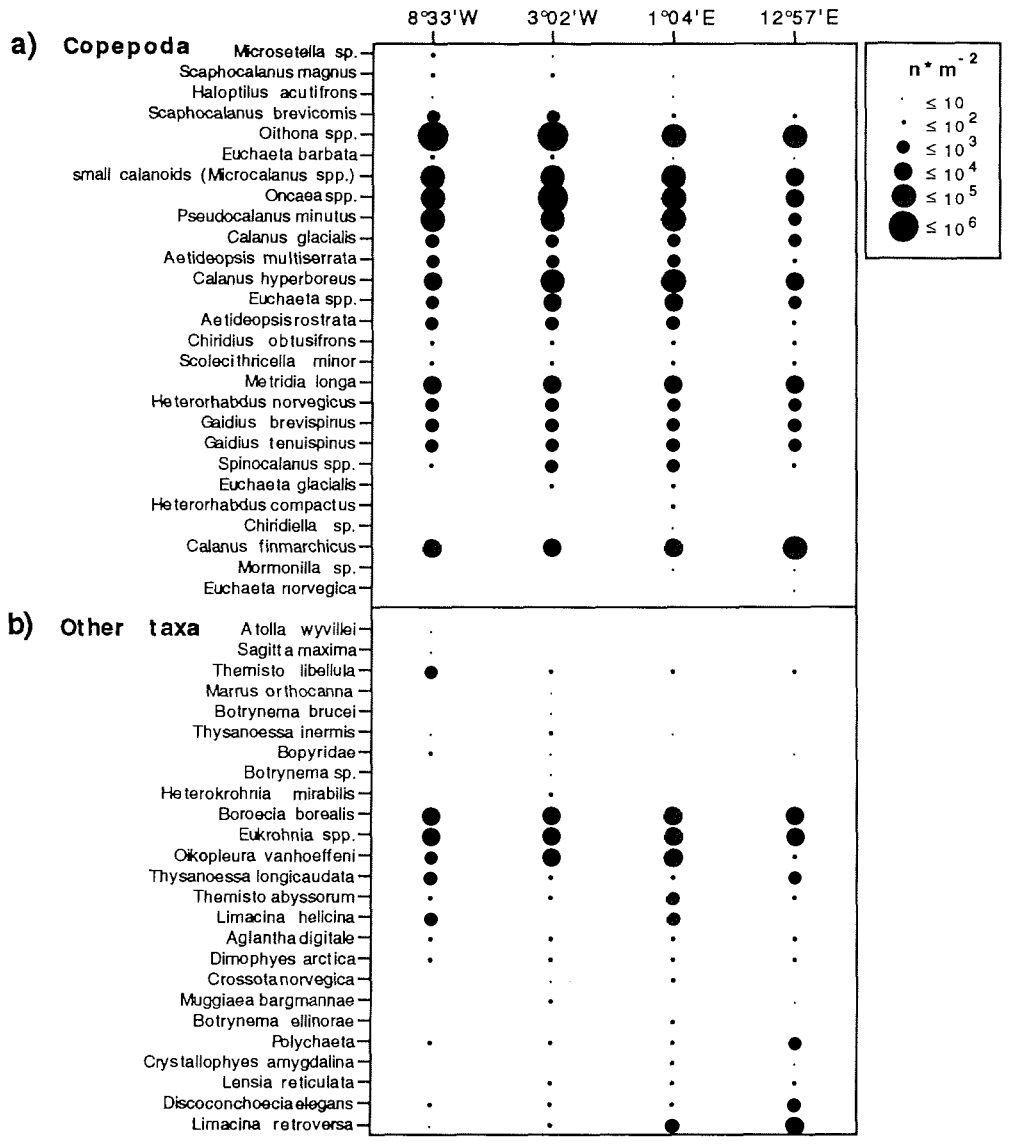

Fig. 4.16: 'Mumm-plot' of species abundances for the regional transect across the Greenland Sea in November 1988, separated for copepods (a) and 'other taxa' (b). Species are ranked according to their zonal center of distribution; species with a westerly distribution are listed above, those with an easterly distribution below.

abundant in the WSC (13°E). This station differs from the gyre stations in generally lower abundances (except for the stated taxa), but no clear zonal pattern is detectable due to the coarse logarithmic scale, the paucity of stations and the ubiquity of the commoner taxa.

The 'Mumm-plot' for the seasonal distribution of copepods is shown in Fig. 4.17a. Taxa with highest occurrences in the dark season are listed in the upper panel, those abounding during the light season at the lower end.

Disregarding the incidental reports of those taxa represented by only single or scattered specimens, virtually no copepods represent the winter type and few, if any, the summer type. The rectangular array of the occurrences rather indicates that all the common copepods are present in the GSG throughout the year. Furthermore, all occur in fairly high numbers, irrespective of season.

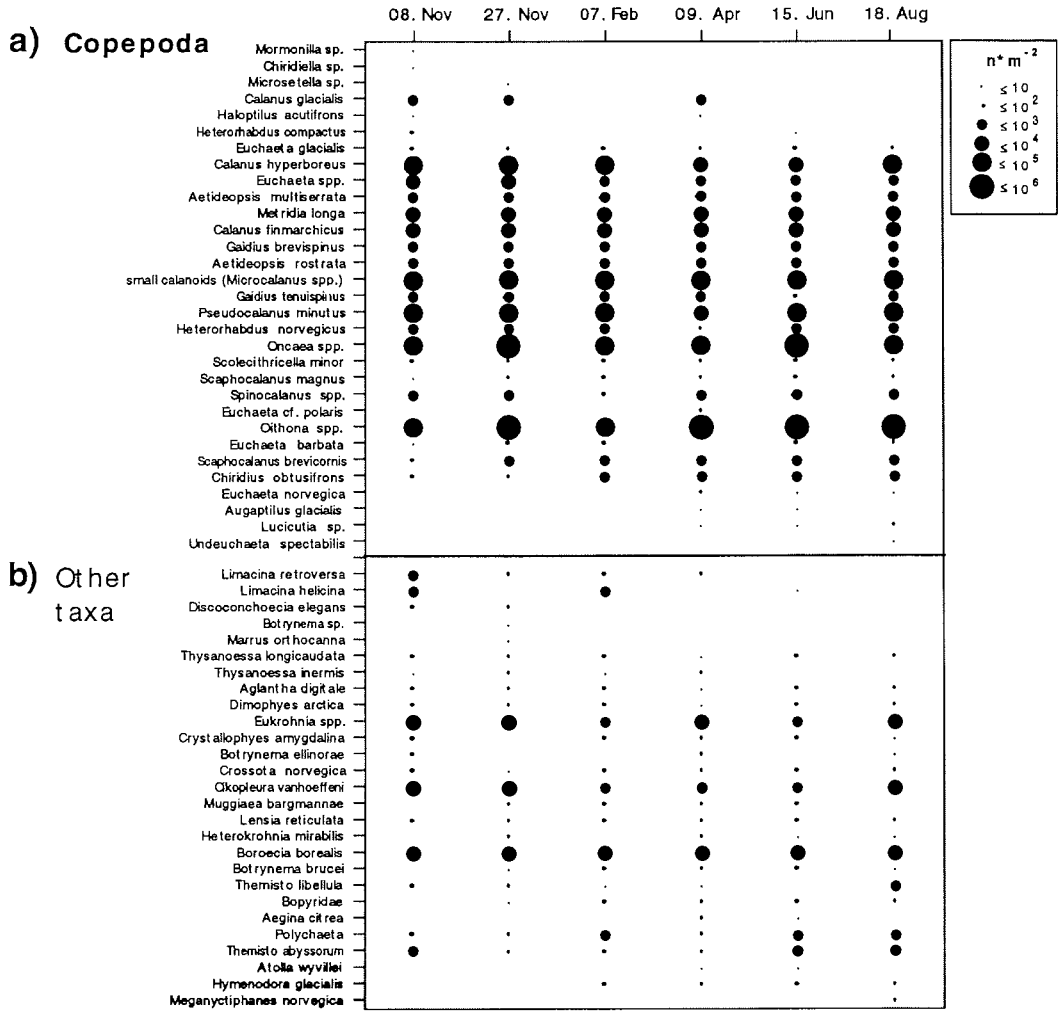

Fig. 4.17: 'Mumm-plot' of species abundances for the seasonal study in the Greenland Sea Gyre, separated for copepods (a) and 'other taxa' (b). Species are ranked according to their seasonal center of distribution; species with highest occurrences in winter are listed above, those with highest occurrences in summer below.

The array takes a more slanted appearance for the other taxa (Fig. 4.17b) and it is noteworthy that some of the species which are common in late fall (*Limacina retroversa, L. helicina, Discoconchoecia elegans*) vanish in summer. while none of the summerly occurring taxa are absent in winter, two incidental macroplankton species notwithstanding. These findings have to be born in mind when discussing advective versus biological causes of population changes in the Greenland Sea Gyre (GSG).

The yearly-averaged vertical distribution of GSG zooplankton is depicted in Fig. 4.18. A clear pattern separates surface from deep dwellers in both, copepods and other taxa. The trapezoidal array of occurrences shown in the plot reveals the interesting observation that the designated 'surface' dwellers do occur throughout the water column down to the

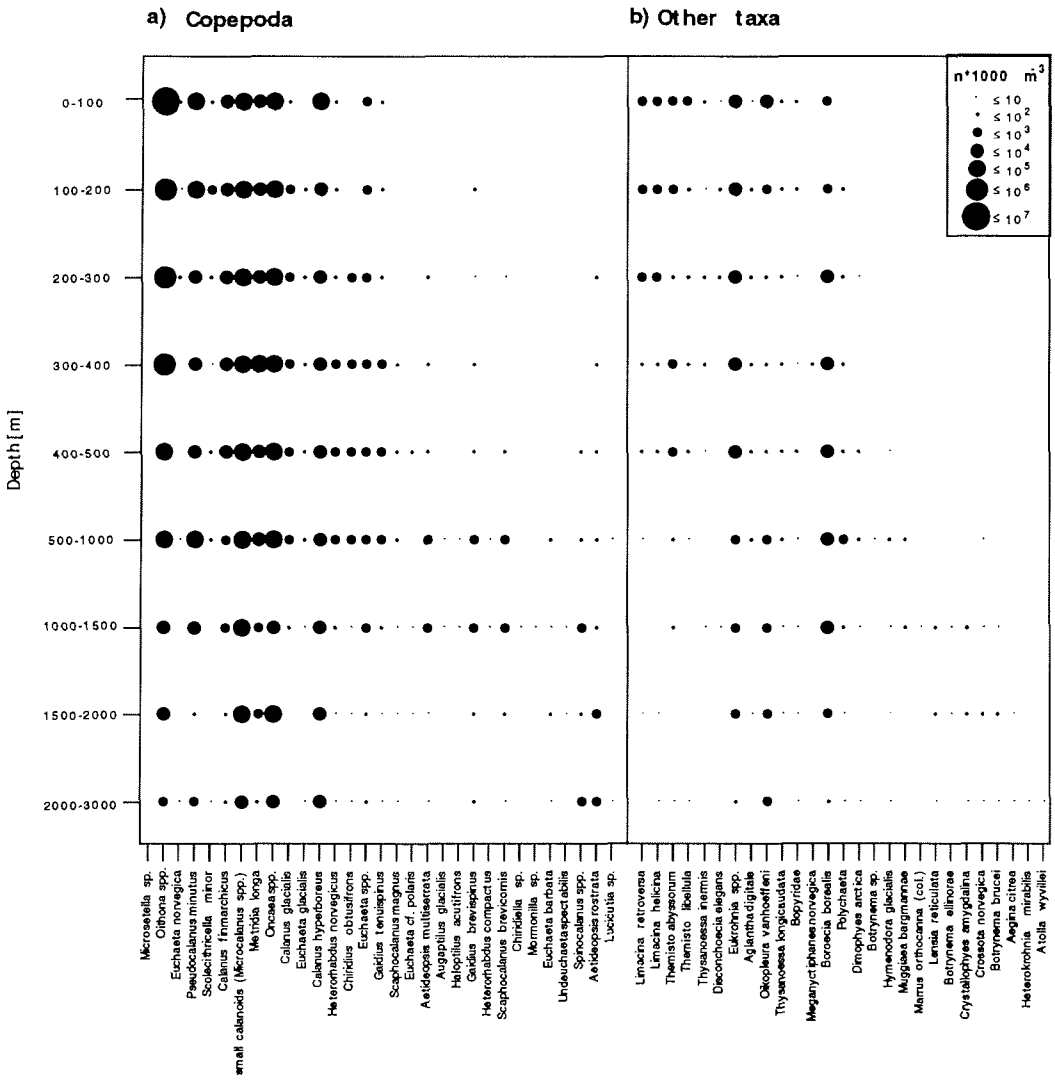

Fig. 4.18: 'Mumm-plot' of species abundances of copepods (a) and 'other taxa' (b) in the nine depth strata. Species are ranked according to their vertical center of distribution; species with a surface-biassed distribution are listed above, those with a deep distribution below.

greatest depths, whereas deep dwellers do not extend into the surface layers. This is most evident for the 'other' taxa, e.g. the hydromedusan and siphonophoran species which occur in low numbers but regularly and exclusively in the bathypelagic range (Fig. 4.18b). Copepods seem to be less restricted in their vertical range. However, a layered distribution of copepods is discernible at intermediate and great depths. Most of the species following this distribution pattern belong to the family Aetideidae. About half of the taxa encountered of both, copepods and 'others', have a very broad vertical range on a yearly basis, extending from the surface to the deep sea. These are also the numerical (*Oithona, Oncaea*) as well as biomass (*Calanus hyperboreus, Eukrohnia hamata, Boroecia borealis*) dominants (cf. Table 4.2)

It will be shown in the following, that many of these species undergo seasonal vertical migrations and abound in much narrower depth ranges on a shorter time scale. Furthermore, it appears that the ranking of the species within this category reflects the range of seasonal migration. This issue will be taken up again in section 4.3 on distribution patterns of selected species.

4.2 Community structure

It was already emerging from the foregoing chapters, that vertical structure appears to be more evident than horizontal structure in the distribution patterns of zooplankton in the Greenland Sea. The ANOSIM permutation test for depth versus time effects on community patterns among samples leads to rejection of H_{01} („no depth effects") at virtually any significance level one cares to nominate (Table 4.4). The observed ρ_{av} is larger than its value in any of the 5000 permutations under H_{01} ($p<0.0002$).

By contrast, the test of the hypothesis H_{02} („no time effects") yields a ρ_{av} which is exceeded by almost half of the simulated values under H_{02} and the null hypothesis cannot be rejected ($p= 0.487$). The test leads to the conclusion that depth is a highly significant factor in shaping the zooplankton community whereas season is not.

Table 4.4: ANOSIM permutation test for differences between time groups (averaged across 9 depth groups) and differences between depth groups (averaged across 6 time groups) in zooplankton samples from the Greenland Sea Gyre. Two-way crossed layout without replication.

Test for difference between	time groups	depth groups
Sample statistic ρ_{av}	-0.006	0.684
Number of permutations	5000	5000
Number of permuted statistics $\geq\rho_{av}$	2432	0
Significance level of ρ_{av}	48.7% (n.s.)	<0.02% (***)

n.s.= not significant, *** highly significant

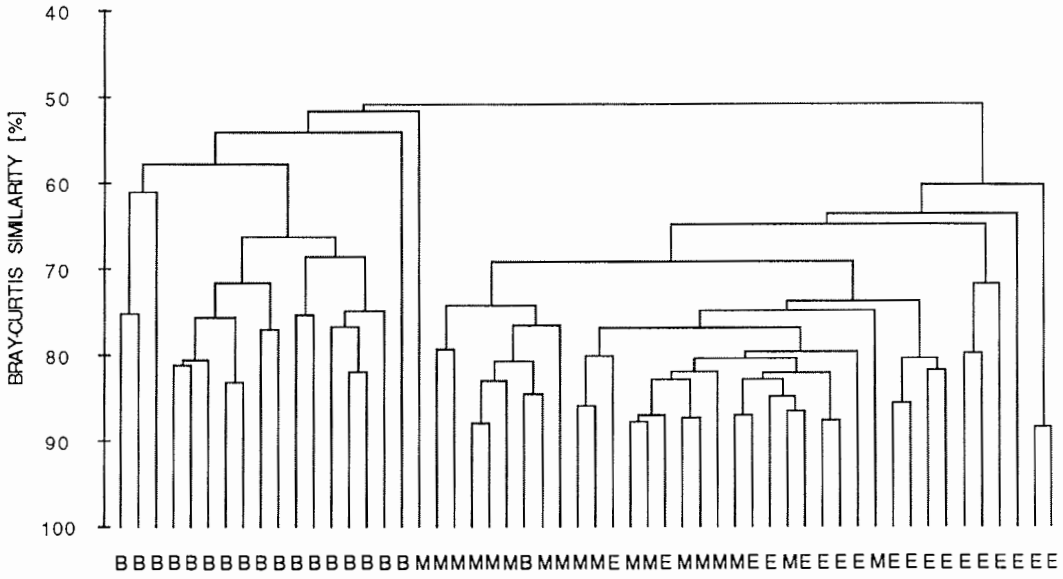

Fig. 4.19: Cluster dendrogram showing classification of 54 zooplankton samples in the Greenland Sea Gyre (fourth-root transformed abundances, Bray-Curtis similarity, group average linking). Samples are labelled according to depth (E= 0-300 m; M= 300-1000 m; B= 1000-3000 m).

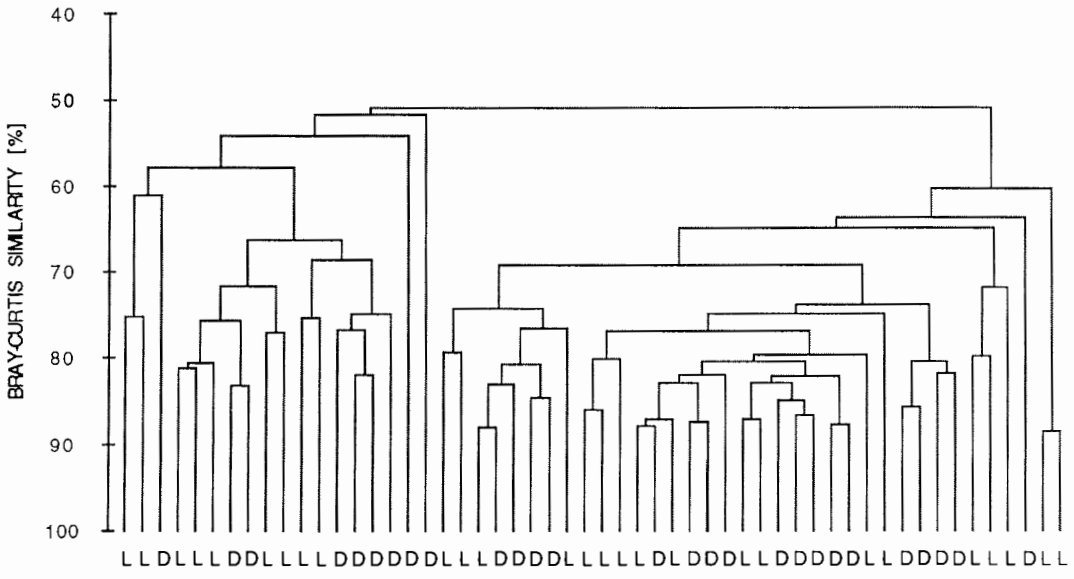

Fig. 4.20: Same dendrogram as in Fig. 4.19. Samples are labelled according to time [L= light season (09 Apr, 15 Jun, 18 Aug); D= dark season (08 Nov, 27 Nov, 07 Feb)].

As expected from the ANOSIM test, subsequent classification analysis results in a clustering of samples according to depth: Epi (E)-, meso (M)- and bathypelagic (B) samples are grouped in conspicuous clusters (Fig. 4.19). Season, by contrast, appears to be irrelevant to the observed grouping of samples (Fig. 4.20).

The same depth dependence is borne out by the MDS ordination yielding a near total separation of bathypelagic from epi- and mesopelagic samples (Fig. 4.21). The separation of epi- and mesopelagic samples is even more evident than in the cluster dendrogram, but the overlap of the E and M labels shows that they are part of a continuum. The isolated E and M samples in the plot, denoted by an asterisk, correspond to the seasonal extremes in total abundance in mid-June (surface layer) and February (400-500 m, cf. Fig. 4.13). The MDS plot with samples labelled according to season bears no structure at all (Fig. 4.22).

Classification and ordination was repeated for the 39 species (Figs. 4.23 and 4.24). The resulting dendrogram reveals six species clusters (Fig. 4.23). Cluster 1 is composed of cnidarians, which all occur exclusively and fairly regularly, but in low numbers in the bathypelagial (cf. Fig. 4.18). Cluster 2 is more heterogeneous in phyletic composition grouping species of regular occurrence in the mesopelagial. The third cluster assembles the biomass and abundance dominants, which all undergo more or less pronounced seasonal vertical migrations. The next two clusters are heterogenous assemblages of meso- and bathypelagic organisms, which is more difficult to interpret. Cluster 6, finally, groups the pteropods *Limacina helicina* and *L. retroversa*, which were shown to have a regionally, seasonally and vertically biassed distribution (Figs. 4.16-18).

The most conspicuous of these clusters, namely 1, 3 and 6 are also easily recognizable assemblages in the MDS plot (Fig. 4.24), and it is not surprising to find the 'predictible' deep dwellers of cluster 1 and the 'unpredictable' surface-biassed pteropods (cluster 6) on opposite sides of the plot. The representatives of cluster 3 project downwards from a diffuse center assemblage, and the array '*Oithona*, *Oncaea*, nauplii, etc.' reads like the 'top

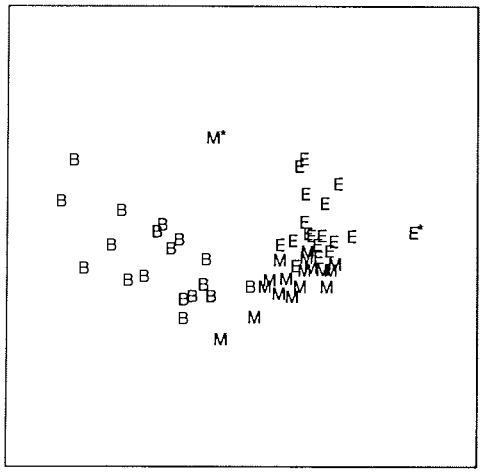

Fig. 4.21: Ordination of 54 zooplankton samples in the Greenland Sea Gyre in 2 dimensions using multi-dimensional scaling on the same similarity matrix as in Fig. 4.19. Axis scales are arbitrary. Asterisks denote the seasonal extremes in total abundance (cf. text). For legend cf. Fig. 4.19.

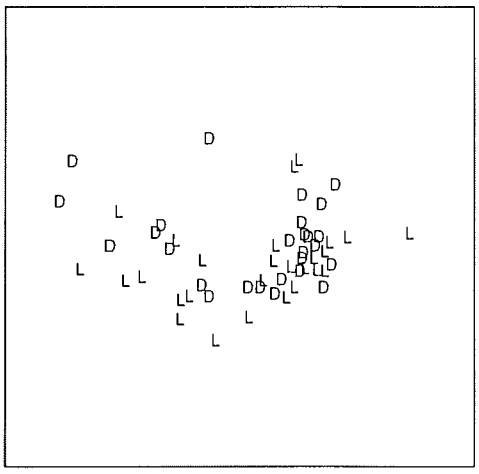

Fig. 4.22: Same MDS plot as in Fig. 4.21. Samples are labelled according to time (cf. Fig. 4.20). Axis scales are arbitrary.

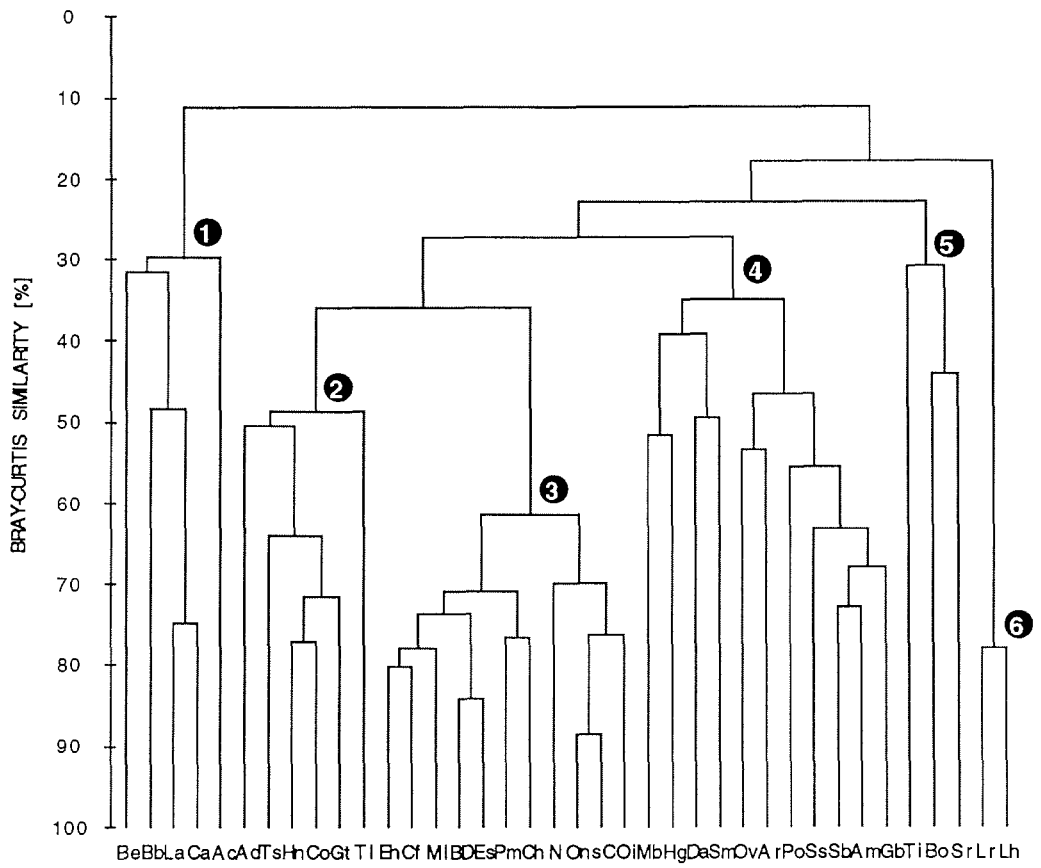

Fig. 4.23: Cluster dendrogram showing classification of 39 zooplankton taxa in the Greenland Sea Gyre (fourth-root transformed abundances, Bray-Curtis similarity, group average linking). Clusters are numbered 1 to 6.

(Be=*Botrynema ellinorae*, Bb= *Botrynema brucei*, La= *Lensia reticulata*, Ca= *Crystallophyes amygdalina*, Ac= *Aegina citrea*, Ad= *Aglantha digitale*, Ts= *Themisto* sp., Hn= *Heterorhabdus norvegicus*, Co= *Chiridius obtusifrons*, Gt= *Gaidius tenuispinus*, Tl= *Thysanoessa longicaudata*, Eh= *Eukrohnia* spp., Cf= *Calanus finmarchicus*, Ml= *Metridia longa*, BD= *Boroecia/Discoconchoecia*, Es= *Euchaeta* spp., Pm= *Pseudocalanus minutus*, Ch= *Calanus hyperboreus*, N= nauplii, On= *Oncaea* spp., sC= small calanoids, Oi= *Oithona* sp., Mb= *Muggiaea bargmannae*, Hg= *Hymenodora glacialis*, Da= *Dimophyes arctica*, Sm= *Scaphocalanus magnus*, Ov= *Oikopleura vanhoeffeni*, Ar= *Aetideopsis rostrata*, Po= Polychaeta, Ss= *Spinocalanus* spp., Sb= *Scaphocalanus brevicornis*, Am= *Aetideopsis multiserrata*, Gb= *Gaidius brevispinus*, Ti= *Thysanoessa inermis*, Bo= Bopyridae, Sr= *Scolecithricella minor*, Lr= *Limacina retroversa*, Lh= *Limacina helicina*

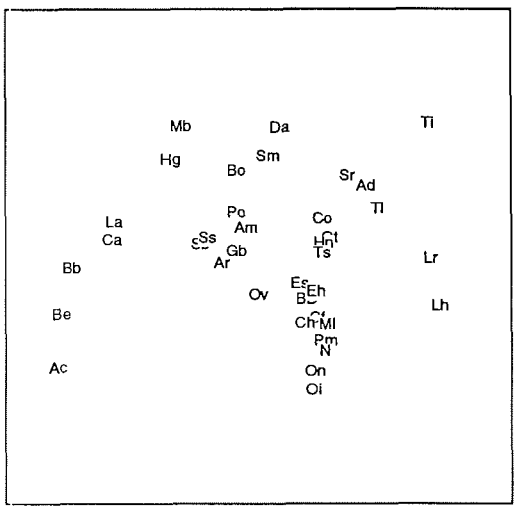

Fig. 4.24: Ordination of 39 zooplankton taxa in the Greenland Sea Gyre in 2 dimensions using multidimensional scaling on the same similarity matrix as Fig. 4.23. Axis scales are arbitrary. For legend *cf.* Fig. 23

ten' list of abundances (Table 4.2). In the center of the plot we find species of the meso- and bathypelagic copepod family Aetideidae. It is noteworthy that their alignment matches their vertical centers of distribution, as will be shown later, with the mesopelagic *Chiridius obtusifrons* and *Gaidius tenuispinus* to the right and the truly bathypelagic *G. brevispinus* and *Aetideopsis rostrata* to the left of the array.

4.3 Selected species

This section highlights the distribution and quantitative composition of those taxa which were shown to be dominant or to represent a particular distribution type. Where appropriate, the chapters are followed by short interpretations of the results (in italics) to set the stage for the discussion of the life history of these groups in the Greenland Sea (cf. chapter 5.4).

Numerical dominants (Cyclopoida and small Calanoida)

Oithona

Oithona is by far the most abundant taxon encountered during this study, contributing to about half of total zooplankton numbers (Table 4.2). But due to its relatively small size, it constitutes only about 2% and 4% of total biomass, averaged across the regional transect in late fall, and across all seasons in the Greenland Sea Gyre (GSG), respectively.

Figure 4.25 reveals marked regional and seasonal differences of abundance and length composition across the Greenland Sea, and within the GSG, respectively.

The lowest numbers of individuals are found at 13°E ($22*10^3$ $n*m^{-2}$) in late fall, while about seven-fold higher values are recorded to the west of the Arctic Front (Fig. 4.25a). These abundance differences are compounded by conspicuous changes in the length distribution between the Atlantic and the arctic stations. The former displays a clear bimodal distribution with modal classes of +0.6 and +1.2 mm total length[4], while the larger-sized mode is entirely absent in the gyre, not only in late fall, but throughout the investigation period (Figs. 4.25a and b, note the scale difference between a and b). Microscopic identification confirms the presence of two species at 13°E but of only one further west. *Oithona similis* (0.8 mm total length) occurs throughout the Greenland Sea, while the larger *O. atlantica* (up to 1.4 mm total length) is confined to 13°E.

Additional regional variability occurs within the lower-sized mode: The length frequency changes from a broad-range left[5]-skewed distribution dominated by large +0.8 mm animals at the western station towards a narrow-range right-skewed distribution dominated by smaller +0.6 mm animals at the eastern station. The center station at 1°E displays a more or less symmetrical distribution around a plateau-like mode of constant frequencies between 0.6 and 0.9 mm. It is very likely that this pattern arises from overlapping 'eastern' and 'western' distribution types described above.

[4] + denotes the left bin edge of a 0.05 mm size class

[5] left and right refers to the small and large size ends, respectively

Abundances in the GSG vary five-fold on a seasonal scale between minimum values in early February and peak values in mid-June (Fig. 4.25b). These quantitative changes are again accompanied by qualitative changes in the length-frequency distributions. The fall population displays a broad size range and a left-skewed size-frequency distribution, indicative of several overlapping modes, dominated by large animals (+0.8 mm total length). Fall through spring the size range progressively narrows and the distribution approaches the unimodal normal type centered at +0.7 mm. The abundance peak in early summer coincides with a clear cut bimodal distribution dominated by young recruits of *O. similis* (+0.45 mm modal length) and a smaller mode of presumptive first generation adults (males and females) at +0.75 mm, as confirmed microscopically. This latter gradually advances to again fall values of +0.8 mm by end of summer. By that time, the mode of the obviously fast growing second generation has merged with the former, giving rise to a left-skewed distribution, with an identical size range as in early November. The reappearance of <0.4 mm animals in late fall is somewhat surprising. It was already evident in the size distributions of the regional transect, especially on the western side.

The vertical distribution of length-frequencies in late fall (Fig. 4.26a) leaves no doubt about the authenticity of this observation, as the occurrence of small specimens is a prominent feature of the surface layer. It recurs at all gyre stations, however most evident west of the prime meridian. This layer also coincides with the abundance maximum at the western station (Fig. 4.26b), but a more homogenous vertical distribution of abundance prevails at the other stations on the transect, in spite of the vertical changes in size. It is interesting to note that size tends to increase with depth down to about 1500 m, while a seemingly different distribution is apparent below (e.g. at 8°33'W and 1°04'E). This is, however, of no quantitative importance to the overall size distribution at the stations (Fig.

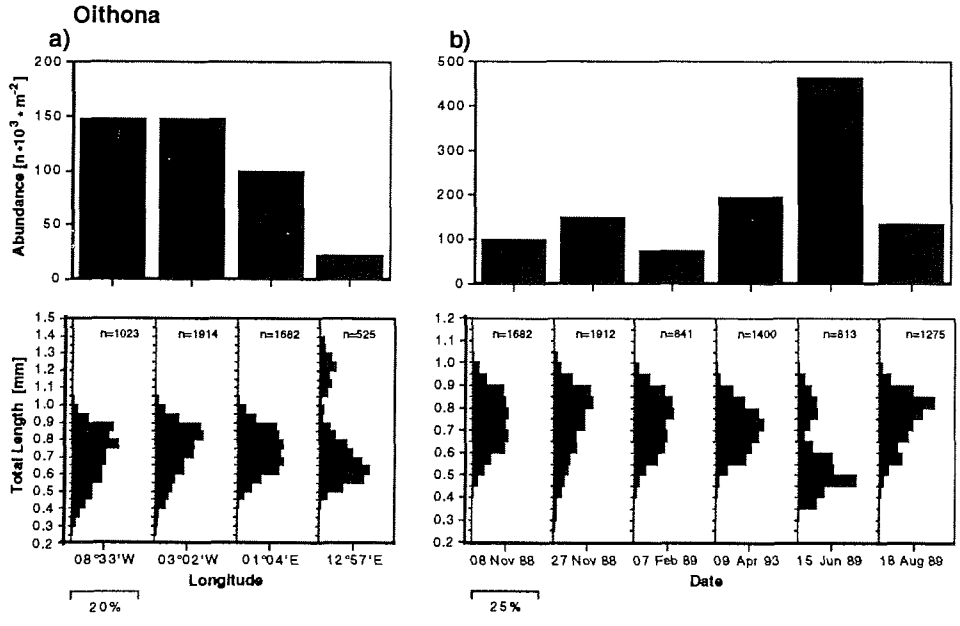

Fig. 4.25: Integrated abundance and length-frequency distribution of *Oithona* spp. along a regional transect across the Greenland Sea in November 1988 (a) and for different seasons within the Greenland Sea Gyre (b). 'n' indicates the number of specimens measured. Note the scale changes between (a) and (b).

4.25a), as the deep population represents only a minute fraction of the total number of individuals (Fig. 4.26b).

The vertical distribution of abundance and size on a temporal scale is shown in Fig. 4.27. Highest concentrations of animals occur in the epipelagial throughout the year (Fig. 4.27b). There is, however, considerable seasonal variation in the acuteness and vertical extent of the maximum. During the dark season uniformly high concentrations of about 200 $n*m^{-3}$ are found in the upper 300 to 400 m, with considerably lower values below. A surface peak develops as early as April and culminates in mid-June, where almost the entire population is aggregated in the top 100 m (4500 $n*m^{-3}$, Fig. 4.27b). This surface-

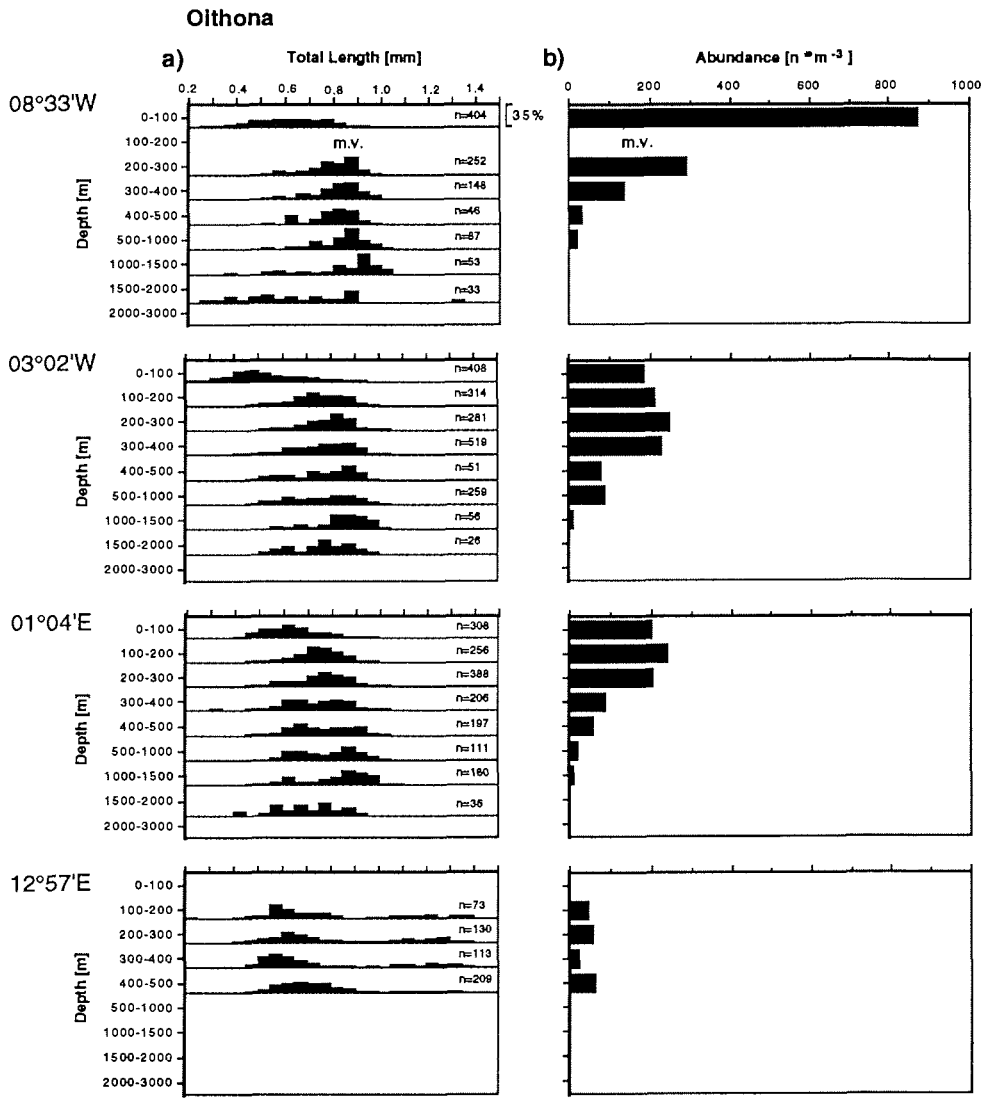

Fig. 4.26: Vertical distribution of length-frequency (a) and abundance (b) of *Oithona* spp. along a regional transect across the Greenland Sea in November 1988 (a). 'n' indicates the number of specimens measured, 'm.v.' denotes missing value.

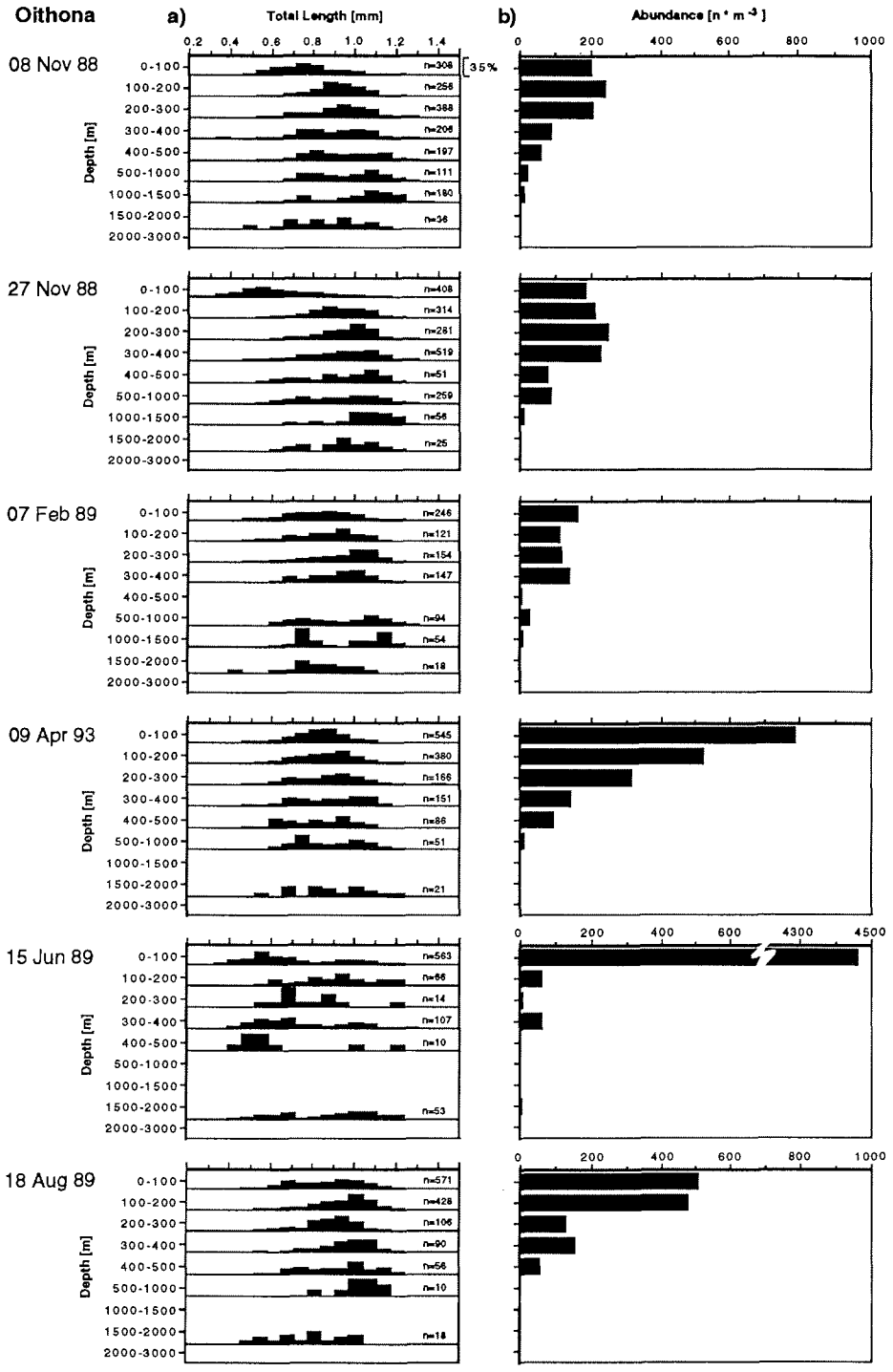

Fig. 4.27: Vertical distribution of length-frequency (a) and abundance (b) of *Oithona* spp. for different seasons in the Greenland Sea Gyre. 'n' indicates the number of specimens measured. Note the scale break for 15 June 1989.

biassed distribution disintegrates by the end of the light season, as part of the population moves into the subsurface, giving way to the distribution pattern already described for the dark season.

The vertical size distribution of *Oithona* over the season repeats the weak trend of increasing size with depth. Only in early summer the prominent bimodal distribution in the surface layer transcends the deeper layers, with dominance of small animals throughout the range. This vertical pattern is, however, obstructed by a somewhat confusing size distribution between 100 and 300 m.

Bimodal distributions are a recurrent feature in meso- and bathypelagial but these latter are based on low concentrations of animals (<100 $n*m^{-3}$). Two modes are evident in the early November, February, April and June histograms, with the larger-sized mode located between 0.85 and 0.95 mm and the smaller-sized mode between 0.55 and 0.65 mm. The length-frequency distribution in the epipelagial, by contrast, was shown to be uni-modal, except in summer, where bimodal distributions coincide with *high* abundances of individuals.

Interpretation

OITHONA SIMILIS is a cold-adapted species with highest occurrence in arctic waters. It maintains high stocks in the epipelagic zone year-round, showing continued development even in the absence of autotrophic production in winter. A minor reproduction event occurs in fall, followed by mortality of spent females over winter. However, the main breeding occurs in early summer in the surface layer. This generation needs one year to complete its life cycle, spawns in the following early summer and dies.

Oncaea

Oncaea comes second in abundance in the Greenland Sea, making up about one fifth of total zooplankton numbers (Table 4.2). But due to its minute size, it is insignificant in terms of biomass (<1%).

Regional variations of abundance are larger than temporal changes, and exceed one order of magnitude between the minimum at 13°E (<$10*10^3$ $n*m^{-2}$) and the maximum at 3°W (>$100*10^3$ $n*m^{-2}$, Fig. 4.28a). These drastic abundance differences are contrasted by only minor regional changes in the size composition. A left-skewed distribution dominated by large +0.65 mm modal animals is found throughout the transect, with varying portions of smaller animals to the west, and conspicuously fewer to the east of the Arctic Front. The regional abundance maximum is associated with the highest shares of smaller size classes constituting an only barely visible second mode at +0.5 mm. A similar feature, albeit at +0.4 mm, is visible at the westernmost station. While these smaller modes appear to be rather spurious projections on a broadly skewed size distribution, it should be borne in mind that they are based on a very large number of independent measurements (n=2076 and n=809, cf. Fig. 4.28a).

The integrated abundance values fluctuate rather wildly on a seasonal scale, between $40*10^3$ and $100*10^3$ $n*m^{-2}$, with highest numbers of individuals in late November and mid June (Fig. 4.28b). The corresponding size distributions follow a more coherent pattern.

Bimodality is apparent throughout the observation period, except perhaps for late summer and fall, where size overlap obscures a clear separation of modes. The larger-sized mode at +0.65 mm predominates throughout most of the year, while the smaller (+0.4 mm) gains greatest importance in early summer.

A near perfect separation of modes is apparent along the vertical axis, with the larger animals inhabiting the upper and the smaller animals the lower half of the water column (1500-3000 m, Figs. 4.29a and 4.30a). This is due to the presence of two vertically segregating species of different size, as confirmed microscopically. The larger *Oncaea borealis* (0.6-0.7 mm total length) dominates in the epi- and mesopelagial, while *Oncaea* cf. *curta* of 0.45-0.5 mm length prevails in the bathypelagial.

This vertical pattern is confounded by the appearance of ≤0.45 mm animals in the epipelagial in fall (Fig. 4.29a), winter and early summer (Fig. 4.30a). These are males (0.45-0.5 mm) and young copepodite stages of *O. borealis*, as again verified through the microscope. They are, however, easily identified in the vertical length-frequency plots due to their surface-biassed distribution, while progressively higher portions of larger-sized animals are found deeper down in the water column. As a result, the distribution changes from bimodal in the epipelagial to unimodal in the mesopelagial. This is most evident during the dark season (Fig. 4.30a). In early summer, a bimodal distribution extends from the subsurface throughout the upper water column, as young copepodids of *O. borealis* are found (in decreasing numbers and proportions) from the surface to about 500 m. By late summer, the small size-classes have disappeared from the lower mesopelagial (500-1000 m), while they endure above. At the same time, the bulk of the population has moved from the surface into the mesopelagial, where it remains during the rest of the year (Fig. 4.30b). Only low concentrations of *Oncaea* are found in the bathypelagial.

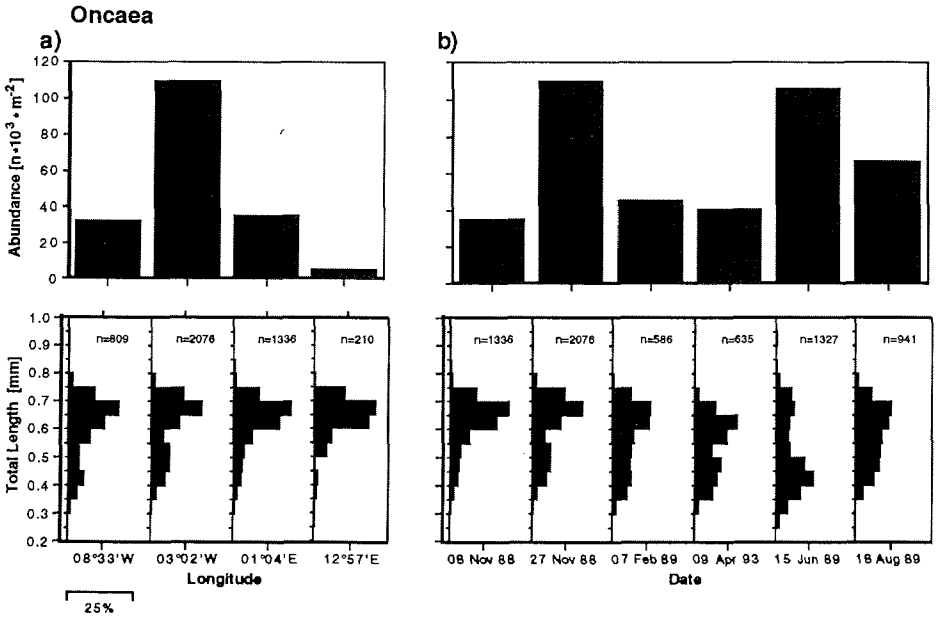

Fig. 4.28: Integrated abundance and length-frequency distribution of *Oncaea* spp. along a regional transect across the Greenland Sea in November 1988 (a) and for different seasons within the Greenland Sea Gyre (b). 'n' indicates the number of specimens measured.

No obvious seasonal pattern is discernible for the bathypelagic *O.* cf. *curta.* This is not surprising, for judging by the small size of the adults, it must be assumed that younger copepodite stages are not retained in the 150 µm mesh employed.

Interpretation

ONCAEA BOREALIS is a cold-adapted species with highest occurrence in arctic waters. It maintains high stocks in the mesopelagial year-round, but reaches highest concentrations in the epipelagial in summer. The reproduction period is extended relative to OITHONA, peaking in fall and early summer in the epipelagial, with high mortality of spent females during the dark season. Growth is rapid during the summer months but slow during winter, where the species endures in the mesopelagial. Development takes one year for both the summer and fall generations.

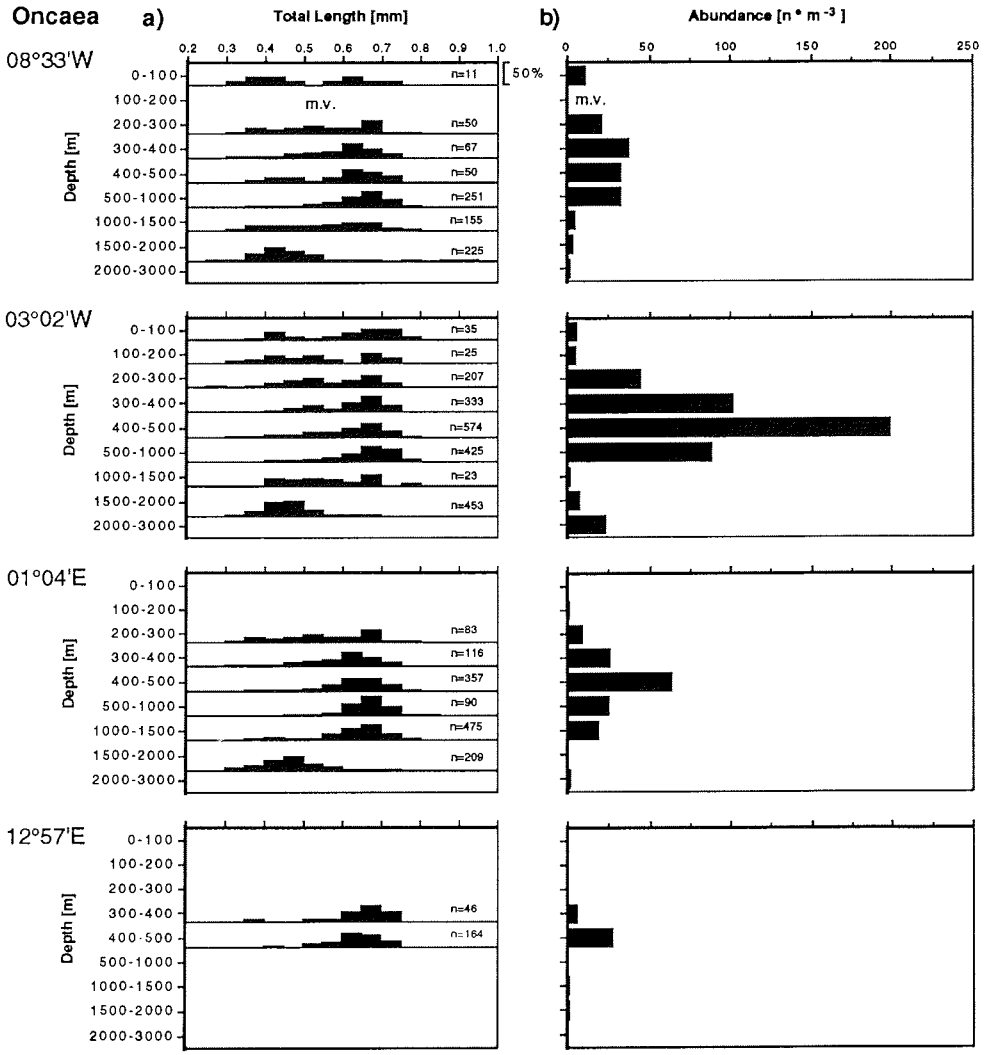

Fig. 4.29: Vertical distribution of length-frequency (a) and abundance (b) of *Oncaea* spp. along a regional transect across the Greenland Sea in November 1988 (a). 'n' indicates the number of specimens measured, 'm.v.' denotes missing value.

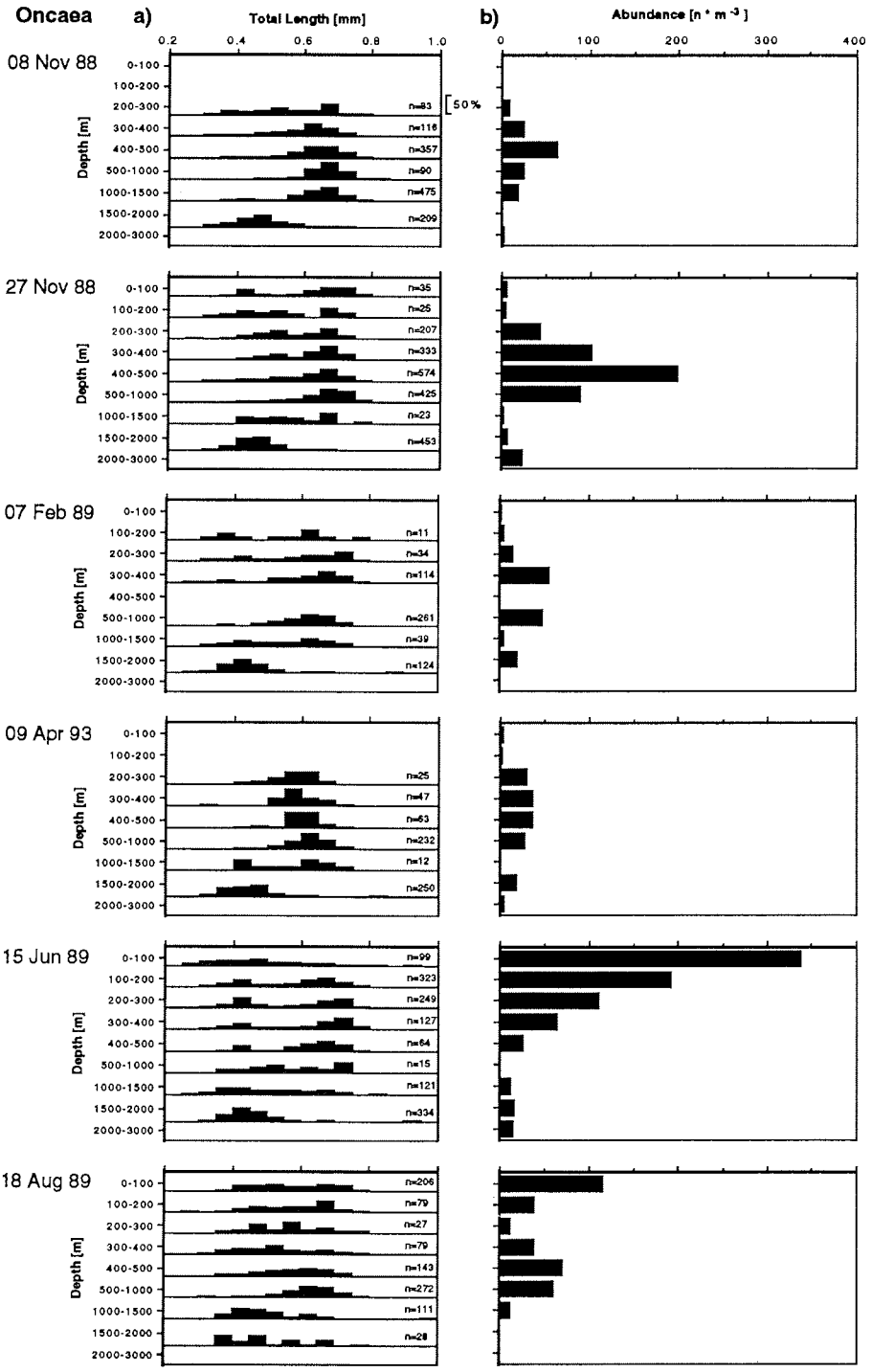

Fig. 4.30: Vertical distribution of length-frequency (a) and abundance (b) of *Oncaea* spp. for different seasons in the Greenland Sea Gyre. 'n' indicates the number of specimens measured.

Pseudocalanus minutus

Pseudocalanus minutus ranks fourth in zooplankton numbers and seventh in biomass, in the Greenland Sea (Table 4.2). *P. minutus* was the only species of the genus *Pseudocalanus* encountered during this investigation.

This species is most abundant in the center of the GSG (>20*10^3 n*m^{-2}), while only half these numbers are found to the west and barely 1*10^3 n*m^{-2} on the eastern end of the regional transect in late fall (Fig. 4.31a).

The length-frequency distributions are quite similar for all gyre stations, approaching a normal size distribution centered around +0.95 mm. At 13°E the distribution is somewhat more skewed towards the larger size end, but it is dominated by the same +0.95 mm modal class.

The size distribution remains practically unchanged through winter, except for the main mode which moves from +0.9 mm to +0.95mm between early and late November (Fig. 4.31b). In spring the shape of the envelope changes as more animals move into the +1.0 and +1.05 mm size classes, beyond which there is an abrupt drop-off in relative frequencies. These size changes are accompanied by a gradual decline in the standing stock of the species, which is at its yearly minimum in spring (7*10^3 n*m^{-2}). The summer increase in numbers is accompanied by the appearance of small specimens in early summer and it was confirmed subsequently that the apparent peaks at the +0.4, +0.5, +0.7 and +1.0 mm size classes correspond to copepodite stages CI, CII, CIII and CVI females.

The abundance maximum occurs remarkably late, i.e. at the end of the summer season, when the youngest stages are no longer visible. A staircase-distribution is characteristic of this period, representing increasing portions of CIII, CIV and CV copepodite stages.

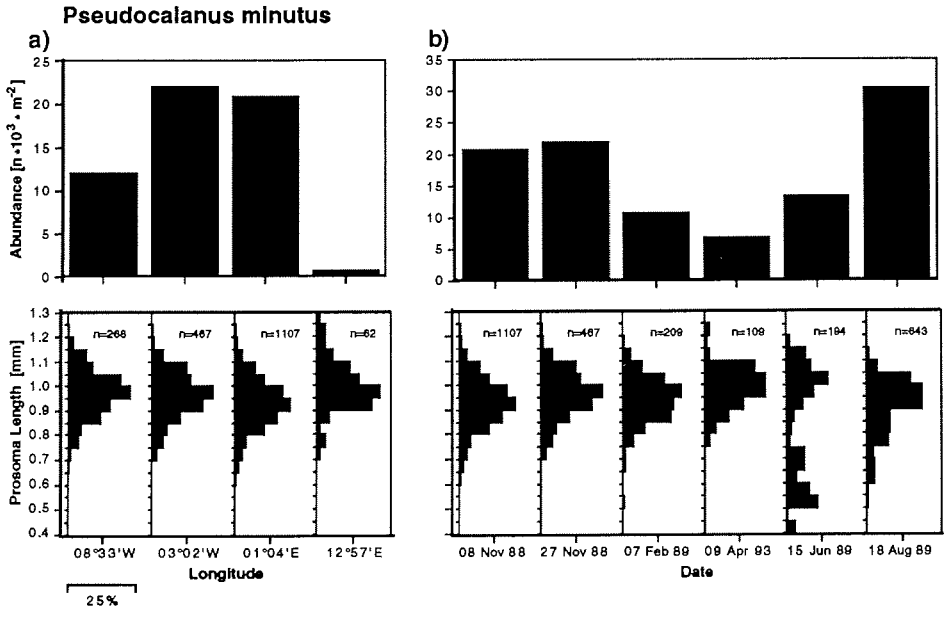

Fig. 4.31: Integrated abundance and length-frequency distribution of *Pseudocalanus minutus* along a regional transect across the Greenland Sea in November 1988 (a) and for different seasons within the Greenland Sea Gyre (b). 'n' indicates the number of specimens measured. Note the scale changes between (a) and (b) abundances.

The latter two were virtually absent two months earlier, as evidenced by the trough between the +1.0 mm and +0.7 mm modes of adult females and CIII in mid-June. The dominating early summer mode of +1.0 mm females phases out by end of the light season and the +0.95 mm mode of presumptive next generation CV copepodids becomes the dominant wintering stage.

Figures 4.32 and 4.33 show pronounced regional and seasonal differences in the vertical distribution of *Pseudocalanus minutus*. In late fall, a vertical split of the population is evident throughout the GSG. Part of the population (between 10 and 25% in terms of total numbers) gathers in the surface layer reaching high concentrations (>50 $n*m^{-3}$ at 1°E, Fig. 4.32b). However, the bulk of the population is centered around 500 m, with

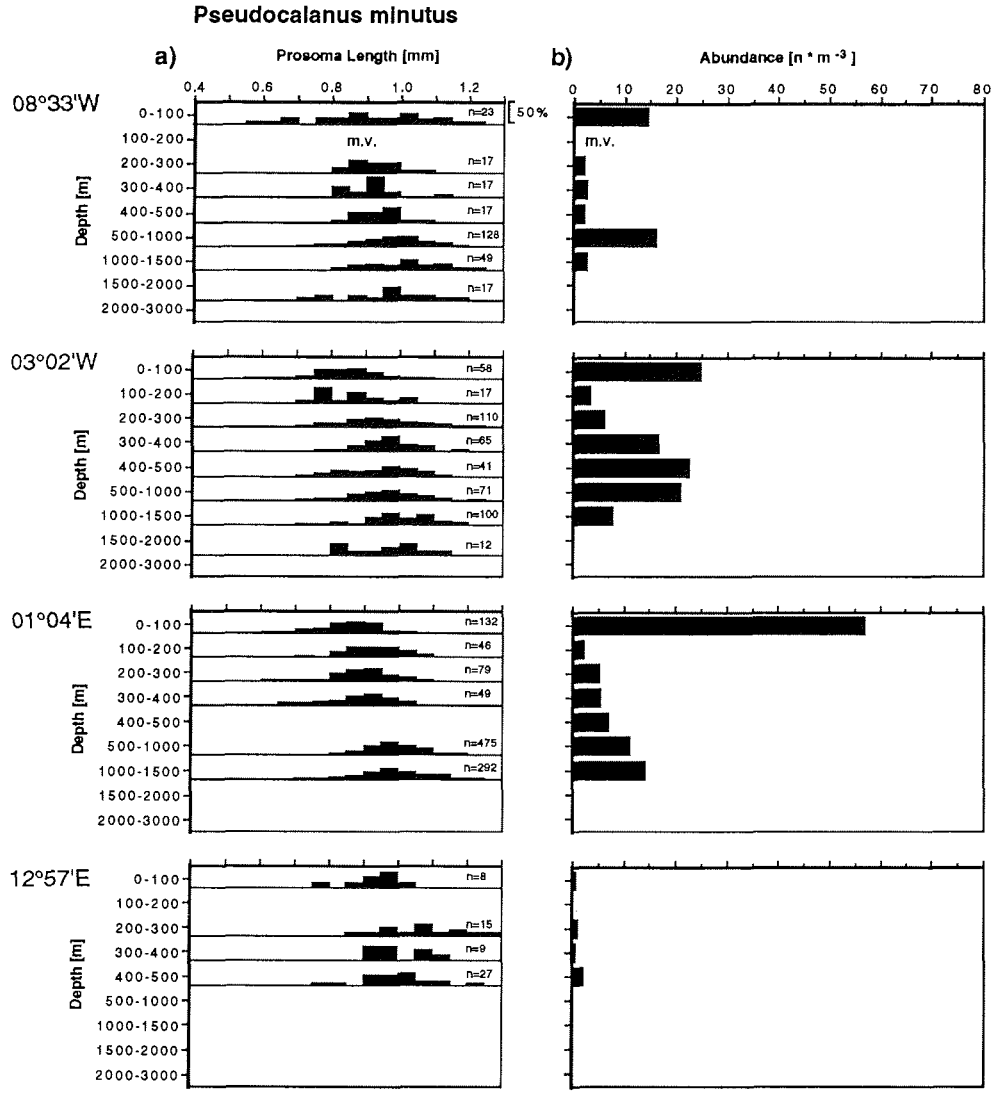

Fig. 4.32: Vertical distribution of length-frequency (a) and abundance (b) of *Pseudocalanus minutus* along a regional transect across the Greenland Sea in November 1988 (a). 'n' indicates the number of specimens measured, 'm.v.' denotes missing value.

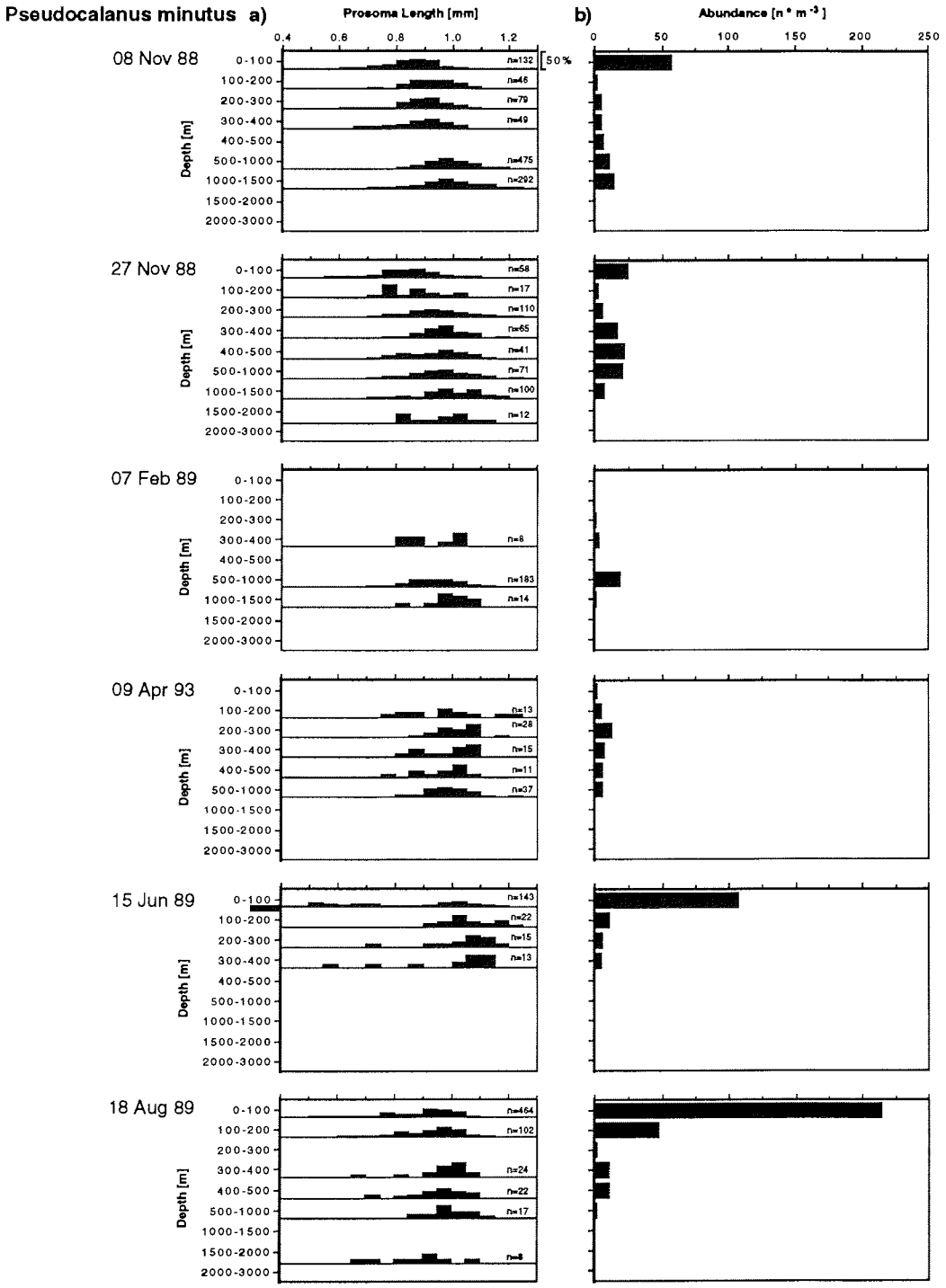

Fig. 4.33: Vertical distribution of length-frequency (a) and abundance (b) of *Pseudocalanus minutus* for different seasons in the Greenland Sea Gyre. 'n' indicates the number of specimens measured.

concentrations exceeding 10 $n*m^{-3}$. This deep part of the population is mainly composed of large animals (+0.95 mm), while the surface population encompasses a wide range of sizes, including small animals (<0.7 mm, Fig. 4.32a). These latter are absent below.

The acute and somewhat surprising surface maximum in early November disappears in the course of the dark season, and in winter almost the entire population is located between 500 and 1000 m (20 $n*m^{-3}$, Fig. 4.33b). The broad size range within this layer indicates a pronounced overlap of presumably +0.85 mm and +0.95 mm modes, while <0.7 mm animals have by that time disappeared from the scene (Fig. 4.33a).

The spring transition from a +0.95 mm to a +1.0 mm dominated population was already mentioned above (Fig. 4.31b). Figure 4.33a shows that this transition occurs between the epi- mesopelagial, for the larger mode dominates in the 200-400 m layer and the smaller +0.95 mm mode below. Microscopic examination corroborates the assumption that these are indeed different stages, i.e. adult females and CV copepodids, respectively.

The reappearance of specimens in the surface layer indicates that the spring time ascent from overwintering depths is already under way. Surface crowding and reproduction lead to a pronounced surface maximum in early summer which persists through fall, but a vanguard of >0.95 mm animals appears to be on its descent as early as August.

Interpretation

PSEUDOCALANUS MINUTUS is a cold-adapted species with highest occurrence in arctic waters. It is an annual species carrying out extensive vertical migrations, hibernating as CV at intermediate depths and rising as early as spring, thereby molting to adulthood. A single spawning peak occurs in early summer, after which the spent females die. Growth of the new generation proceeds at the surface until attaining copepodite stage CV, which leaves the surface to overwinter. This may take until late in the dark season, where growth obviously depends on heterotrophic food.

Biomass dominants (large Calanoida)

Calanus hyperboreus

In terms of biomass, *Calanus hyperboreus* is the most important species in the Greenland Sea Gyre (GSG). It is also the most abundant of the larger zooplankton (>0.1 mg mean ind. DW, Fig. 4.15).

Highest numbers of individuals are found in the center of the GSG ($18*10^3$ $n*m^{-2}$), decreasing to less than half this value at its western periphery and to only one sixth of it in the WSC (13°E, Fig. 34a). The abundance changes are also reflected in the stage distribution of the species. The dominant copepodite stage at 13°E is CIV (60% of the population) while in the center of the gyre it is CIII (>65%). The western station (08°33'W) is somewhere in between the two, with about half of the population at stage CIII, and roughly one quarter at CIV. There appears to be good overall correspondence between total abundance of the species and relative abundance of the CIII stage, indicating that CIII copepodids are the main contributors to the observed abundance changes in the Greenland Sea in late fall.

From Fig. 4.34b it is apparent that CIII is also the main overwintering stage, making up two thirds of the population during the dark season. Somewhat surprisingly, this period coincides with the seasonal abundance maximum of the species ($15*10^3$ $n*m^{-2}$). However, except for April 1993 where all stages were enumerated, sample counts for CI and CII copepodids were not available at the time of preparation of this manuscript (cf. Table 3.2), and a full account of the stage distribution of this species will be available soon (Hirche, in prep.). It is therefore almost certain that an abundance peak of young second generation animals was missed in summer 1989. This can be inferred from the changes in the stage distribution of the >CII copepodids over the seasons. CIII copepodids phase out in course of the early light season, probably molting to CIV, which is the dominant (large) stage in early summer (70%). By the end of the summer season, CIII copepodids reappear on the scene, and this is again accompanied by an abundance increase of the population to near fall values ($14*10^3$ $n*m^{-2}$). These are presumptive second generation animals which will form the bulk of the following overwintering stock, as will be discussed in chapter 5.4. CV copepodids constitute only a small fraction of the population throughout the year and especially during the dark season, where they comprise less than 5% of the investigated stock. Females are found year-round, with largest relative importance in the early light season (50%), while males occur only from November through April, in low but constant fractions. They are absent in the Atlantic domain of the Greenland Sea in late fall (13°E, Fig. 4.34a). The observed stage composition, the low incidence of (second generation) CIII in particular, and the low overall abundance of the species at the latter station, may be interpreted as evidence for an expatriate population of *C. hyperboreus* in the Atlantic domain of the Greenland Sea, dominated by (first generation) CIV copepodids.

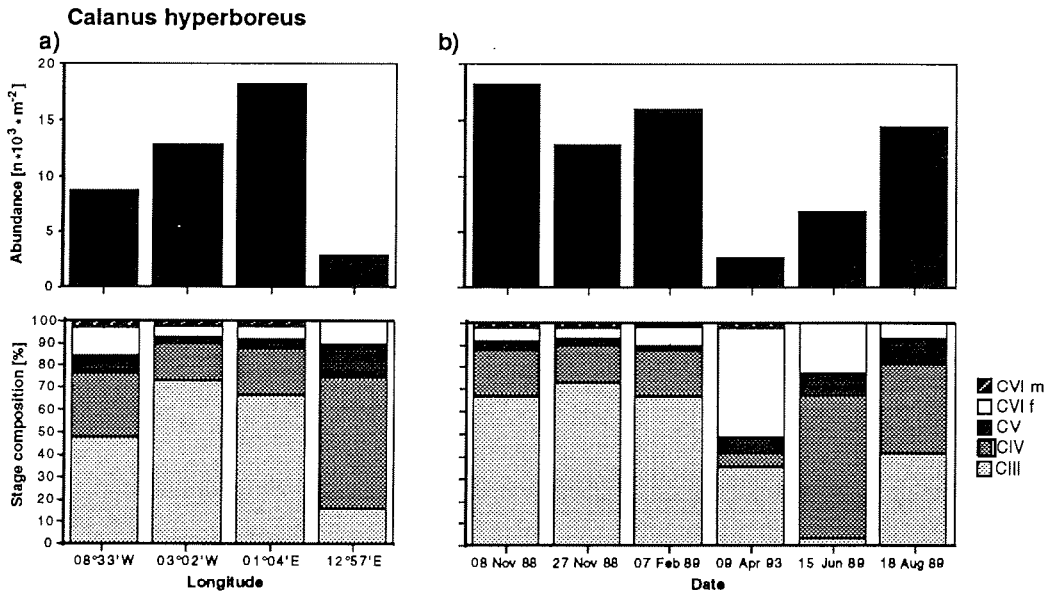

Fig. 4.34: Integrated abundance and stage composition of *Calanus hyperboreus* along a regional transect across the Greenland Sea in November 1988 (a) and for different seasons within the Greenland Sea Gyre (b). No data for CI and CII copepodids.

The vertical distribution of abundance and stage composition along the regional transect in late fall is shown in Fig. 4.35. In all instances, the bulk of the population is located in the bathypelagial, with highest concentrations in the 1000-1500 m layer. Furthermore, the younger copepodids predominate in the lower, and the older stages in the upper water column.

The resulting vertical partitioning of the water column between the stages persists through spring (Fig. 4.36a), and reverses hereafter. Thus, in late summer, there is a gradual progression from near total dominance of CIII at the surface to CIV between 500 and 1500 m and CV-CIV females below. While the dominances in the deeper layers are based on only scattered specimens, the CIII and CIV dominance peaks are paralleled by distinct

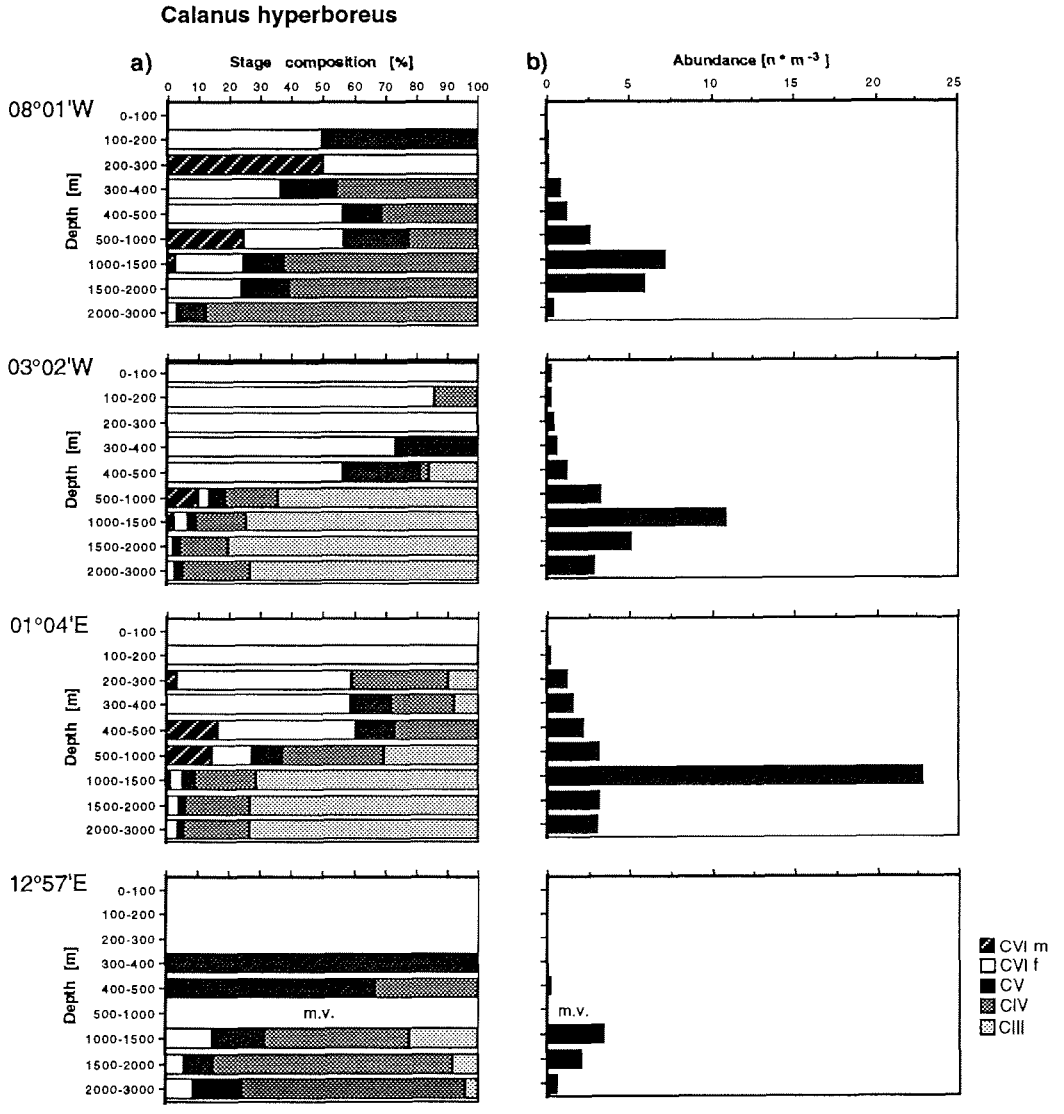

Fig. 4.35: Vertical distribution of stage composition (a) and abundance (b) of *Calanus hyperboreus* along a regional transect across the Greenland Sea in November 1988 (a). No data for CI and CII copepodids. 'm.v.' denotes missing value.

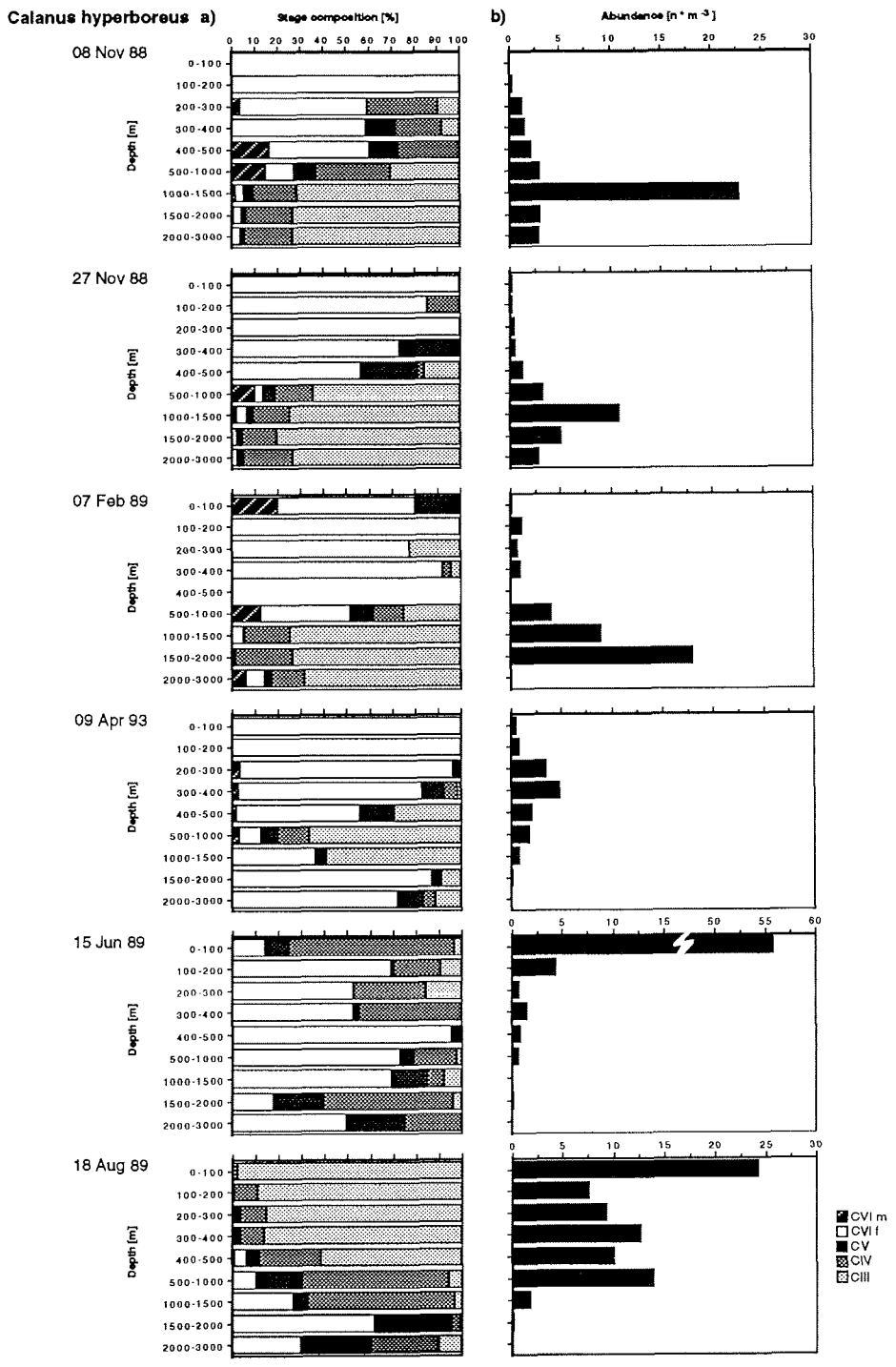

Fig. 4.36: Vertical distribution of stage composition (a) and abundance (b) of *Calanus hyperboreus* for different seasons in the Greenland Sea Gyre. No data for CI and CII copepodids. Note the scale break for 15 June 1989.

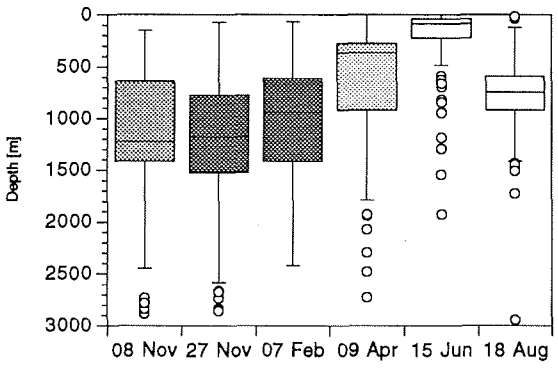

Fig. 4.37: Seasonal translocation of z_{50} depths of *Calanus hyperboreus* biomass in the Greenland Sea Gyre. These are the depths above which 50% of the biomass is distributed. Shading illustrates seasonal illumination.

abundance maxima in the respective depths (Fig. 4.36b). It is noteworthy that the intermediate CIV maximum in late summer is preceded by a pronounced surface maximum of the named stage two months earlier. The CIII maximum, by contrast, has no obvious precursor, reinforcing the earlier postulation of high CI and CII occurrences in the early summer surface layer.

The period of maximum surface concentrations of *C. hyperboreus* is brief, and the bulk of the population is located in the subsurface for most of the year. The vertical range of the abundance maxima over the year is considerable, reaching down to 2000 m by the end of the dark season (Fig. 4.36b). In terms of biomass, it is somewhat reduced and the z_{50} depths extend from 100 m in summer to 1200 m in late fall (Fig. 4.37).

The vertical and temporal distribution of eggs and nauplii was investigated from winter through early summer, i.e. during and after the period of co-occurrence of adult male and female *Calanus hyperboreus* (Figs. 4.38 and 4.39). There is only little likelihood of confusion with the early life stages of other copepods, since these are smaller [cf. review of Marshall and Orr (1972)] and occur later in the year (e.g. Conover 1988). The observed large-sized (>0.4 mm) eggs and nauplii were not identified.

Approximately equal numbers of eggs are found in February and April ($11*10^3$ $n*m^{-2}$, Fig. 4.38). There are, however, differences in the size and vertical distribution of the eggs (Figs. 4.38, 4.39b). Winter eggs are larger (+0.175 mm modal length[6]) and concentrate in the surface layer, while the smaller eggs observed in spring 1993 (+0.15 mm) tend to be more dispersed, featuring an only slight abundance maximum at 200-300 m just above the spring abundance maximum of adult female *C. hyperboreus* (Fig. 4.36). No vertical differences in egg size are discernible (Fig. 4.39a).

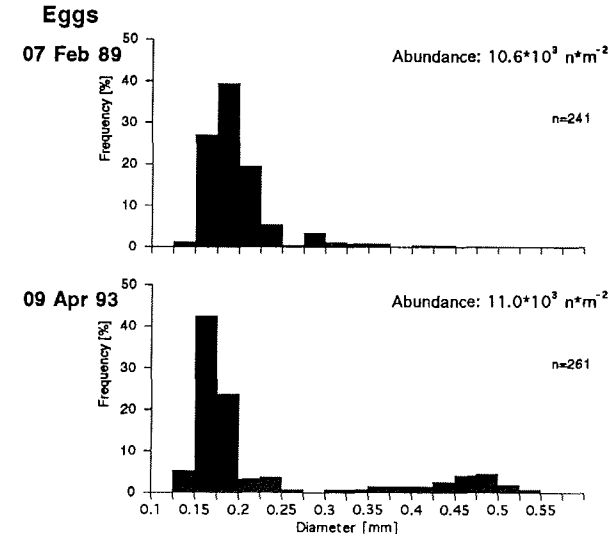

Fig. 4.38: Integrated abundance and length-frequency distribution of copepod eggs for February 89 and April 93 in the Greenland Sea Gyre (b). 'n' indicates the number of specimens measured.

The nauplii, by contrast, increase in both, numbers and size, while the vertical distribution pattern of abundance remains essentially the same throughout the observation period (Figs. 4.40 and 4.41b) Naupliar numbers increase almost five-fold from winter through early summer

[6] + denotes the left bin edge of a 0.025 mm size class

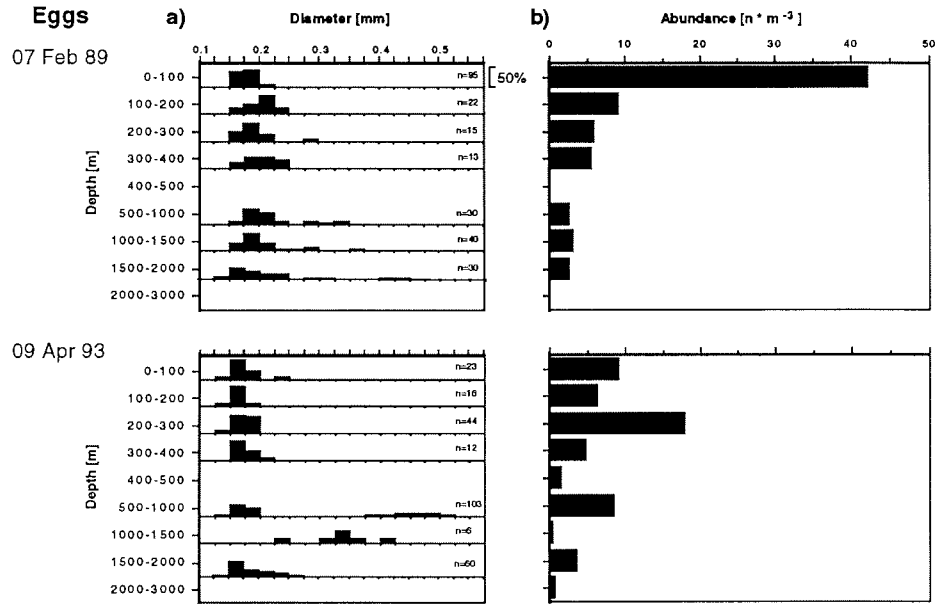

Fig. 4.39: Vertical distribution of length-frequency (a) and abundance (b) of copepod eggs in February 1989 and April 1993 in the the Greenland Sea Gyre. 'n' indicates the number of specimens measured.

($55*10^3$ $n*m^{-2}$) and crowd into the surface layer. During the same period the size distribution of the main mode changes from right-skewed to left-skewed, and the modal sizes increase from +0.20 to +0.325 mm (Fig. 4.40). The distribution plots for separate depth intervals compound the earlier notion of a bimodal length distribution of nauplii in February (Fig. 4.41a). This feature is most apparent in the upper part of the water column between 100 and 400 m, where modes at +0.20 mm and +0.30 mm are clearly separated. This size difference, however, progressively narrows as one moves deeper into the meso- and bathypelagial, and both modes eventually lose their identity, converging into a unimodal distribution centered around +0.275 mm. The winterly abundance maximum at the surface is almost exclusively composed of small nauplii.

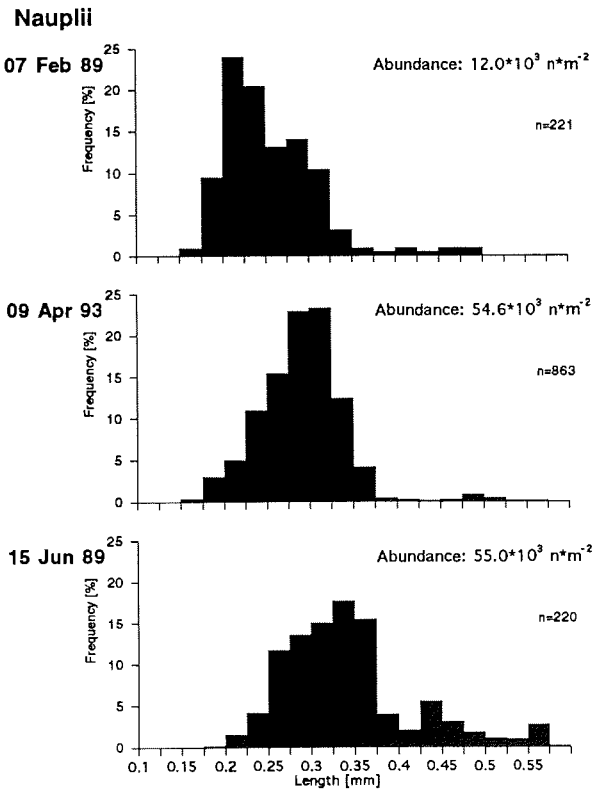

Fig. 4.40: Integrated abundance and length-frequency distribution of copepod nauplii in the Greenland Sea Gyre. 'n' indicates the number of specimens measured.

A different situation is encountered in spring, where the largest animals are found in the surface layer (+0.30 mm mode). Modal lengths decrease almost continuously down to the lower mesopelagial (+0.225 mm). Below 1000 m, the modal length is an invariable +0.275 mm, i.e. the same as two months earlier.

The summerly length-distribution is highly surface-biassed (Fig. 4.41b) and characterized by a high degree of scatter in the deeper layers. The observed seasonal and vertical differences in egg and naupliar sizes and numbers will be later discussed with respect to Conover's 'developmental ascent' hypothesis for *Calanus hyperboreus* (Conover et al. 1991, Conover and Huntley 1991).

Interpretation

CALANUS HYPERBOREUS takes (at least) two years to complete its development in the Greenland Sea Gyre. It overwinters as copepodite stage CIII during the first year and (probably) CV during the second. These molt to adulthood in the course of winter where spawning occurs in the absence of food. Spent females survive through summer, few of which apparently survive a third winter.

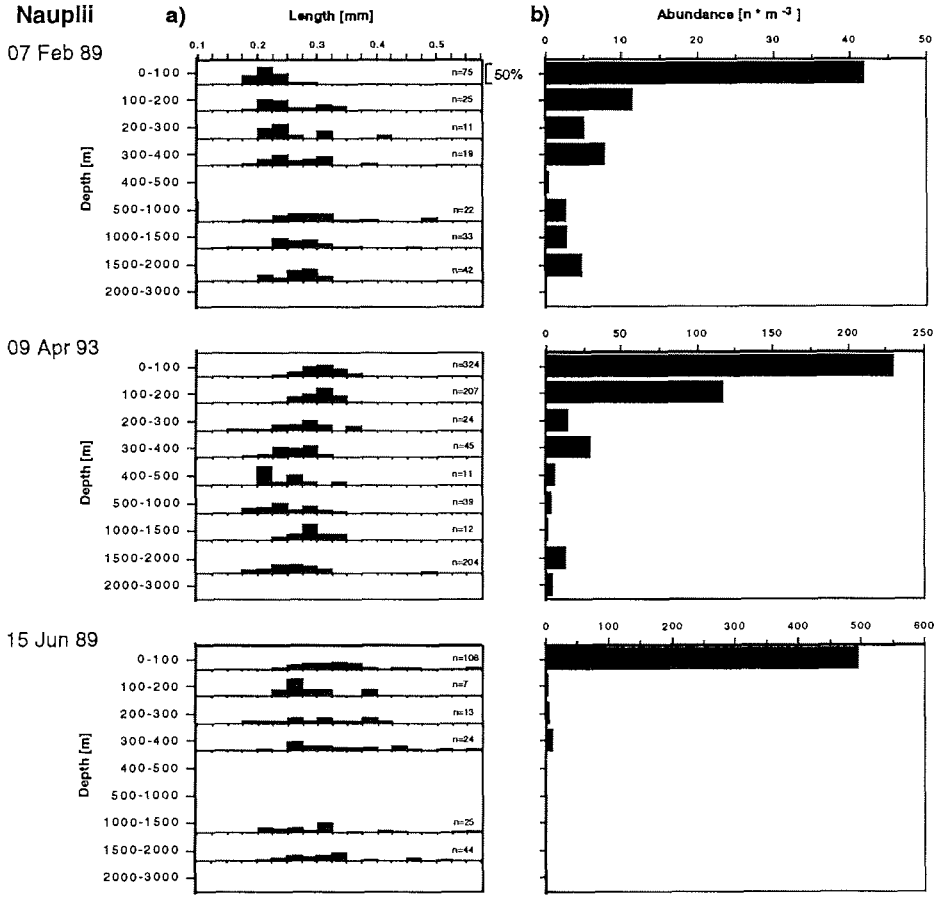

Fig. 4.41: Vertical distribution of length-frequency (a) and abundance (b) of copepod nauplii in the Greenland Sea Gyre. 'n' indicates the number of specimens measured.

Calanus finmarchicus

Calanus finmarchicus is the second important copepod species in the Greenland Sea, in terms of biomass. It was found to be of overriding abundance and biomass in the Atlantic domain of the WSC.

The high regional variability in *C. finmarchicus* occurrence, which is apparent in late fall, contrasts with a remarkably uniform stage distribution along the transect (Fig. 4.42a). A single dominance shift occurs between the westernmost station (60% CIV) and the other arctic stations, whereas virtually no differences are noticeable between the latter two and the WSC station.

The CV stage prevails in the GSG in late fall (60%) and also during the rest of the year (Fig. 4.42b), only surpassed by CIV during spring. Abundances vary rather erratically around $2.5*10^3$ $n*m^{-2}$, but again, this is spurious, for CI and CII stages are wanting (cf. Table 3.2). Adult males appear in spring and vanish in course of the light season, never amounting to more than 5% of the population.

The vertical distribution of abundance and stage composition on the regional transect is shown in Fig. 4.43. The vertical distribution patterns are similar for all the gyre stations (08°33'W through 01°04'E). The population is rather evenly distributed over the upper 2000 m, with only moderate abundance maxima in the lower epipelagial (100-300 m, Fig.

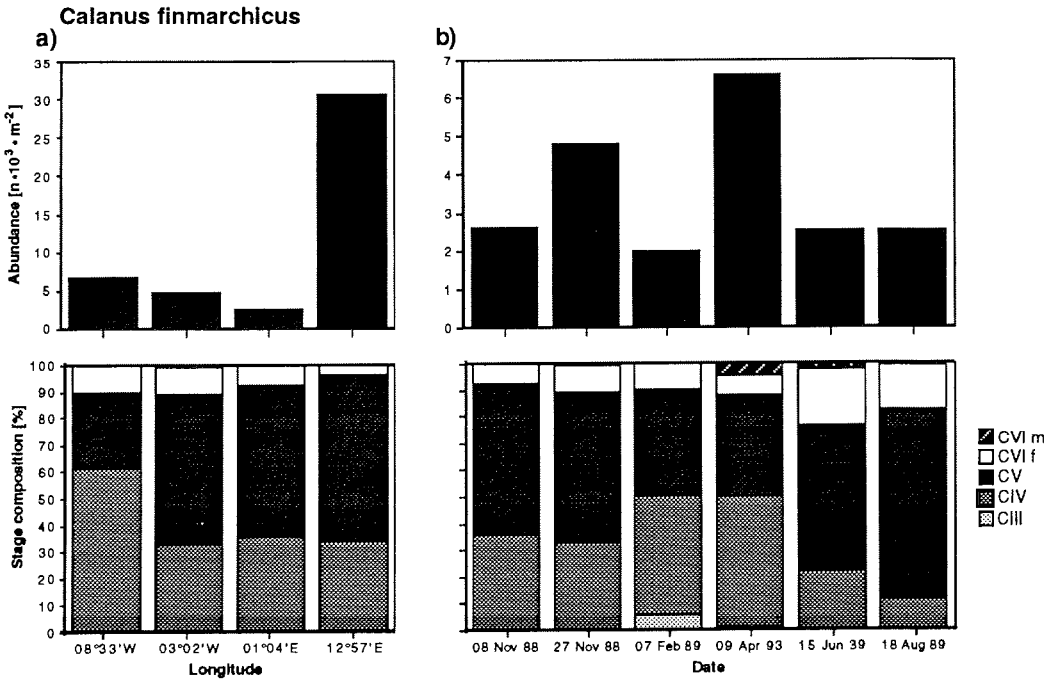

Fig. 4.42: Integrated abundance and stage composition of *Calanus finmarchicus* along a regional transect across the Greenland Sea in November 1988 (a) and for different seasons within the Greenland Sea Gyre (b). No data for CI and CII copepodids.

4.43b). The WSC population, by contrast, is concentrated in the mesopelagial, displaying a pronounced maximum around 500 m.

The stage distribution is characterized by a vertical segregation of adult females, CV, and CIV copepodids from the surface to intermediate depths (Fig. 4.43a). The apparent increase of CV below is based on only few specimens.

The stage distribution pattern persists through winter, and (probably) reverses afterwards (e.g. 18 August, Fig. 4.44a), although this again is based on only few deeper dwelling

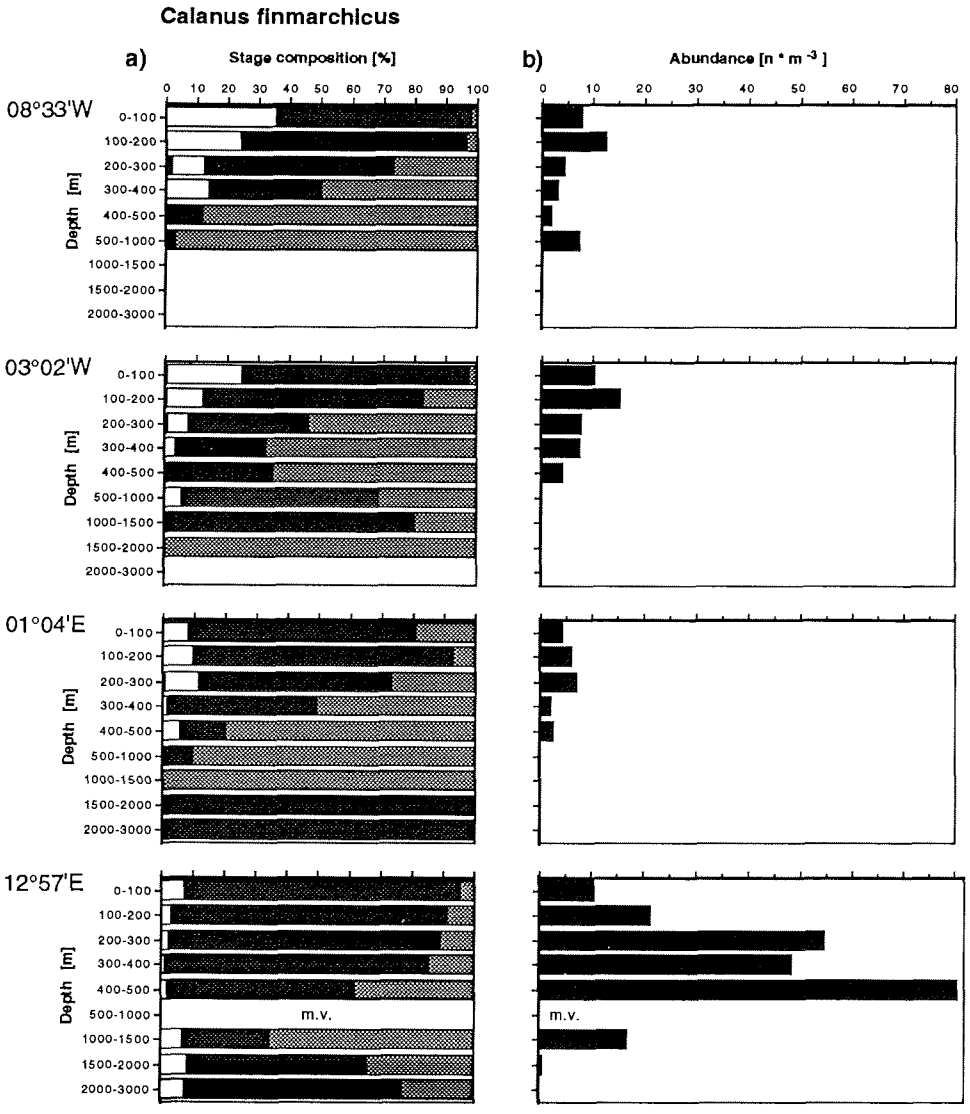

Fig. 4.43: Vertical distribution of stage composition (a) and abundance (b) of *Calanus finmarchicus* along a regional transect across the Greenland Sea in November 1988 (a). No data for CI and CII copepodids. 'm.v.' denotes missing value.

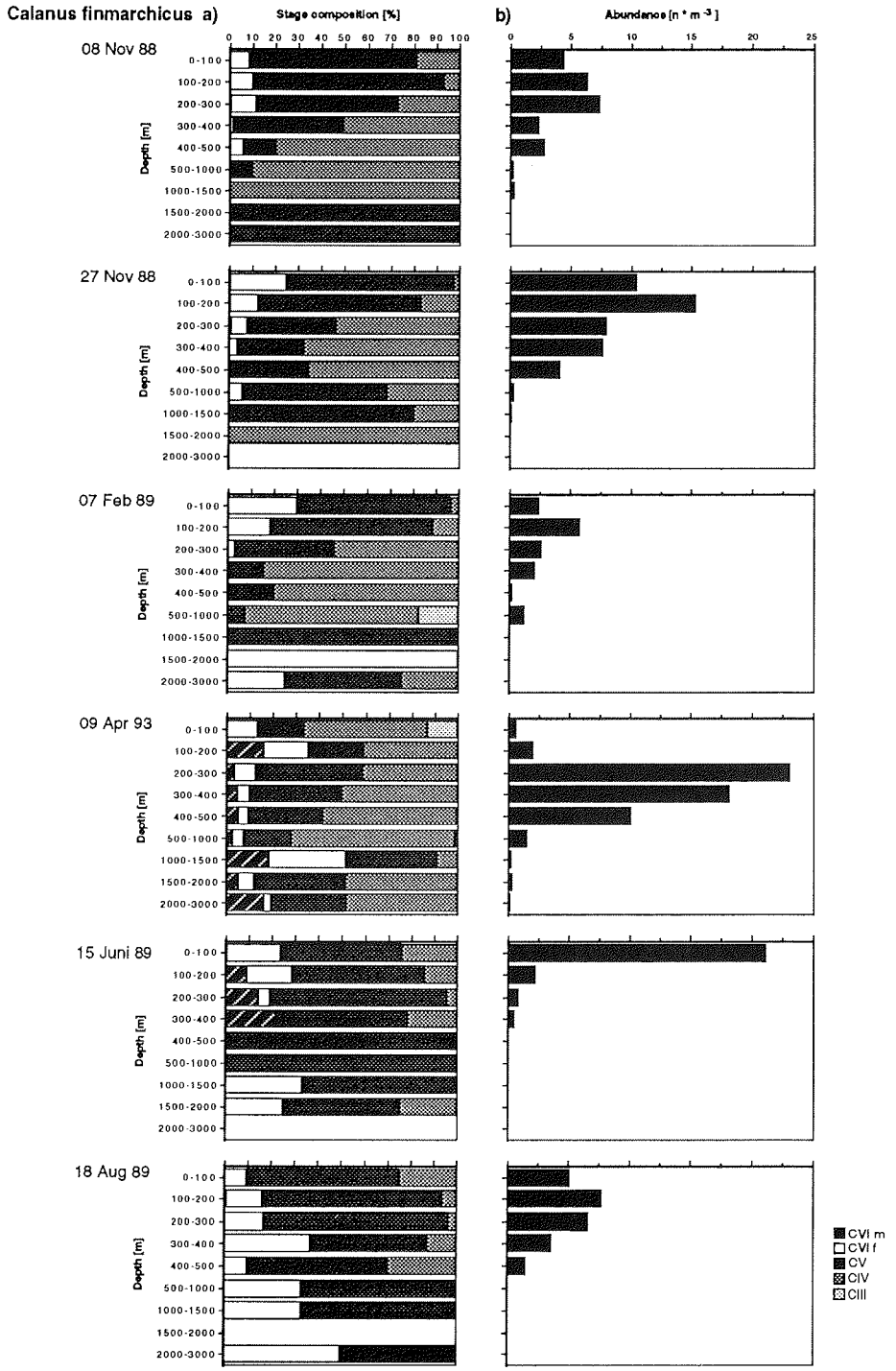

Fig. 4.44: Vertical distribution of stage composition (a) and abundance (b) of *Calanus finmarchicus* for different seasons in the Greenland Sea Gyre. No data for CI and CII copepodids.

specimens. The abundance maximum is shallow (Fig. 4.44b), as compared to *C. hyperboreus*. It never exceeds 300 m in the GSG, while in the WSC it was shown to be deeper. A surface maximum, however, appears only briefly in early summer and the late summer distribution is not any different from the ones encountered during the rest of the year.

Metridia longa

Metridia longa is the third important copepod species in the Greenland Sea, in terms of biomass (Table 4.2). Only the temporal variations in numbers and stage distributions will be considered here, as the species is currently investigated by Scherzinger (1994, in prep.). The present data base for *M. longa* is punctured by the absence of sample counts for copepodite stages ≤CIII in winter and summer of 1989. However, reliable sample counts of all stages are available for the GSG in late fall 1988 (Scherzinger, in prep.) and spring 1993 (this study). From these stations, it is evident that young copepodids occur remarkably late in the year, for more than half of the fall population consists of CIII copepodids or younger (Fig. 4.45). Development continues through winter, as evidenced by the waxing and waning of successive copepodite stages, leading to a summer population of CV and adults. It can only be speculated upon the timing of the new generation, but from the incidence of CI and CII in late fall, recruitment of youngest copepodids probably takes place during the late summer period.

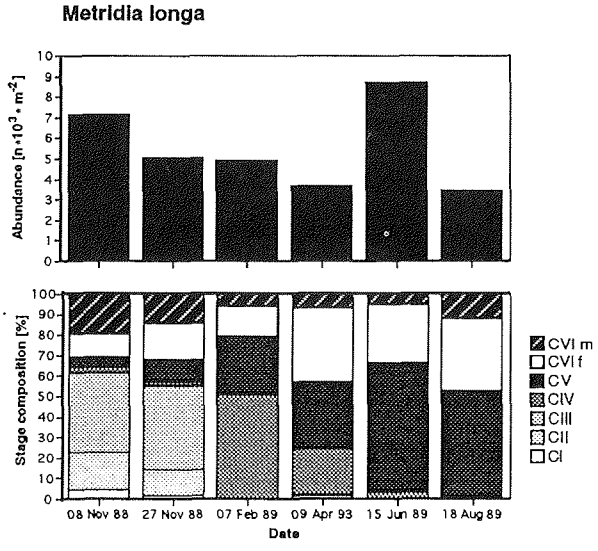

Fig. 4.45: Integrated abundance and stage composition of *Metridia longa* along a regional transect across the Greenland Sea in November 1988 (a) and for different seasons within the Greenland Sea Gyre (b). No data for CI-CIII copepodids in February, June and August.

Males occur throughout the year and may constitute as much as 20% of the population during the dark season.

Abundance values vary two-fold between early and late summer, but no seasonally recurring pattern is evident.

The seasonal variations in the vertical distribution of *M. longa* abundance and stage composition are shown in Fig. 4.46. Maximum concentrations are always in the subsurface, shallower in winter (100-200 m) and deeper in early summer (400-500 m, Fig. 4.46b). No pattern is obvious for the stage distribution, and there is only a slight tendency of adult females to occur above the maximum of males (Fig. 4.46a).

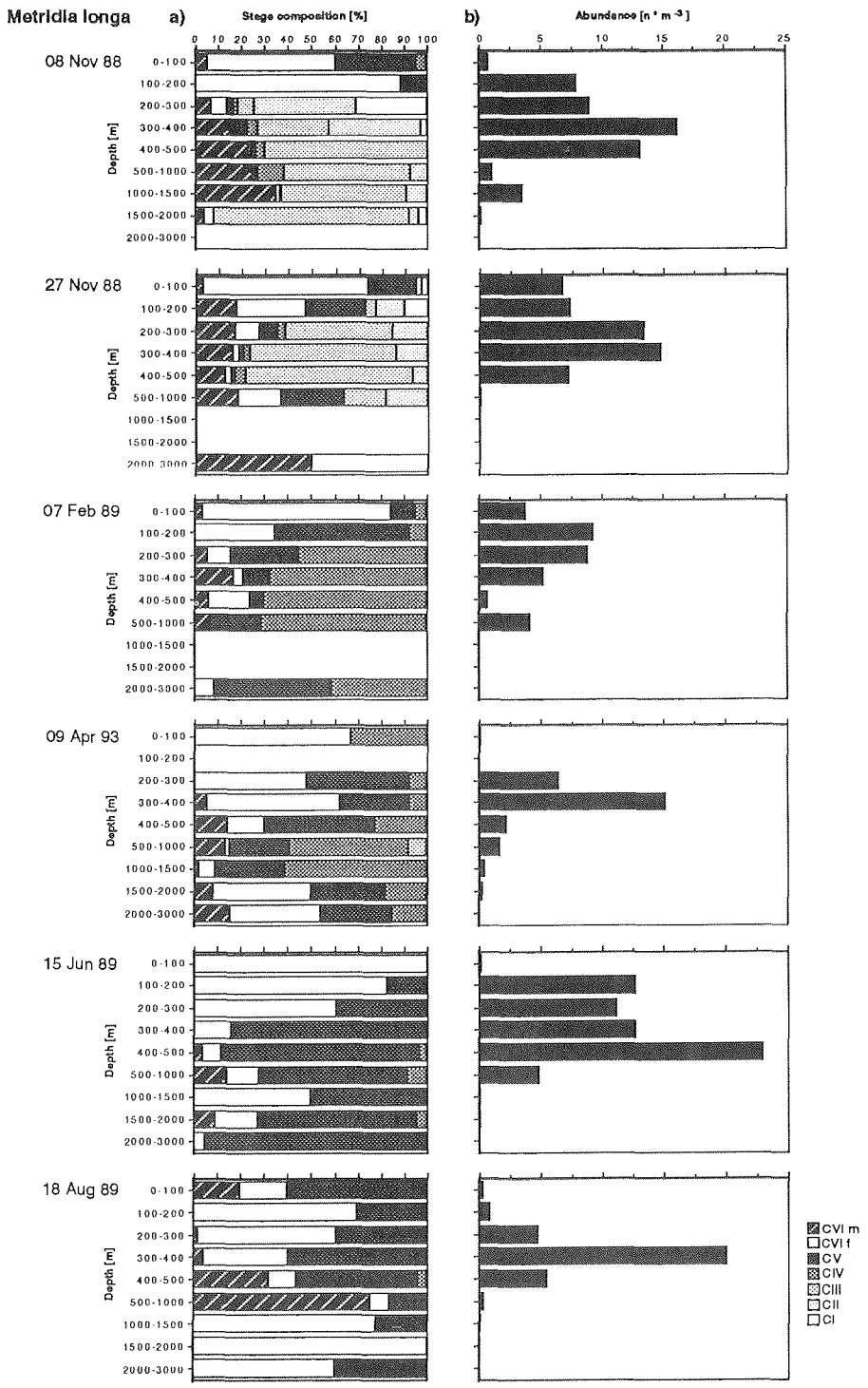

Fig. 4.46: Vertical distribution of stage composition (a) and abundance (b) of *Metridia longa* for different seasons in the Greenland Sea Gyre. No data for CI-CIII copepodids in February, June and August.

Meso- and bathypelagic Copepoda (Aetideidae)

In contrast to the taxa in the foregoing chapters, which, on a wide spatio-temporal scale, are all distributed over a wide depth range, the members of the copepod family Aetideidae have a more restricted vertical distribution. This was already visible in the 'Mumm-plot' (Fig. 4.18) and suggested by the MDS species plot (Fig. 4.24).

All species occur in fairly low numbers and constant portions throughout the investigation (Fig. 4.47). *Gaidius tenuispinus* dominates to the east of the Arctic Front (40%), while to the west there is only slight, if any, dominance of *Aetideopsis multiserrata* (about 30%, Fig. 4.47a). However, there is a greater proportion of the larger *A. rostrata* in spring and roughly the same number of *G. brevispinus* in late November (Fig. 4.47b). The smaller *Chiridius obtusifrons* is only poorly represented in the Greenland Sea, both seasonally and regionally, but seems to gain greater importance in the GSG in summer (>20%).

Aetideidae dwell in the deeper layers of the Greenland Sea, mainly below 300 m, and down to greatest depths. They are only occasionally caught in the epipelagial (Figs. 4.48b and 4.49b). The average concentration throughout the range is about 0.5 $n*m^{-3}$, but more or less acute abundance maxima of three times the average may occur, both regionally (13°E, Fig. 4.48b) and seasonally (April and August, Fig. 4.49b).

The vertical species distribution resembles a multi-layered pie, regardless of longitude or season, reflecting a vertical partitioning of the water column between the species (Figs.

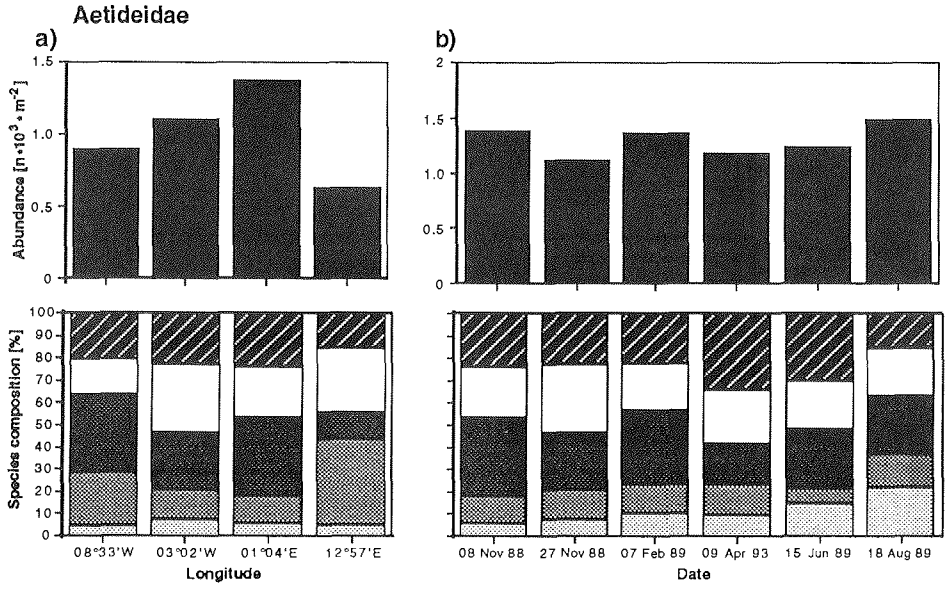

Fig. 4.47: Integrated abundance and species composition of Aetideidae along a regional transect across the Greenland Sea in November 1988 (a) and for different seasons within the Greenland Sea Gyre (b).

4.48a, 4.49a). *Chiridius obtusifrons* and *Gaidius tenuispinus* dominate in the upper mesopelagial, *Aetideopsis multiserrata* in the lower mesopelagial/upper bathypelagial, and *Gaidius brevispinus* and in particular *Aetideopsis rostrata* in the deeper bathypelagial. Considerable overlap between the species' depths ranges, however, occurs and in many

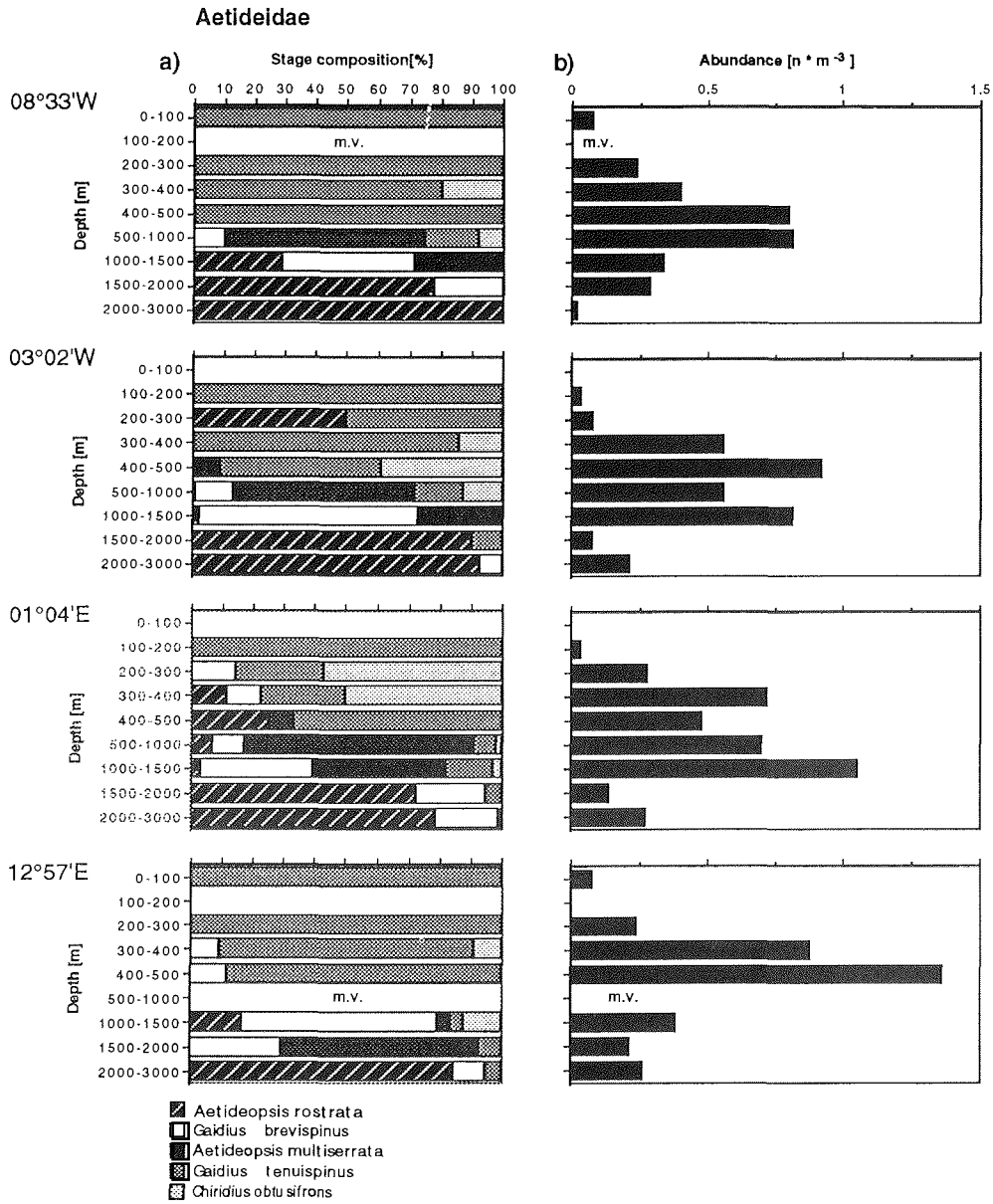

Fig. 4.48: Vertical distribution of species composition (a) and abundance (b) of Aetideidae along a regional transect across the Greenland Sea in November 1988 (a). 'm.v.' denotes missing value.

instances these layers of maximum co-occurrence coincide with the abundance maximum (1°E, Fig. 4.48; February, June, August, Fig. 4.49), but this is not always the case (e.g. 13°E, Fig. 4.48).

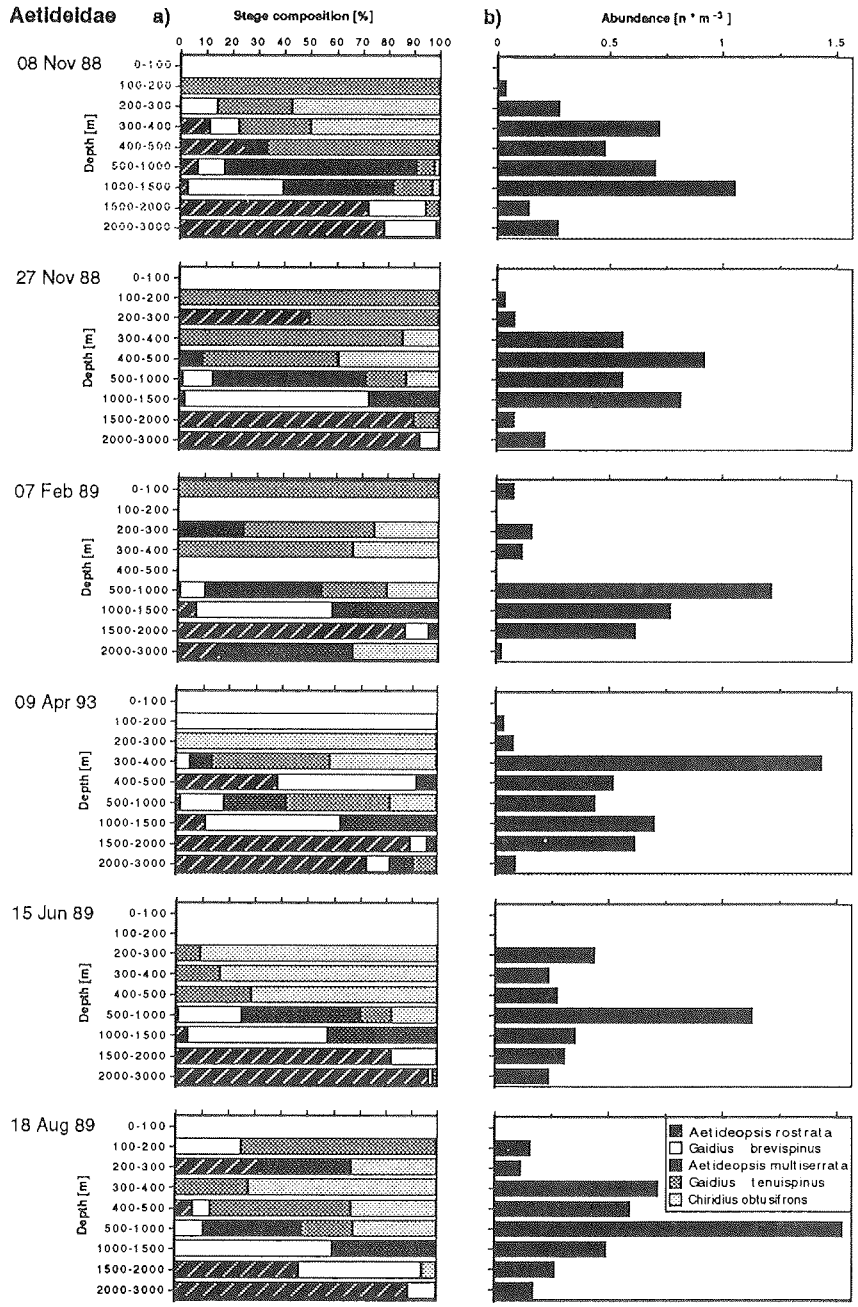

Fig. 4.49: Vertical distribution of species composition (a) and abundance (b) of Aetideidae for different seasons in the Greenland Sea Gyre.

Vertical partitioning of the water column also occurs intraspecifically, as illustrated by *C. obtusifrons*. Younger stages, where present, tend to occur below the older copepodids and adult females. This is especially evident in summer (Fig. 4.50).

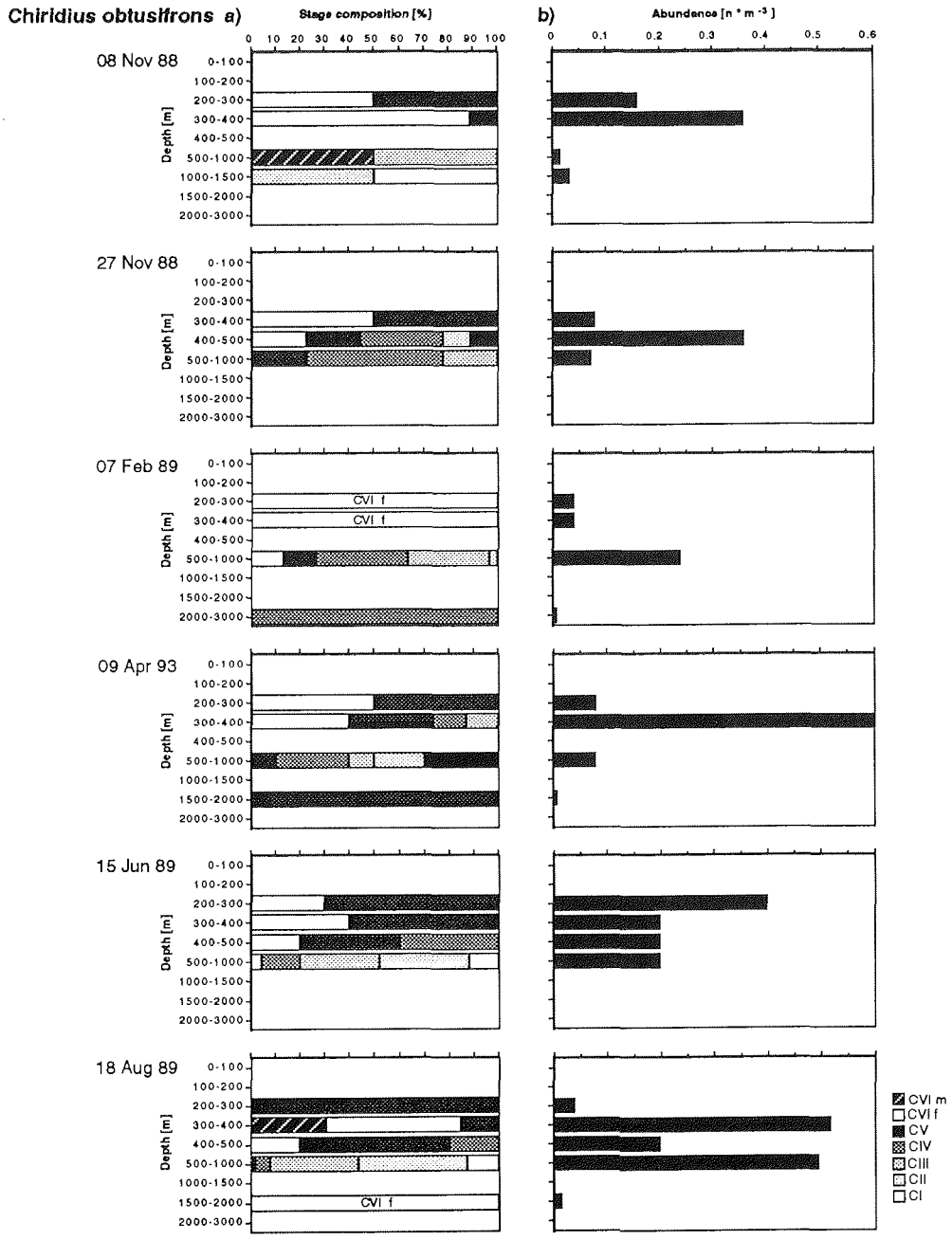

Fig. 4.50: Vertical distribution of stage composition (a) and abundance (b) of *Chiridius obtusifrons* for different seasons in the Greenland Sea Gyre.

Other important biomass contributors (Chaetognatha, Ostracoda)

Eukrohnia sp.

The chaetognath *Eukrohnia* sp. is second to *Calanus hyperboreus*, in terms of biomass, while it ranks only ninth in terms of abundance (Table 4.2).

Probably two species of *Eukrohnia* occur in the Greenland Sea, *E. hamata* and *E. bathypelagica*. While the differentiating morphological criteria still raise some doubts among taxomomists, separation of immatures is virtually impossible on a routine basis (Kapp and Hagen, pers. comm.). Probably the most trenchant differentiating criterion is the ratio of tail length to total length (Alvariño 1962). While her Fig. 22 shows two clearly separated linear regressions of tail to total length for both species, the Greenland Sea specimens follow the *E. hamata* regression line, but there is a high degree of variance for the larger animals (Fig. 4.51). A similar observation was reported by Dawson (1968) for the Arctic Ocean.

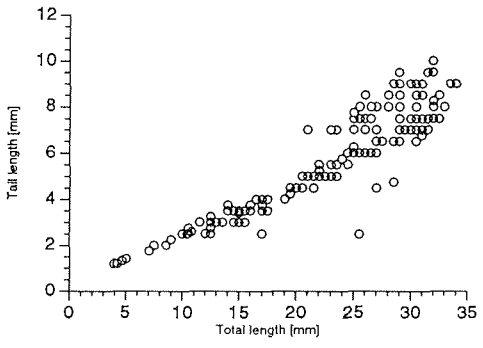

Fig. 4.51: Tail length versus total length of *Eukrohnia* sp. in the Greenland Sea Gyre, pooled data for 27 November 1988 and 15 June 1989.

Regional and seasonal differences in *Eukrohnia* abundance and size distribution over the entire water column are shown in

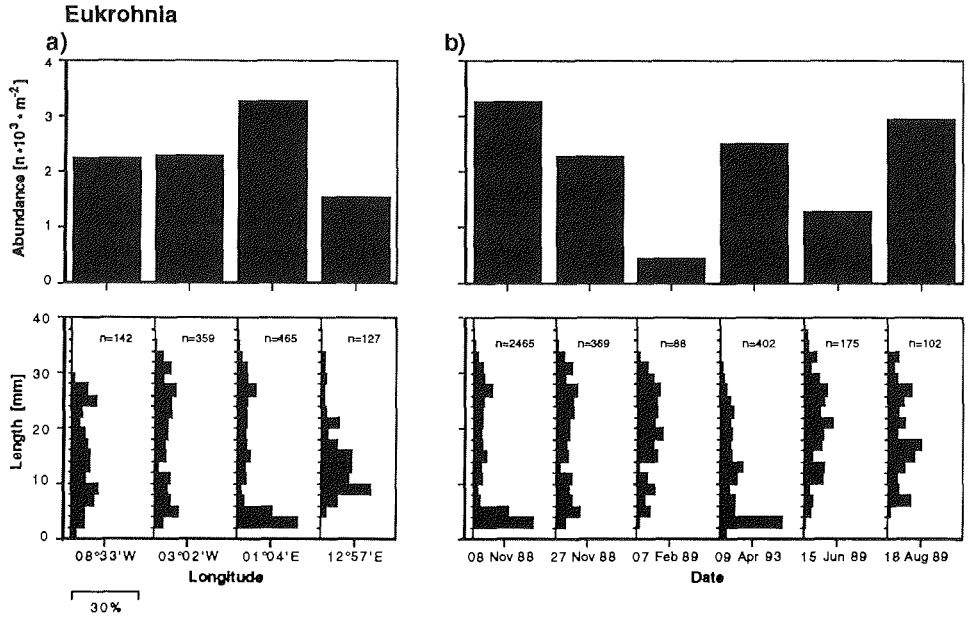

Fig. 4.52: Integrated abundance and length-frequency distribution of *Eukrohnia* sp. along a regional transect across the Greenland Sea in November 1988 (a) and for different seasons within the Greenland Sea Gyre (b). 'n' indicates the number of specimens measured.

Fig. 4.52. Abundances range from $1.5*10^3$ to $3.3*10^3$ $n*m^{-2}$ on a regional scale, and the regional maximum at 1°04'E is clearly associated with a conspicuous peak of 3 mm[7] specimens in the size distribution (Fig. 4.52a). No such feature is present at the other stations of the transect, which show quite dissimilar size distribution patterns. In fact, the only recurring feature is a 26 mm mode at stations 3°W and 1°E in the center of the Greenland Sea Gyre. The size distributions are generally very broad, spanning the entire length range up to 38 mm, indicating the presence of two or probably more overlapping modes.

The seasonal distribution of abundances in the GSG shows a five-fold decline of chaetognath numbers from fall 1988 through winter 1989 (Fig. 4.52b). This decline

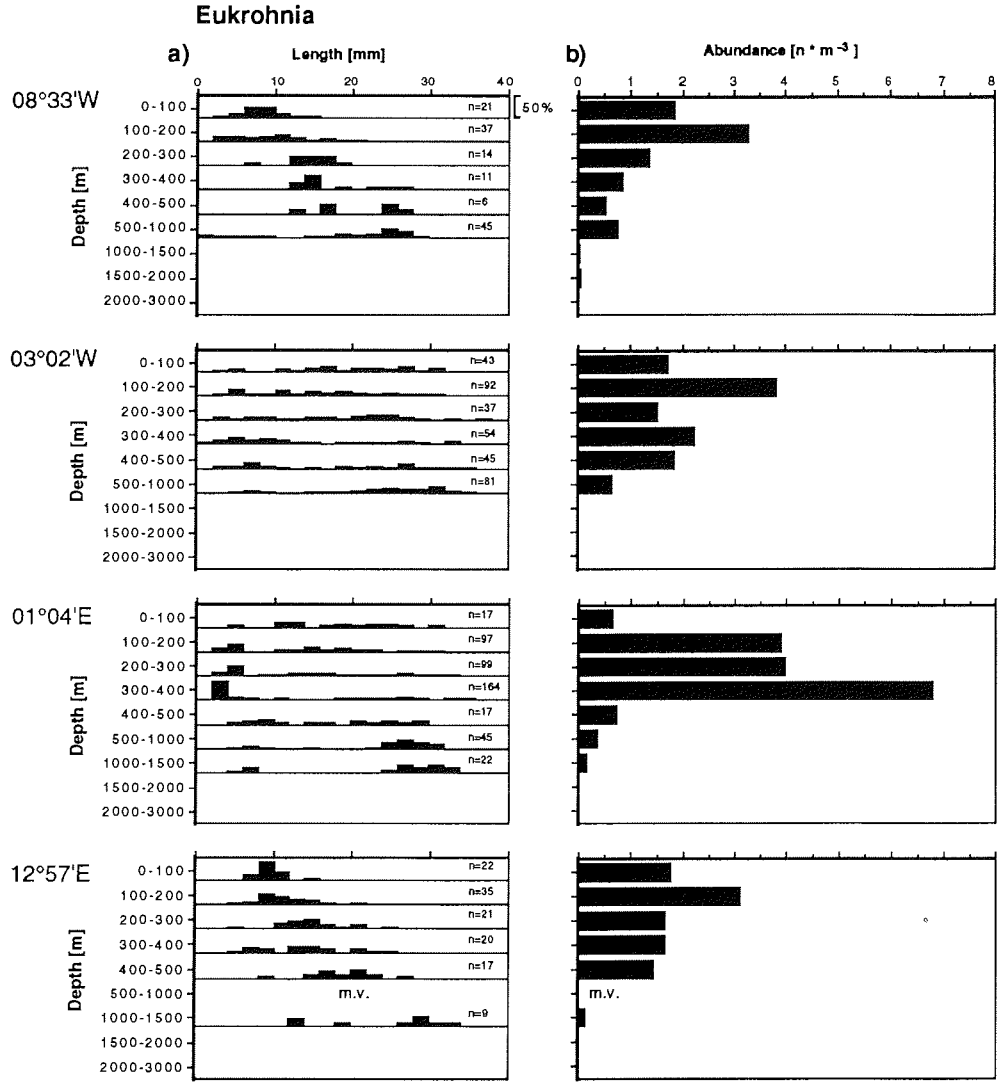

Fig. 4.53: Vertical distribution of length-frequency (a) and abundance (b) of *Eukrohnia* sp. along a regional transect across the Greenland Sea in November 1988 (a). 'n' indicates the number of specimens measured, 'm.v.' denotes missing value.

[7] center value of a 2 mm size class

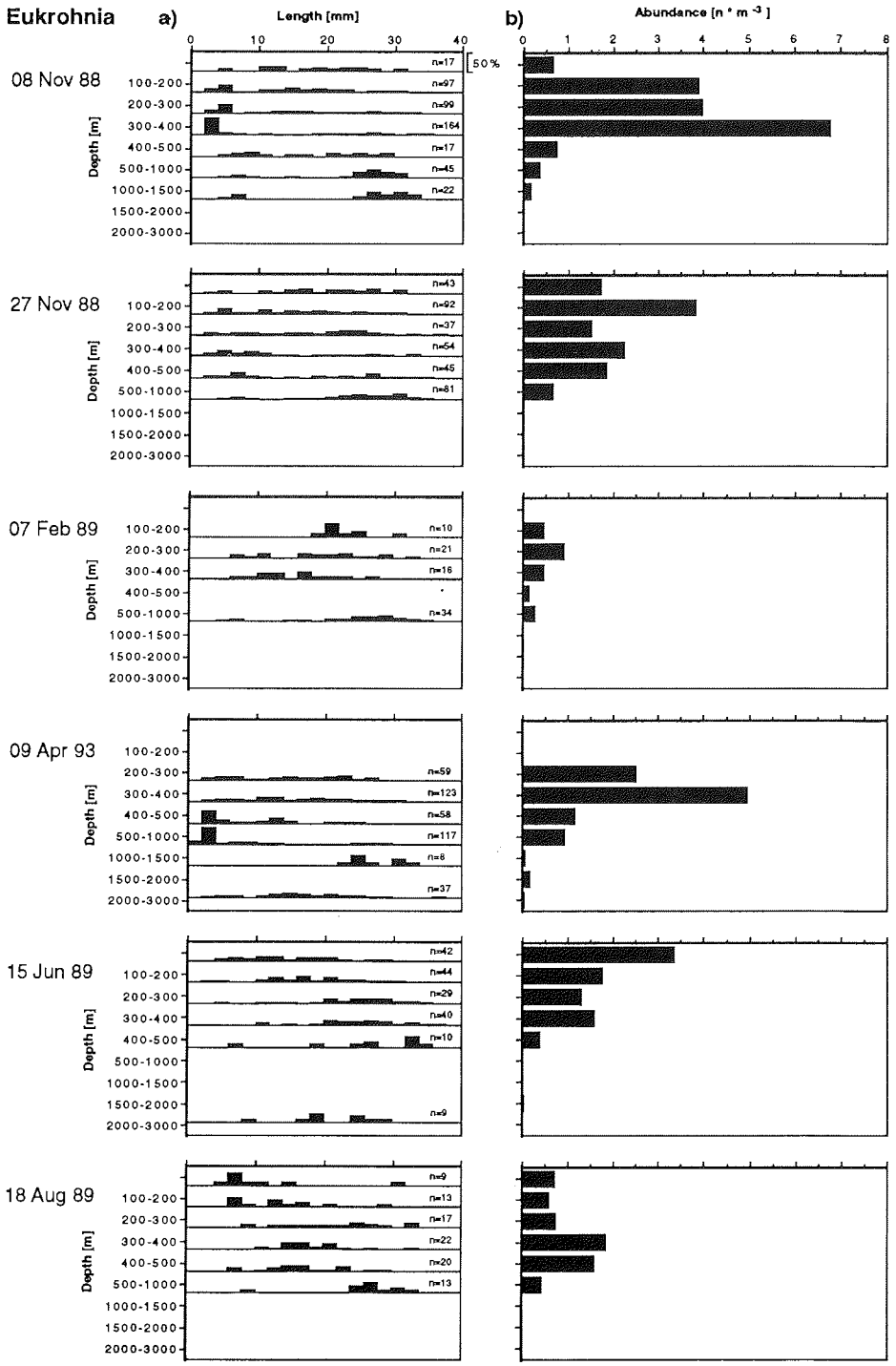

Fig. 4.54: Vertical distribution of length-frequency (a) and abundance (b) of *Eukrohnia* sp. for different seasons in the Greenland Sea Gyre. 'n' indicates the number of specimens measured.

is accompanied by a reduction of the smaller size classes. Spring 1993 shows again high abundances and high frequencies of 3 mm animals. In fact, this pattern is very similar to the one encountered in early November 1988. While the early summer decline to about $1*10^3$ $n*m^{-2}$ can be again explained with lower frequencies at the lower size end, the late summer increase to again fall levels of $>2*10^3$ $n*m^{-2}$ is not paralleled by the appearance of young.

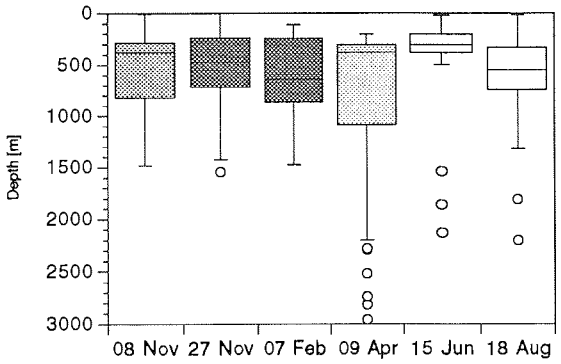

Fig. 4.55: Seasonal translocation of z_{50} depths of *Eukrohnia* sp. biomass in the Greenland Sea Gyre. These are the depths above which 50% of the biomass is distributed. Shading illustrates seasonal illumination.

The vertical distribution of *Eukrohnia* along the transect shows fairly high concentrations throughout the upper 1000 m (Fig. 4.53b). A subsurface abundance peak of about 3.5 $n*m^{-3}$ recurs in the 100-200 m layer, but at 1°04'E a pronounced maximum (7 $n*m^{-3}$) is located some 200 m deeper. This latter is composed almost exclusively of small 3 mm animals while the former is due to a number of different size classes (Fig. 4.53a). Both center stations show no conspicuous vertical trends with respect to size as individuals of widely different sizes occur at any one depth. By contrast, at both ends of the transect, a gradual increase of size with depth is evident, with 9 mm animals dominating in the surface layer, and >25 mm animals in the deep sea. With this pattern in mind, the putatively random distribution of sizes over depth at the center stations can be re-interpreted as the result of two superposing patterns: while the larger >8 mm classes seem to comply with the described size increase with depth, the smaller <8 mm classes appear to distribute invariantly with depth (cf. 1°04'E).

This view is supported by the temporal sequence of vertical distribution patterns in the GSG (Fig. 4.54a). April closely resembles early November 1988 with a pronounced 3 mm mode at intermediate depths. As this mode phases out in the course of the light season, the vertical size segregation of the population becomes evident.

The abundance maximum is located in the subsurface for most of the year, except in early summer, where it is found in the surface layer (Fig. 4.54b). The seasonal translocation of biomass is only moderate, and the median depth fluctuates between 300 and 650 m (Fig. 4.55).

Boroecia borealis

The ostracod *Boroecia borealis* is an important biomass component in both, the arctic and Atlantic domain of the Greenland Sea, ranking among the top three and four species, both seasonally and regionally (Table 4.2).

The zonal transect carried out in late fall shows uniformly high numbers of individuals at the gyre stations ($2.5*10^3$ $n*m^{-2}$, Fig. 4.56a). East of the Arctic Front, only about half

these numbers are found. These quantitative differences are accompanied by qualitative changes in the size distribution of the species, which is remarkably uniform within the gyre and quite different at 13°E. The former stations show almost identical length-frequency distributions, characterized by two pronounced modes at 2.3 mm[8] and 3.3 mm carapace length, while the latter displays a broad size distribution with four modes of more or less equal strength.

The lower-sized modes at 13°E are already detectable in the size distribution of the neighboring station, and the 1.7 mm mode may in fact be traced all the way back to 8°33'W.

There appears to be a gradual increase in relative frequencies of small animals as one moves eastwards across the Greenland Sea in late fall.

The seasonal development of ostracod numbers and sizes is shown in Fig. 4.56b. Low numbers of individuals occur during the dark season, and high numbers during the light season, with about six-fold differences between the February minimum and the June maximum ($6*10^3$ $n*m^{-2}$).

The size distribution is polymodal and reveals five recurrent modes throughout the investigation period, most conspicuous in early summer. These modes are located at 3.3, 2.3, 1.5, 1.1 and between 0.7 and 0.5 mm, respectively. It will be shown later, that the latter are actually two separate modes (at 0.7 and 0.5 mm, respectively), so that a total of six modes are identified. These modal classes are virtually identical to the ones found by Haberstroh (1985) in the Fram Strait. Following her terminology, they will be termed VIII, VII, VI, V, IV and III, respectively (cf. chapter 5.4), as they very likely represent the

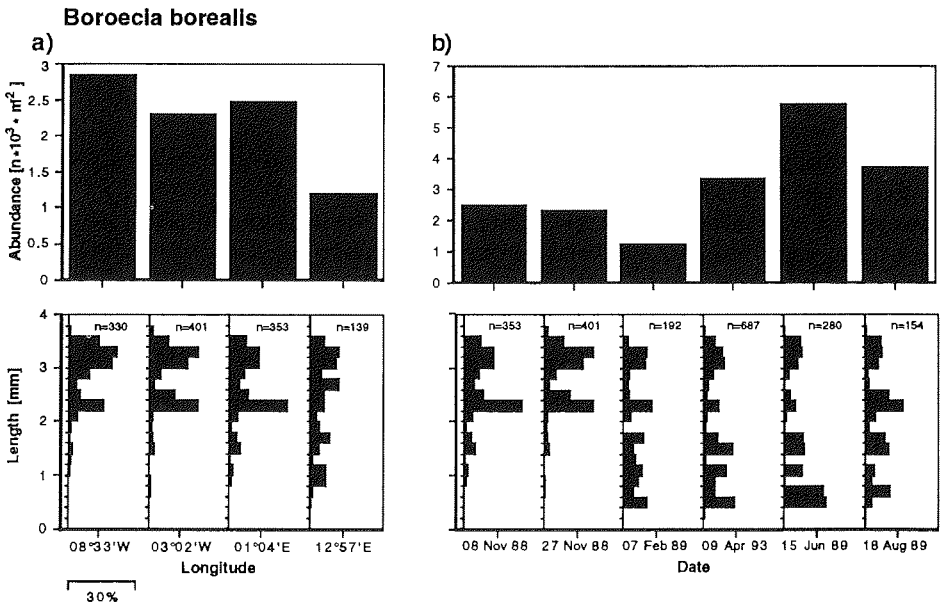

Fig. 4.56: Integrated abundance and length-frequency distribution of *Boroecia borealis* along a regional transect across the Greenland Sea in November 1988 (a) and for different seasons within the Greenland Sea Gyre (b). 'n' indicates the number of specimens measured. Note the scale difference between (a) and (b) abundances.

[8] center value of a 0.2 mm size class

corresponding ostracod stages. However, the identity of the two was not ascertained in this study.

Small individuals appear as early as February and become dominant by early summer, when the III and IV modes alone account for almost 40% of the population. The III/IV peak thus coincides with the seasonal abundance maximum of the species in June. By the end of summer, only few III remain (<5%), and IV specimens amount to less than half their early summer values. Only scattered specimens persist through fall. Large-sized animals dominate in November. The prominent VII mode, which makes up 40% of the population in late fall gradually thins out through early summer (<10%). The broader VIII mode, which comprises about half of the population in fall, remains at a relatively

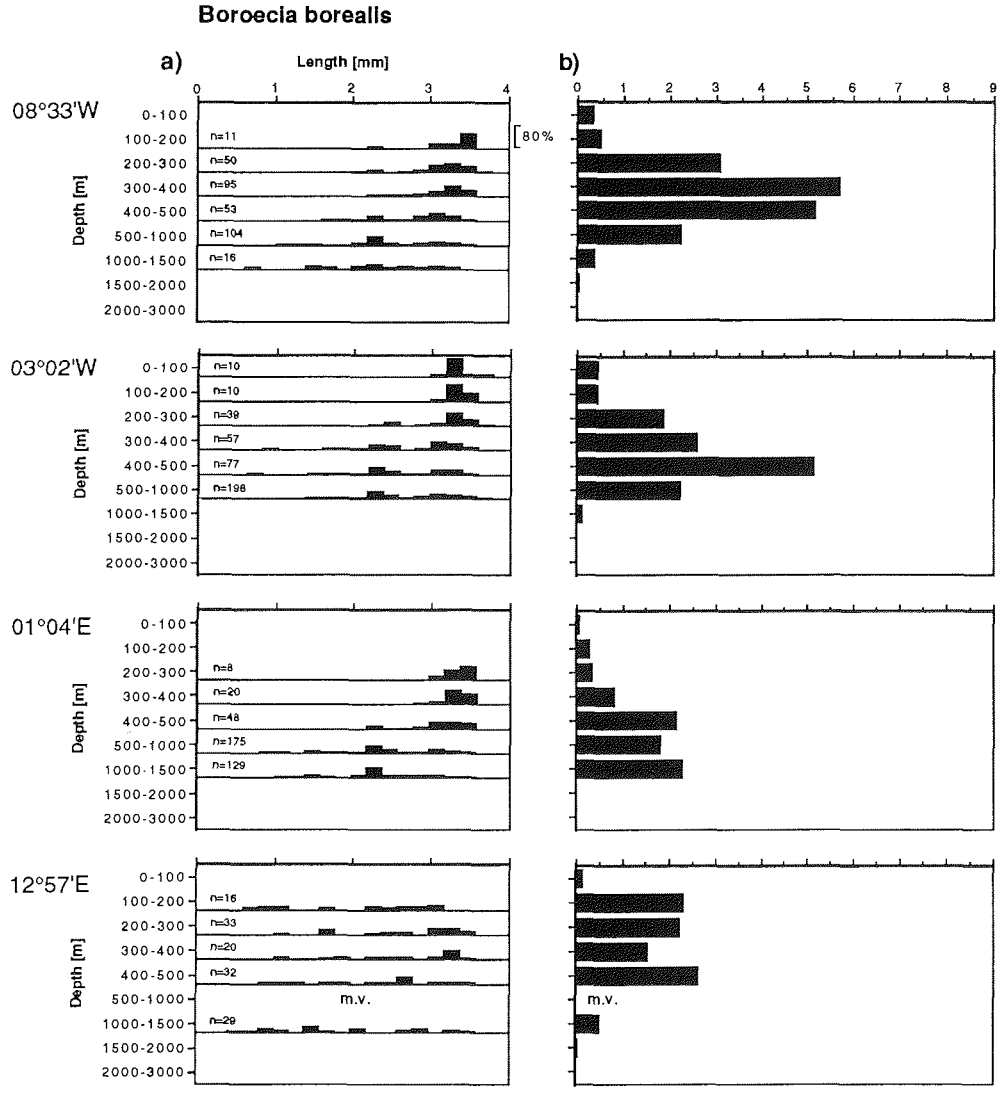

Fig. 4.57: Vertical distribution of length-frequency (a) and abundance (b) of *Boroecia borealis* along a regional transect across the Greenland Sea in November 1988 (a). 'n' indicates the number of specimens measured, 'm.v.' denotes missing value.

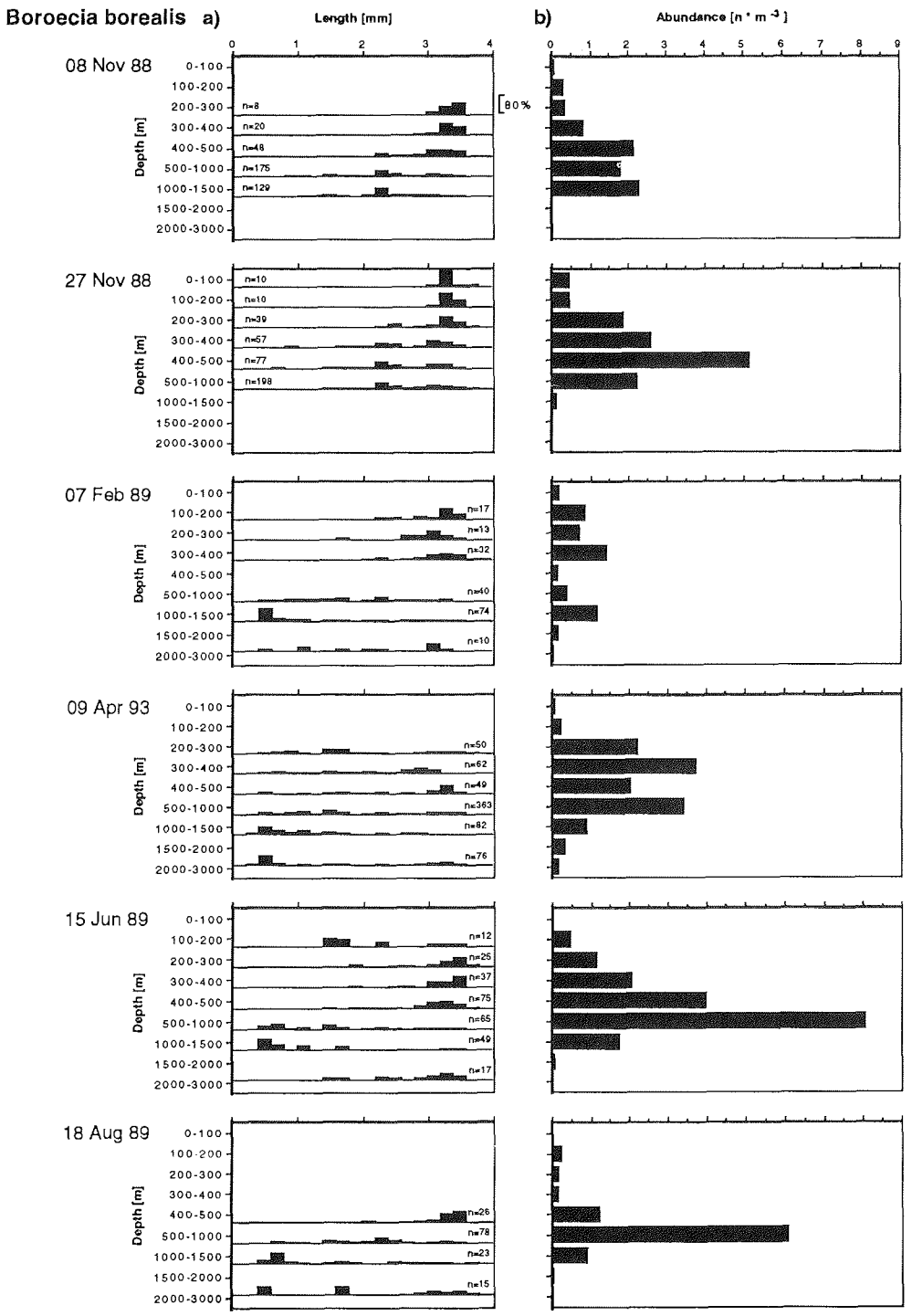

Fig. 4.58: Vertical distribution of length-frequency (a) and abundance (b) of *Boroecia borealis* for different seasons in the Greenland Sea Gyre. 'n' indicates the number of specimens measured.

constant 20-25% during the rest of the year. Likewise, the VI mode, barely visible in fall, remains at a relatively constant 15%, whereas V appears to be thinning from winter (>10%) through late summer (>5%).

The vertical distribution of *Boroecia borealis*, in terms of abundance and size, shows some interesting features in space and time (Figs. 4.57 and 4.58).

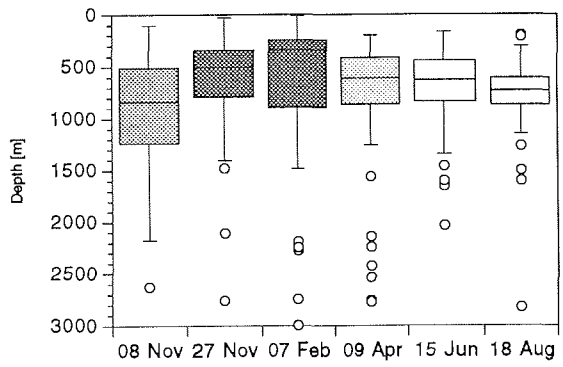

Fig. 4.59: Seasonal translocation of z_{50} depths of *Boroecia borealis* biomass in the Greenland Sea Gyre. These are the depths above which 50% of the biomass is distributed. Shading illustrates seasonal illumination.

Along the regional transect in late fall, high concentrations (>2 $n*m^{-3}$) are found over a wide depth range, i.e. between 100 m (13°E) and 1500 m (1°E) (Fig. 4.57b). Conspicuous maxima occur west of the prime meridian between 300 and 500 m (>5 $n*m^{-3}$). No such feature is apparent to the east, where two smaller peaks are present.

The size distribution is clearly surface-biassed in the GSG, for the upper water column is devoid of small individuals and almost exclusively inhabited by mode VIII specimens (Fig. 4.57a). Smaller size classes appear in the deeper layers leading to a gradual transition towards a broader size distribution with increasing depth. The distribution at 13°E is markedly different, displaying a fairly homogeneous length distribution over the entire depth range.

The temporal sequence of the abundance and size distributions in the GSG shows an apparent rise of the population from below 1000 m to above 400 m between fall and winter, and a concomitant appearance of a second deep maximum in February (Fig. 4.58b). This latter is composed of small mode III specimens, while the former is dominated by the VIII class (Fig. 4.58a). The shallow abundance maximum fades away in course of the light season, while the deep maximum shifts upwards into the lower mesopelagial and becomes the dominant feature in summer. Mode III animals remain in the 1000-1500 m layer through summer, while the larger size classes prevail above. This biassed distribution pattern is most prominent during the dark season and only barely visible in spring.

The seasonal displacement of biomass covers a 400 m range, in terms of z_{50} depths (Fig. 4.59). It follows the above described winter rise with shallowest depths attained by February (400 m) and deepens in course of the light season, reaching maximum depths in early November. The translocation of biomass is thus reverse to the one observed for *Calanus hyperboreus*. It is, however, less pronounced and never extends into either epi- or bathypelagial.

5 Discussion

5.1 Methodical constraints

This chapter discusses methodical problems of data acquisition, processing and presentation.

Sampling design and equipment

One of the key questions associated with any spatio-temporal investigation of plankton distribution is 'how representative are point samples in space and time?' This boils down to one of the central issues of plankton ecology, namely the one of 'patchiness', i.e. the natural horizontal, vertical and temporal variability in plankton distribution (e.g. Steele 1978). Obviously, this issue is difficult to address in the absence of replicate samples, and its effect on the present study can only be inferred from literature.

Horizontal variability is high in hydrographically dynamic areas, such as coastal or upwelling regions, where lateral advection may introduce considerable population changes in both, zooplankton stock size (Blackburn 1979) and composition (Smith et al. 1981). In the central Greenland Sea, however, lateral advection is weak over a large area: mean horizontal current velocities during 1988/89 were in the order of <1 $cm*s^{-1}$ (Visbeck 1993) and 40-hour-averaged current velocities never exceeded 20 $cm*s^{-1}$ (Schott et al. 1993). It can therefore be assumed that physically induced horizontal patchiness is not a great problem in the low advective régime of the Greenland Sea Gyre (GSG). However, horizontal variability is expected to be high in the Greenland Sea periphery, due to the higher current velocities of the boundary currents, the billowing of fronts, and the generation of eddies (e.g. Johannessen et al. 1987).

Usually, vertical variability in plankton (as in physical parameters) is considered to be higher than horizontal and in the open ocean the most important cause of patchiness is the thermocline (Hamner 1988). In the GSG vertical temperature gradients are small (<1°C over the entire water column, Quadfasel and Meincke 1987) and a shallow thermocline develops only in summer. Vertical stratification is weak and wintertime mixing may homogenize the water column down to more than 1000 m (Rudels et al. 1989). The low vertical stability in the GSG is thus not conducive to patch formation and winter mixing will, on the contrary, rather tend to randomize the plankton within the mixed layer.

The occurrence of diel vertical migrations (DVM) may seriously jeopardize the interpretation of the observed distribution patterns. However, DVMs are considered to be of only minor importance in the Arctic (Longhurst 1976, Longhurst et al. 1989) and may be entirely suppressed during continuous daylight (Bogorov 1946). However, moored Acoustic Doppler Current Profilers (ADCP) revealed intense DVMs of backscattering particles under conditions of alternating day and night in the Greenland Sea (Fischer and Visbeck 1993). Peak migration velocities were around 1.5 $cm*s^{-1}$ and covered a ~300 m depth range. Judging by the size selectivity of the ADCPs with an optimum response

around 1 cm the authors point at the euphausiid *Thysanoessa longicaudata* as a likely candidate for these migrations. This species was present in the Multinet samples, albeit in low numbers. Due to its potential net avoidance, it was probably not quantitatively caught (Mumm 1991). *Calanus hyperboreus* as another potential candidate was never shown to perform DVMs (Kosobokova 1978, Longhurst et al. 1984) and it is therefore unlikely that it did so in the GSG.

Temporal variability is high on a seasonal scale, in both a qualitative and a quantitative sense, as high latitude populations are tightly geared to the seasonal production cycle (e.g. Heinrich 1962). The pulsed availability of food results in a largely synchronous development and long generation times, dampening out smaller and larger scale temporal variability. Given that seasonality is the driving factor in high latitude systems (Nemoto and Harrison 1981) it was assumed that interannual variability is *comparatively* small. This was the rationale for including the 1993 spring data in the 1988/89 sequence. However, a system never turns twice in exactly the same way (Margalef 1989), and interannual variability is likely to have introduced an unknown amount of bias.

In addition to the natural variability of zooplankton, there are drawbacks due to the many factors involved in sampling (e.g. UNESCO 1979). However, this sampling variability is probably inferior to the natural variability (about 5%, Cushing 1962). The sampling error associated with the Kiel Multinet has been thoroughly discussed by Mumm (1991) and Kurbjeweit (1993).

Of special concern to the present study is the systematical error induced by mesh selection and avoidance. Hopkins et al. (1993) found striking discrepancies between 30 l bottle samples and 162 µm plummet net catches for <1 mm zooplankton in the Antarctic. Although the same genera were dominant in both, the bottle and net catches, nauplii, cyclopoid and small calanoid copepod species were severely underestimated in the net catches by up to three orders of magnitude! Conversely, large and motile plankton are most likely to be undersampled by the Multinet, due to the relatively small mouth area (0.25 m^2) and the towing bridles in front of the net. Mumm (1991) believes that chaetognaths and large crustaceans (euphausiids, amphipods and large carnivorous copepods) escape the net, but gives no estimate. Obviously, no single net can quantitatively sample the entire size spectrum (e.g. Clutter and Anraku 1979) and the shortcomings of a given net are to some extent compensated by the large number of investigations carried out with the same net type (for Multinet: e.g. Haberstroh 1985, Diel 1991, Hirche et al. 1991, Mumm 1991, Kurbjeweit 1993, Metz 1993, Morales 1993) and mesh size (150 µm: e.g. Alshuth 1989, Hirche 1991, Düsterloh 1994, Scherzinger 1994).

The next question concerns the spacing of samples with respect to the (estimated) natural and sampling variability discussed above. Obviously, four stations constitute a very crude, if any transect at all and six observations in time a rather incomplete time series. A finer resolution, e.g. of the summer months, of the surface layer and of the frontal structures in the Greenland Sea periphery, as well as replicate samples would clearly have been desirable. However, this was out of the scope of the present investigation, which is concerned with the large-scale features including the deep sea. Given the restrictions in available ship time and in manpower for processing the samples this had to be at the expense of fine resolution and replication.

Whatever the potential limitations of the present data set, the clear trends in the observed large-scale regional and temporal distributions agree well with what one would expect from the literature, suggesting that methodical errors did not distort the overall picture.

Biomass calculations

Biomass was not an independent measure during this investigation since it was calculated from abundances and size-weighted or size-independent coefficients, depending on the size range of the taxon under consideration [length-weight relationships and mean individual dry weights (DW_i) are listed in Appendix 1]. This is straightforward as long as the abundances and biomass coefficients are taken from one and the same population. This was not possible for this study and would also have been impracticable due to the various sources of variability under investigation (see above). For instance, it cannot be assumed that surface dwellers have the same body composition (including dry weight) as deep dwellers, for a given taxon at a given time (Båmstedt et al. 1990). Individual dry weights may vary by a factor of four for female and CV copepodids of *Calanus hyperboreus* (Kattner et al. 1989) and temporal variability may be as high (Conover and Corner 1968, Conover and Huntley 1991). Even within a given sample, individual dry weights may vary by a factor of 4-5 (Båmstedt 1988). Given the wide range of variability to be expected, I considered it appropriate in some instances to average over a range of reported values, instead of selecting an (arbitrary) single value. This procedure reduces the bias associated with extrapolating a single value over space and time.

5.2 Species composition and diversity

The composition of zooplankton in the Greenland Sea is characterized by a very uneven distribution of individuals and biomass among species and of species among higher taxa. This was evident from both, regional and seasonal studies and most pronounced in the upper water column.

Copepods are of overriding importance, with small forms (<1 mm) dominating in numbers and large forms (*Calanus*) in biomass. Similar findings are reported for the Arctic Ocean (Brodskii and Pavshtiks 1977, Pavshtiks 1983, Kosobokova 1982), although the importance of small forms in the polar domain has not been unequivocably demonstrated (Johnson 1963, Minoda 1967, Haberstroh 1985, Mumm 1991), probably due to the coarser nets (≥300 µm) employed by these investigators. The lesser importance of small-sized cyclopoids and calanoids in the Atlantic domain, however, appears to be real, as shown by the low incidence of these groups in the eastern Fram Strait (Smith 1988), Davis Strait (Pavshtiks 1968, Huntley et al. 1983), the Norwegian Sea (Østvedt 1955) and the West Spitsbergen Current (this study). Fine mesh sizes (≤200 µm) were used during these investigations. It is not known to what extent these dominance shifts reflect biogeographic differences, as the polar and Atlantic species sets are not fundamentally different (Østvedt 1955, Grainger 1965, Mumm 1991). The species encountered in the arctic domain (Table 4.1) are also common in the Arctic Ocean (e.g. Grainger 1989), whereas some of the true polar species [e.g. *Calanus glacialis*, *Fritillaria borealis* (Grainger 1965)], including neritic and brackish water forms (*Acartia*, *Limnocalanus*, *Pseudocalanus*

acuspes) are not or seldom found in the open Greenland Sea. Likewise, there is good correspondence of the present species list with Østvedt's (1955) inventory from the Norwegian Sea, again excluding neritic genera and species (*Candacia, Evadne, Sagitta elegans, Temora*) and those of clearly southern affiliation (*Pleuromamma, Conchoecia obtusata, Hyperia*). All but three of the copepod species identified in this study are also listed by Brodskii (1967) and Brodskii et al. (1983) for the Greenland Sea. According to these authorities, the present reports of *Spinocalanus horridus, Undeuchaeta spectabilis* and *Euchaeta farrani* are new to the Greenland Sea fauna. However, there is some confusion concerning the taxonomy of *Euchaeta* (Mauchline, pers. comm.), and *E. farrani* is now considered identical with *E. barbata* (Mauchline 1992).

Complying with Mumm (1991), indices of diversity (H') and evenness (J) will be used only to examine the species distribution within the present data set. Regional differences are evident and reflect the abundance distribution along the regional transect in late fall with highest H' and J values coinciding with lowest abundances at the WSC station. A low overall abundance thus appears to be associated with an even distribution of individuals among species, resulting in a high diversity despite the low number of species (S) at this station. Conversely, diversity is comparatively low within the gyre due to the concentration of a large number of individuals in few species, irrespective of the higher number of species (S) encountered here. The species composition was not fundamentally different along the transect, although there were higher portions of typical Atlantic representatives at 13°E, namely *Calanus finmarchicus* among the copepods (Jashnov 1970) and *Limacina retroversa* among the pteropods (Van der Spoel 1967).

The relative constancy of total species numbers in the GSG with time (Fig. 4.2) is encouraging, for it supports the *a priori* postulation of repeated sampling of (essentially) the same community over time. The constancy in species composition, as borne out by the rectangular array of the 'Mumm plot' (Fig. 4.17) and the failure to reject the null hypotheses 'no time effects' (Table 4.4) further strengthens this assumption. The opposite case, i.e. large variations in species numbers and composition has repeatedly frustrated temporal studies of both phyto- and zooplankton in highly dynamic areas, such as upwelling zones (Blasco et al. 1980, Smith et al. 1981, Richter 1990).

Thus, depth appears to be the main element structuring the pelagic community, irrespective of season. This was shown in the 'Mumm plot' (Fig. 4.18), in the highly significant rejection of the null hypothesis 'no depth effects' (Table 4.4) and in the subsequent classification and ordination of the samples (Figs. 4.19, 4.21).

Roughly one half of the species occur throughout the depth range investigated, displaying vertical migrations to a varying extent, while the other half of the species encountered show clear depth preference throughout the investigation period.

Representatives of the former group are *Oithona, Oncaea, Microcalanus, Pseudocalanus minutus, Metridia longa, Calanus finmarchicus* and *C. hyperboreus* among the copepods, and *Eukrohnia, Oikopleura* and *Boroecia* among the other taxa.

Resident species of the latter group are found among the Aetideidae and Scolecithricidae (Copepoda) and among the Cnidaria. These are exclusively meso- and bathypelagic species, and it is noteworthy that no epipelagic residents appear to have established themselves in the Greenland Sea. This is in contrast with the temperate North Atlantic, where e.g. Paracalanidae, Centropagidae and Pontellidae inhabit the epipelagial

throughout the year (Grice and Hülsemann 1965). These copepod families are entirely absent in the arctic and polar domains (Brodskii 1967, Brodskii et al. 1983). The only likely candidates for the surface distribution type among the 'other taxa' are the pteropods *Limacina helicina* and *L. retroversa* (Fig. 4.18). However, they are among the few species that occurred only discontinuously, regionally and seasonally (Figs. 4.16 and 4.17). It must therefore be assumed that they have a smaller-scale distribution, not representatively covered by the widely spaced sampling carried out during this investigation. In fact, the larger *L. retroversa* is considered an opportunistic species with occasional mass occurrences in the Norwegian Sea in late summer and fall, followed by population collapses (Bathmann et al. 1991). It is not known, whether such mortality events occur further north. However, the available seasonal carbonate flux data (Honjo 1990) do not support such a scenario for the Greenland Sea.

Along the vertical axis, both species numbers and evenness add up to higher diversities with increasing depth, irrespective of abundance changes. While the high species numbers in the lower meso- and upper bathypelagial may partly be attributable to (five-fold) larger sample sizes relative to above (Hurlbert 1971), the steady increase with depth within the upper 500 m of constant sample volume (25 m^3) suggests that this is a 'real' phenomenon. This view is supported by similar observations for the calanoid copepod fauna from the Arctic Ocean, the Norwegian Sea, North Atlantic, North Pacific, Antarctic and Subantarctic (Table 5.1). It is hard to decide whether the drop in total and calanoid species numbers towards the lower bathypelagial is spurious or real, due to the very low concentrations of individuals and the likely occurrence of (numerous) 'cryptic' species (e.g. among the Spinocalanidae, Damkaer 1975) in the Greenland Sea samples. However, Table 5.1 shows that a similar decrease is also apparent for the Calanoida in other regions of the world ocean. With regard to the total numbers of species, the Norwegian and especially the Greenland Sea harbor a strikingly poor calanoid fauna relative to the adjacent North Atlantic as well as to the Arctic Ocean (Østvedt 1955, this study). Vinogradov (1970) attributed the depletion of the calanoid fauna in the Norwegian Sea to the intense modifications of its water masses (winter cooling), leading to a selection of

Table 5.1: Absolute (and relative) numbers of species of calanoid copepods living at various depths in different regions of the world ocean.

Depth [m]	Arctic Ocean		Atlantic				Pacific	Antarctic[h]
	Canadian Basin[a]	Eurasian Basin[b]	Greenland Sea[c]	Norwegian Sea[d]	50°-70° N[e]	30°-50°N[f]	Bering Sea[g]	and Subantarctic
0-100	25 (54)	20 (54)	10 (36)	16 (33)	24 (17)		17 (26)	30 (19)
100-200	34 (74)	26 (70)	12 (48)		34 (24)	91 (59)	18 (28)	37 (24)
200-300			16 (57)					
300-500			18 (64)	32 (67)	48 (35)	123 (79)	42 (65)	56 (36)
500-1000	40 (87)	31 (84)	23 (82)	25 (52)	105 (76)	120 (77)	45 (69)	80 (52)
1000-1500			24 (86)					
1500-2000			17 (61)	31 (65)	95 (68)	70 (45)		
2000-3000	31 (68)	25 (68)	19 (68)		55 (40)	57 (37)	4 (6)	

[a]Brodskii and Nikitin 1955, Johnson 1963; [b]Virketis 1957; [c]this study; [d]Østvedt 1955; [e]Thompson 1903 in Vinogradov 1970, Wolfenden 1904, Jespersen 1934, Lysholm and Nordgaard 1945; [f]Farran 1926, Lysholm and Nordgaard 1945, Grice and Hülsemann 1965; [g]Brodskii 1957; [h]Vervoort 1957.

especially cold-adapted oceanic species. Cooling and deep mixing is more intense in the Greenland Sea, and the rapid flushing of the deep waters (in the order of ten years!, Smethie et al. 1988) relative to an estimated residence time of 1000 years for the oceanic stratosphere (Rudels 1993) sets very different time scales for the evolution of a deep sea fauna between the North Atlantic and the Nordic Seas. The rise in species numbers in the Arctic Ocean can be explained accordingly by the lower flushing rates (50 to 500 years, Rudels 1993) especially in the Canada Basin, whose stagnant bottom waters have allowed the evolution of a number of endemic deep sea species [e.g. *Chiridiella reducta, Pseudochirella spectabilis, Scaphocalanus polaris* (Brodskii 1967)].

5.3 Biomass

It was already stated that regional comparisons of abundances based on different sampling equipment (mainly mesh size) may lead to spurious results. Biomass better suits this purpose, as in high latitudes biomass is mainly determined by large-bodied organisms (e.g. Hempel 1985). Nevertheless, there still remain many unknowns (i.a. avoidance and conversion between different biomass units) which have to be borne in mind when carrying out such analyses [cf. chapter 5.1. (this study) and Mumm (1991)]. Fig. 5.1. depicts

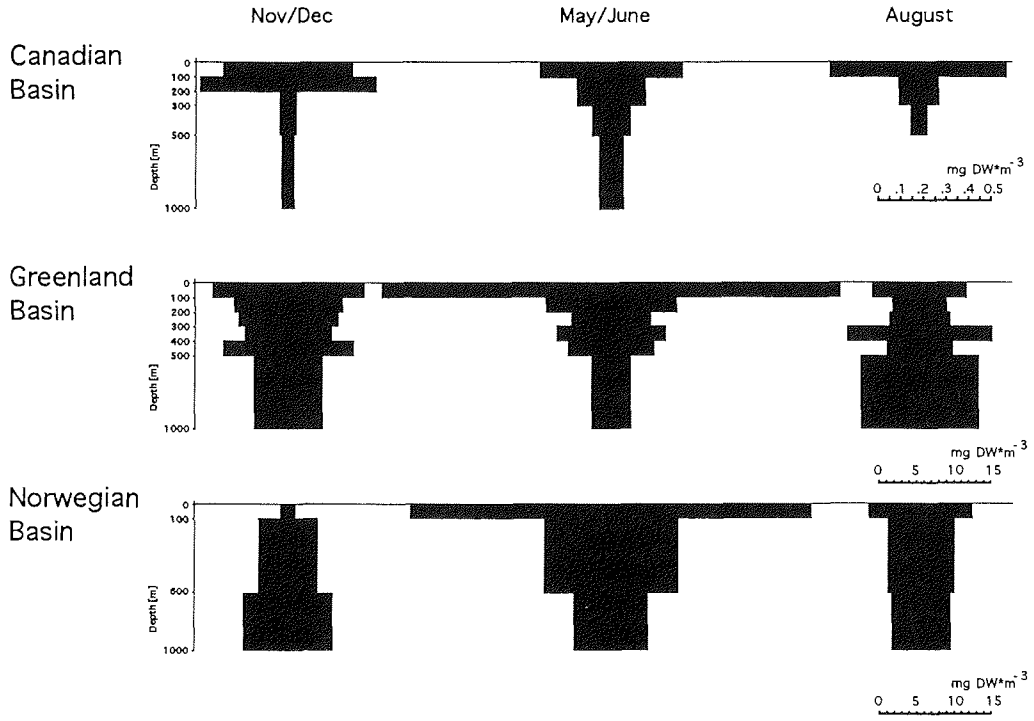

Fig. 5.1: Vertical distribution of zooplankton biomass (mg DW*m^{-3}) at different seasons in the Arctic Ocean, the Greenland Sea and Norwegian Sea. Note the 30x scale difference between the upper and the two lower rows. [Data from Hopkins (1969), this study, and Wiborg (1954). Wiborg's data converted according to Raymont (1983): 1 ml = 160 mg DW].

the probably only available data sets for the seasonal variability of zooplankton biomass in the polar, arctic and Atlantic deep water domains down to 1000 m (Wiborg 1954, Hopkins 1969, this study). Total biomass, integrated over all depths, is considerably lower in the Arctic Ocean [average 0.2 g DW* m^{-2} (Hopkins 1969)], with more than 50-fold higher values in both, the Greenland and Norwegian Seas [13.5 g DW*m^{-2} (0-1000 m this study) and 12.1 g DW*m^{-2} (calculated form Wiborg 1954)]. These are high standing stocks, approaching the seasonal average for the highly productive Bering Sea [14.9 g DW*m^{-2}, calculated from Vinogradov's (1970) wet weight values in a 500 m water column, assuming WW*0.17=DW (Båmstedt 1986)]. A good compilation of zooplankton standing stocks in other polar and subpolar seas is given by Boysen-Ennen et al. (1991), Conover and Huntley (1991) and Mumm (1991). From these it is evident that Hopkins' (1969) data for the Arctic Ocean are among the lowest reported. Kosobokova (1982) gives about one order of magnitude higher values for the Canadian Basin and the Transpolar Drift regions [1.6 and 2.2 g DW*m^{-2} for May to October, calculated from wet weight values, assuming WW*0.17=DW (Båmstedt 1986)], but does not discuss this discrepancy with regard to Hopkins' (1969) data. Whatever the 'true' value for the Arctic Ocean, both studies agree in that seasonal changes are confined to the upper 500 m water column. The surface maximum extends well into the dark season and disappears as late as February through early May (not shown in Fig 5.1.), the deeper layers remaining relatively unaffected throughout the year.

In striking contrast, the surface maximum appears to be a rather acute and ephemeral structure in both, the Greenland and Norwegian Basins, disintegrating as early as August.

Considerable translocation of biomass occurs during this period, leading to a homogeneous distribution over the entire water column in the Norwegian Sea. An intermediate maximum between 300 and 500 m pervails in the Greenland Sea throughout the year. It is not known whether such a feature also occurs in the Norwegian Sea, due to the coarser sampling intervals employed. However, it is clearly not present in the Arctic Ocean, neither in Hopkins' (1969), nor in Kosobokova's (1982) observations. It was shown that the intermediate biomass maximum in the Greenland Sea Gyre coincides with the distribution maximum of the chaetognaths, which are second to copepods in terms of biomass. This group, and the meso- (and bathypelagic) community as a whole, appears to be only poorly developed in the Arctic Ocean, in quantitative terms [Dawson 1968, Hopkins (1969), Kosobokova (1982)], whereas in qualitative terms the Arctic Ocean harbors a richer, i.e. a more diverse assemblage (e.g. Brodskii 1967, cf. also Mumm 1991) compared to the GSG.

In winter, only low concentrations of biomass are left in the surface of the Norwegian Sea, and the bulk of the population is located in the lower mesopelagial. In the Greenland Sea, however, fairly high concentrations are found throughout the upper 1000 m, and the surface minimum was shown to appear later in winter (February, not shown in Fig. 5.1.) and to persist through spring (Fig. 4.13.). With respect to the timing of the surface minimum, there are thus parallels with the situation in the Arctic Ocean. The persistence of relativly high surface concentrations far into the dark season raises some speculations about the possible causes. Ice-algal food may still be available under the Arctic pack-ice (cf. Mel'nikov 1989), but obviously not in the open waters of the Greenland Sea Gyre during periods of nil phototrophic production. However, large numbers of the large thecate dinoflagellate *Ceratium arcticum* were encountered in the winter samples, but it is

Table 5.2: Ratios of the annual minimum and maximum biomass in different regions of the world ocean.

Region	0-100 m	0-1000 m	Reference
Arctic Ocean, Canadian Basin	1:16	1:6.3	Hopkins 1969
Arctic Ocean, Eurasian Basin	1:18	1:3.3	"
Greenland Sea	1:17	1:1.9	this study
Norwegian Sea, station "M"	1:40	1:2.3	Wiborg 1954
Northwest Pacific and Bering Sea	1:12	1:3.0*	Vinogradov 1970
Northeast Pacific, station "P"	1:10	1:2.0	McAllister 1961
Subantarctic	1:5	1:1.8	Foxton 1956
Antarctic	1:3	1:1.9	"

*collections from 0-500 m

not known to what extent this probably mixotrophic protist is a potential food source. Its temperate congener *C. tripos,* typical of autumn blooms in the Baltic Sea, is considered a rather unattractive food item for herbivorous zooplankton (Smetacek 1988).

Table 5.2. summarizes the available data on the seasonal variabilities of biomass at the surface and in the upper 1000 m for temperate and high latitude regions. Absolute numbers are not given due to the lack of congruence in the biomass units employed (wet weight, dry weight, displacement volume per hauling hour, etc.). The highest seasonality is recorded for the 100 m surface layer of the Norwegian Sea, with 40-fold biomass changes between the early summer maximum and the winter minimum (cf. also Fig. 5.1.). In the Antarctic, surface biomass varies only by a factor of 3 in the course of the year. For the whole 1000 m water column the range is reduced to 1.9. This latter is identical to the ratio observed for the Greenland Sea. If integrated over the entire 3000 m investigated, the ratio decreases to only 1.5 (not shown in Table 5.2.). This is the lowest value observed and illustrates the remarkable stability of zooplankton stocks in this high latitude open ocean system in spite of the extreme seasonality in primary production (e.g. Smith and Sakshaug 1990).

High stocks are maintained by a low number of well adapted species and an efficient partitioning of the limiting food resources, as will be outlined in the following section: Ecological niches appear to be delimited by body size within calanoid herbivores (*Pseudocalanus, Calanus finmarchicus, C. hyperboreus*), determining food spectrum, storage capacity and range of seasonal migrations, and by depth among calanoid omnivores (*Aetideidae*) and gelatinous carnivores (Cnidaria). Main carnivores and omnivores are represented by single genera of chaetognaths and ostracods, which dwell at intermediate depths.

The abounding cyclopoids and small calanoids appear to be to some extent uncoupled from the seasonal supply of food and probably subsist on a rich auto-mixo- and heterotrophic protistan food web (Auf dem Venne 1990), depending on season.

5.4 Life histories of selected taxa in relation to the seasonal production cycle in the Greenland Sea

The following discussion summarizes the available physical and biological oceanographical information for the observation period and presents a general life history scenario for the most important taxa (cf. chapter 4.3).

From the numerous physical oceanographical observations carried out during the 1988/89 field phase of the Greenland Sea Project (GSP group 1990, Budéus et al. 1993, Schott et al. 1993, Visbeck 1993) it appears that a shallow (50 m) layer of Arctic Surface Water originating in summer 1988 persisted far into fall of the same year. By November this low salinity layer was found at near-freezing temperatures (-1.9°C). Two successive convection events in February and March of 1989 deepened the mixed layer down to 300 and 1000-1500 m, thereby entraining warmer intermediate water and raising the mixed-layer temperature to -1.3°C. Thermal stratification of the nearly homogenous water column started in early June, and a shallow thermocline persisted through mid-October at a fairly constant 40 m depth. In mid-June the vernal phytoplankton bloom was already under way (Legendre et al. 1993), with high primary production (up to 1 g $C*m^{-2}*d^{-1}$) and lowered silicate concentrations in the productive layer. High P/B ratios for the >5 µm phytoplankton indicated heavy grazing on this fraction, leading to a shift of the phytoplankton community towards ≤5 µm cells.

These observations provide a valuable basis for the interpretation of the zooplankton data from the present study. Virtually all potentially herbivorous taxa had by that time crowded into the surface layer, obviously taking advantage of the favorable growth conditions. Thus, the mid-June surface layer was teeming with spawning adults and young developmental stages of the annual species (cyclopoids, *Pseudocalanus minutus, Calanus finmarchicus*?) as well as older first generation and young second generation stages of the biennial species like *Calanus hyperboreus*. The marked growth, as infererred from the length and stage increments of the named species as well as from the general biomass increase between early and late summer, indicates that primary production remained favorable during that period. Unfortunately, though, there are no phytoplankton data to support this assumption.

By late summer, large numbers of *C. hyperboreus* had already descended to their wintering depths, which is in agreement with Conover (1988). It appears that the older first generation stages ≥CIV are the first to leave the surface, while the young second generation of ≤CIII copepodids remains in the productive layer, until presumably attaining a 'critical mass' for hibernation. While Conover and Huntley (1991) maintain that 'overwintering is probably not a great hardship', failure to attain the critical size for overwintering might explain the massive recruitment losses of *C. hyperboreus* repeatedly reported for the Arctic Ocean (Brodskii and Pavshtiks 1977, cf. also Mumm 1991). CIII was the main overwintering stage in the Greenland Sea and smaller stages did not survive through winter.

A similar selection mechanism can be invoked to explain the seasonal distribution pattern of *Pseudocalanus minutus*, which is a considerably smaller species of only 0.4% of the former's body mass (Conover and Huntley 1991) and which lives for one year only (Digby 1954, Østvedt 1955, McLaren et al. 1989). Spawning coincided with the early phytoplankton bloom (cf. Østvedt 1955, McLaren 1969), and growth proceeded at the

surface until late in the season. The abundance maximum occurred but late in the summer in the surface layer, where a sizeable portion of the population remained until late fall. The size distribution proved that these specimens were indeed smaller than the ones that had left the surface layer, reinforcing the earlier notion of a size threshold for wintering. This limit corresponds to the CV copepodite stage in *Pseudocalanus,* which accumulates large amounts of lipids at the end of the growing season (McLaren et al. 1989, Norrbin 1991), and is the dominant stage from late summer through winter (McLaren et al. 1989, this study).

Not only the timing but also the range of the seasonal vertical migration appears to be related to body size. *P. minutus* was shown to overwinter between 500 and 1000 m, while the bulk of the wintering *C. hyperboreus* was located at the remarkable depth of 1500-2000 m. Østvedt's (1955) data reveal similar differences for the Norwegian Sea. Both species attain their seasonal abundance minimum in spring, when they are already on their rise to the surface. This might be due to increased mortality from molting to maturity which in both species is reported to take place before and during this period (Sømme 1934, Ussing 1938, Østvedt 1955), or from increased predation mortality while traversing the mesopelagic zone.

Unfortunately, we know nothing about mesopelagic fish stocks in the GSG, and the following discussion can only account for the potential invertebreate predation on the migrating calanoid stocks. The highest concentrations of chaetognaths were found in the mesopelagial and the recruitment peak of *Eukrohnia (hamata)* in spring indicates favorable feeding conditions prior to or during this period. A second spawning peak was observed in fall, i.e after the late summer descent of the wintering herbivore stocks. This somehow unusual timing of reproduction is an indication that the species might actually benefit from the seasonal migration of its potential prey. The recurrence of four conspicuous size modes during the investigation period confirms previous reports of a 2 year life cycle for the species in the Nordic Seas (Sands 1980). Vertical segregation of the old and young generation is evident, with the offspring rising to the surface, thereby reducing the risk of falling prey to their parents and at the same time increasing the encounter probabilities with prey organisms of an adequate size. Sullivan (1980) showed that juvenile *E. hamata* fed preferentially on cyclopoid copepods. The prevalence of *Oithona* in the epipelagic zone during the dark season might therefore be a prerequisite for chaetognath recruitment success in fall, and the observed narrowing length-frequency distribution of *Oithona* over winter might be explained by differential mortality by predation on the lower size end. Older chaetognaths appear to prey rather indiscriminately on whatever there is available, including large calanoids (Sullivan 1980, Hopkins 1987). However, Øresland (1990) found only low predation rates of *E. hamata* in the Antarctic in winter. Despite the low feeding rates observed, he postulated that the continued feeding activity amounted to a high cumulative predation impact over the long winter period, with a considerable fraction of the wintering stocks potentially removed. Such a scenario might hold true for *Pseudocalanus* in the Greenland Sea as well, whose wintering stocks indeed seem to experience severe decimation in the upper mesopelagic zone. *Calanus hyperboreus,* however, by virtue of the extraordinary range of its seasonal vertical migration is likely to escape prolonged periods of depredation in its bathypelagic winter refuge. While vertical migrations have been repeatedly associated with avoidance of predators (Longhurst 1976 and references therein), this has been forwarded with respect to visual predators on much shorter time scales. Avoidance of invertebrate predation during long periods of arrested

development might be a plausible mechanism explaining the wide range of migration of *C. hyperboreus* in the Greenland Sea. It would further explain the limited range of migration of the same species in the Arctic Ocean (Dawson 1978), where carnivores, and chaetognaths in particular, are rare (Longhurst 1985, Longhurst et al. 1989). It was already stated that in the Arctic Ocean there appears to be an only depauperate mesopelagic community, in terms of biomass [Hopkins 1969, cf. also Fig. 5.1 (this study)].

Aetideidae and Ostracoda are, in addition to the named chaetognaths, the characteristic components of the meso- and bathypelagic community in the Greenland Sea. These are predominantly omnivorous forms which feed on a wide variety of food items, including algal debris, marine snow, fecal pellets, molts, live prey and carcasses (Esterly 1916, Heinrich 1958, Harding 1974, Angel 1972, Hopkins 1985, 1987). The apparent lack of food-specialization within the Aetideidae is believed to have resulted in a vertical partitioning of the limited resources (Raymont 1983), with a stepwise arrangement of species with regard to depth (Grice and Hülsemann 1965) and a large generic radiation within this family (Razouls 1993). The layered occurrence observed during this study agrees with previous findings from the Norwegian Sea (Østvedt 1955) and the North Atlantic (Grice and Hülsemann 1965).

Breeding of the truly bathypelagic species (*Aetideopsis rostrata, Gaidius brevispinus*) is continuous (Raymont 1983), while the mesopelagic species *Chiridius obtusifrons* is reported to reproduce during winter and summer (Østvedt 1955). Breeding was continuous for all the Aetideidae investigated during this study, irrespective of depth. This was evidenced by the constancy in the stage distribution, encompassing all six copepodite stages at all times, and the year-round incidence of spermatophores on female genital segments. Complete development may take as little as three months in *Chiridius armatus* (Matthews 1964), but Bakke and Valderhaug (1978) report four to five months for the same species to develop from copepodite stage CIII to CVI. Virtually no information is available for the deep-living species encountered during this investigation, which are estimated to have generation times up to five years (Raymont 1983)!

In contrast to the relative large number of species in the Aetideidae only two species of ostracods appear to be successful in the Greenland Sea, of which *Boroecia borealis* is by far the dominant throughout the mesopelagial. In spite of its recognized importance in the deeper layers of Baffin Bay (Sameoto 1984), the Fram Strait (Haberstroh 1985) and southern Nansen Basin (Mumm 1991), there is only limited published information on this species. This might be due in part to the taxomomic confusion at the specific and generic level. The specimens in the present collection correspond to Sars' (1900) description of *Conchoecia maxima* which has alternately been synonymized and separated from *C. borealis* (Skogsberg 1920, Poulsen 1973). However, after revision of the genus (Kock 1992), the appropiate specification now appears to be *Boroecia borealis* (Weigmann-Haass, pers. comm.).

From the present study it seems that this species breeds from winter through summer, with a reproductive peak in June. Breeding activity probably stalls in the second half of the year as evidenced by the disappearence of the smallest modal size classes in late fall (Fig. 4.56, this study). Growth, however, appears to be rapid in this size range, as indicated by the disappearance of the youngest stages between summer and late fall and the re-appearance of the named stages only two months later.

Complete development probably takes one year in the Greenland Sea Gyre as deduced from the ebb and flow of the preadult stage and the aforementioned rapid succession of the youngest stages. How this proceeds remains a mystery, for recruitment not only occurs 'out of season', i.e. during winter but also 'out of range', i.e. in the bathypelagic zone. Breeding in *Boroecia borealis* thus appears to be decoupled from the seasonal production cycle. The observed vertical separation of stages with adults above and young instars below is contrary to what one would expect (cf. *Eukrohnia*) and contradicts previous findings for planktonic ostracod populations in the literature (Angel 1989) as well as the general conception of the pelagic food web, which postulates a size increase within populations with depth (e.g. Vinogradov 1970, Raymont 1983, Rodríguez and Mullin 1986). The vertical separation of the parents and their offspring further requires sinking of the spent eggs and hatching of the nauplii at depth. A similar mechanism has been invoked in the early life cycle of the Antarctic krill (Marr 1962, Hempel and Hempel 1985), where hatching, however, is followed by a developmental ascent of the nauplii to the surface. While food remains a problem in the bathypelagic zone, the selective advantage of staying at depth is probably the same as for overwintering *Calanus hyperboreus* (see above), i.e. protection against predation. This is even more stringent for early developmental stages which constitute a nutritious and easy prey. Thus, sinking might be an adaptation to save the offspring from predation by the omnivorous mesopelagic community.

The adaptional value of this presumptive 'strategy' is illustrated by the opposite case of positively buoyant eggs in *C. hyperboreus* (Marshall and Orr 1972). This species spawns in late winter, supposedly at depth (Conover 1988), thereby depleting its lipid reserves (Conover 1967, Head and Harris 1985). The lipid-rich eggs are believed to rise to the surface, experiencing heavy predation by *Metridia longa* which was found gorging on the eggs (Conover and Huntley 1991, Conover et al. 1991). The authors do not quantify this impact, but they apparently consider it large enough to hypothesize that the early spawning period of *C. hyperboreus* might actually induce reproduction in *M. longa*.

While the present data do not allow to test this hypothesis for *M. longa*, the distribution of females, eggs and nauplii of *C. hyperboreus* support Conover's assumption of egg-laying at depth, and subsequent rise to the surface (Conover 1988, Conover and Huntley 1991, Conover et al. 1991). Early eggs are larger (February) and accumulate in the surface layer. With progressive depletion of lipids (cf. Conover 1967) they become smaller (April), being less positively buoyant and accordingly more dispersed in the water column (cf. Fig. 4.39 b). The distribution of nauplii in February does not fit the postulated 'developmental ascent' of the early stages, as the surface nauplii are smallest, indicating retarded development with respect to the nauplii below (cf. Fig. 4.41). The only plausible explanation for the observed vertical size distribution in February is: hatching at the surface followed by sinking of the early nauplii and subsequent rising of the advanced naupliar stages.

The size distribution in April, by contrast, agrees well with the developmental ascent of nauplii to the surface, as there is a conspicuous length increase of nauplii with decreasing depth.

Naupliar development of *C. hyperboreus* proceeds to stage NV (0.55 mm, Sømme 1934) on stored lipids alone (Conover 1962), and further development obviously depends on the availability of food. While ice-algae are an early source of food in the presence of sea-ice (Conover et al. 1991), naupliar development in the open Greenland Sea depends on the vernal phytoplankton bloom. This in turn depends on the thermal stratification of the

water column, which occurs only late in the season and which may be intercepted by storms (Smith and Sakshaug 1990). The apparent success of the species in the GSG, however, suggests that nauplii may endure at the surface in slow or arrested development in wait of favorable growth conditions.

This 'sit and wait' strategy can probably be extended to *Pseudocalanus minutus*, which was shown to belong to the vanguard of herbivores repopulating the surface layer well in advance of the vernal bloom. The presence of these grazers as well as of the ubiquitous *Oithona* enduring in the epipelagial precludes the build-up of massive phytoplankton stocks in summer. This contradicts the classic North Atlantic paradigm of only loose coupling of primary and secondary production (Heinrich 1962). There is now accumulating evidence that this might not hold true for the gyres of the Greenland and Norwegian Seas (Wassmann et al. 1991, Legendre et al. 1991, this study), which in fact show more resemblance to the situation in the North Pacific than was previously thought.

6 References

Alshuth S (1989) Distribution and abundance of dominant Arctic copepods in early winter. ICES Council meeting 1989, Int Council Explor Sea, Copenhagen, 11 pp

Alvariño A (1962) Two new Pacific chaetognaths, their distribution and relationship to allied species. Bull Scripps Inst Oceanogr 8: 1-50

Angel MW (1972) Planktonic oceanic ostracods - historical, present and future. Proc R Soc Edinburgh, Ser B, 73: 213-228

Angel MV (1989) Does mesopelagic biology affect the vertical flux? In: Berger WH, Smetacek VS, Wefer G (eds) Productivity of the ocean: Present and past. Wiley, Chichester, pp 155-173

Auf dem Venne H (1990) Zur Verbreitung auto-, mixo- und heterotropher Ciliaten im Plankton der Grönlandsee. Diploma thesis, Kiel University, 102 pp

Bakke JLW, Valderhaug AV (1978) Ecological studies on the deep-water pelagic community of Korsfjorden, western Norway. - Population biology, biomass, and caloric content of *Chiridius armatus* (Crustacea, Copepoda). Sarsia 63: 247-254

Båmstedt U (1981) Water and organic content of boreal macrozooplankton and their significance for the energy content. Sarsia 66: 59-66

Båmstedt U (1986) Chemical composition and energy content. In: Corner EDS, O'Hara SCM (eds) The biological chemistry of marine copepods. Clarendon, Oxford, pp 1-58

Båmstedt U (1988) Ecological significance of individual variability in copepod bioenergetics. In: Boxshall GA, Schmincke HK (eds) Biology of copepods. Hydrobiologia 167/168: 43-59

Båmstedt U, Håkanson JL, Brenner-Larsen J, Björnsen PK, Geertz-Hansen O, Tiselius P (1990) Copepod nutritional condition and pelagic production during autumn in Kosterfjorden, western Sweden. Mar Biol 104: 197-208

Båmstedt U, Eilertsen HC, Tande KS, Slagstad D, Skjoldal HR (1991) Copepod grazing and its potential impact on the phytoplankton development in the Barents Sea. In: Sakshaug E, Hopkins CCE, Øritsland NA (eds) Proc Pro Mare Symp 1990. Polar Res 10(1): 339-353

Bathmann UV, Noji TT, von Bodungen B (1991) Sedimentation of pteropods in the Norwegian Sea in autumn. Deep-Sea Res 38: 1341-1360

Blackburn M (1979) Zooplankton in an upwelling area off Northwest Africa: Composition, distribution and ecology. Deep-Sea Res 26: 41-56

Blasco D, Estrada M, Jones B (1980) Relationship between the phytoplankton distribution and composition and the hydrography in the Northwest Africa upwelling region near Cabo Cobeiro. Deep-Sea Res 27: 799-821

Bogorov BG (1946) Peculiarities of diurnal vertical migrations of zooplankton in polar seas. J Mar Res 6: 25-32

Boysen-Ennen E, Hagen W, Hubold G, Piatkowski U (1991) Zooplankton biomass in the ice-covered Weddell Sea, Antarctica. Mar Biol 111: 227-235

Bray JR, Curtis JT (1957) An ordination of the upland forest communities of southern Wisconsin. Ecol Monogr 27: 325-349

Brodskii KA (1957) The fauna of Copepoda (Calanoida) and the zoogeographic division of the northern part of the Pacific Ocean and the adjacent seas [in Russian]. Izd Akad Nauk SSR, Moscow, 222 pp

Brodskii KA (1967) Calanoida of the far eastern seas and Polar Basin of the USSR. In: Pavslovskii EN (ed) Keys to the fauna of the USSR, 35. Israel Progr Sci Transl, Jerusalem, 440 pp

Brodskii KA, Nikitin MM (1955) Observational data of the scientific research drifting station of 1950-1951. Hydrobiological work. Izd Morsk Transp 1: 404-410 [Transl Am Meteorol Soc]

Brodskii KA, Pavshtiks YA (1977) Plankton of the central part of the Arctic Basin. Pol Geogr 1: 143-161

Brodskii KA, Vishkvartseva NV, Kos MS, Markhaseva EL (1983) Calanoid copepods from the seas of the USSR and adjacent waters, 1. [in Russian] Nauka, Leningrad, 356 pp

Budéus G, Maul A-A, Krause G (1993) Variability in the Greenland Sea as revealed by a repeated high spatial resolution conductivity-tempe-rature-depth survey. J Geophys Res 98(C6): 9985-10000

Carmack E, Aagard K (1973) On the deep water of the Greenland Sea. Deep-Sea Res 20: 687-715

Clarke A, Holmes LJ, Gore DJ (1992) Proximate and elemental composition of gelatinous zooplankton from the Southern Ocean. J Exp Mar Biol Ecol 155: 55-68

Clarke KR, Green RH (1988) Statistical design and analysis for a 'biological effects' study. Mar Ecol Progr Ser 46: 213-226

Clarke KR, Warwick RM (1994) Similarity-based testing for community pattern: the two-way layout with no replication. Mar Biol 118: 167-176

Clarke RA, Swift JH, Reid JL, Koltermann K-P (1990) The formation of Greenland Sea Deep Water: double diffusion or deep convection? Deep-Sea Res 37: 1385-1424

Clifford DHT, Stephenson W (1975) An introduction to numerical classification. Academic Press, New York, 229 pp

Clutter RI, Anraku M (1979) Avoidance of samplers. In: Tranter DJ, Fraser HJ (eds) Zooplankton sampling. UNESCO press, Paris, pp 57-76

Conover RJ (1962) Metabolism and growth in *Calanus hyperboreus* in relation to its life cycle. Rapp P-v Réun Cons int Explor Mer 153: 190-197

Conover RJ (1967) Reproductive cycle, early development, and fecundity in laboratory populations of the copepod *Calanus hyperboreus*. Crustaceana 13: 61-72

Conover RJ (1988) Comparative life histories in the genera *Calanus* and *Neocalanus* in high latitudes of the northern hemisphere. In: Boxshall GA, Schmincke HK (eds) Biology of copepods. Hydrobiologia 167/168: 127-142

Conover RJ, Corner EDS (1968) Respiration and nitrogen excretion by some marine zooplankton in relation to their life cycles. J Mar Biol Ass UK 48: 49-75

Conover RJ, Huntley M (1991) Copepods in ice-covered seas - Distribution, adaptations to seasonally limited food, metabolism, growth patterns and life cycle strategies in polar seas. J Mar Syst 2: 1-42

Conover RJ, Harris LR, Bedo AW (1991) Copepods in cold oligotrophic waters - How do they cope? Proc IV Int Conf Copepoda. Bull Plankton Soc Japan (spec vol): 177-199

Cushing DH (1962) Patchiness. Rapp P-v Réun Cons int Explor Mer 153: 152-164

Damkaer DM (1975) Calanoid copepods of the genera *Spinocalanus* and *Mimocalanus* from the central Arctic Ocean, with a review of the Spinocalanidae. NOAA Tech Rep NMFS CIRC-391, 88 pp

Dawson JK (1968) Chaetognaths from the Arctic Basin, including the description of a new species of *Heterokrohnia*. Bull So Calif Acad Sci 67(2): 112-124

Dawson JK (1978) Vertical distribution of *Calanus hyperboreus* in the central Arctic Ocean. Limnol Oceanogr 23(5): 350-357

Dickson RR, Gmitrovitch EM, Watson AL (1990) Deep-water renewal in the northern North Atlantic. Nature 344: 848-850

Diel S (1991) Zur Lebensgeschichte dominanter Copepodenarten (*Calanus finmarchicus, C. glacialis, C. hyperboreus, Metridia longa*) in der Framstraße. Ber Polarforsch 88, 113 pp

Digby PSB (1954) The biology of the marine planktonic copepods of Scoresby Sound, East Greenland. J Anim Ecol 23: 298-335

Düsterloh S (1994) Die Vertikalverteilung des herbivoren Zooplanktons in der Grönlandsee in Beziehung zur Frühjahrsblüte des Phytoplanktons. Diploma thesis, Oldenburg University (in prep)

Esterly CI (1916) The feeding habits and food of pelagic copepods and the question of nutrition by organic substances in solution in the water. Univ Calif Publ Zool 16: 171-184

Faith DP, Minchin PR, Belbin L (1987) Compositional dissimilarity as a robust measure of ecological distance. Vegetatio 69: 57-68

Farran GP (1926) Biscayan plankton collected during a cruise of HMS „Research", 1900, Pt XIV. The Copepoda. J Linn Soc London, Zool, 36: 219-310

Field JG, Clarke KR, Warwick RM (1982) A practical strategy for analysing multispecies distribution patterns. Mar Ecol Progr Ser 8: 37-52

Fischer J, Visbeck M (1993) Seasonal variation of the daily zooplankton migration in the Greenland Sea. Deep-Sea Res 40: 1547-1557

Foxton P (1956) The distribution of the standing crop of zooplankton in the Southern Ocean. Discovery Rep 28: 191-236

Frost B (1989) A taxonomy of the marine calanoid copepod genus *Pseudocalanus*. Can J Zool 67: 525-551

Grainger EH (1965) Zooplankton from the Arctic Ocean and adjacent Canadian waters. J Fish Res Bd Can 22(2): 543-564

Grainger EH (1989) Vertical distribution of zooplankton in the central Arctic Ocean. In: Rey L, Alexander V (eds) Proc VI Conf Comité Arctique Int, 1985. Brill, Leiden, pp 48-60

Grice GD, Hülsemann K (1965) Abundance, vertical distribution and taxonomy of calanoid copepods at selected stations in the northeast Atlantic. J Zool 146: 213-262

GSP Group (1990) Greenland Sea Project. - A venture towards improved understanding of the oceans' role in climate. EOS 71(24): 750-751

Haberstroh D (1985) Die Vertikalverteilung von planktonischen Crustaceen auf einem Schnitt in der nördlichen Framstraße. Diploma thesis, Würzburg University, 140 pp

Hamner WM (1988) Behavior of plankton and patch formation in pelagic ecosystems. Bull Mar Sci 43(3): 752-757

Harding GCH (1974) The food of deep-sea copepods. J Mar Biol Assoc UK 54: 141-155

Head EJH, Harris LR (1985) Physiological and biochemical changes in *Calanus hyperboreus* from Jones Sound, NWT, during the transition from summer feeding to overwintering conditions. Polar Biol 4: 99-106

Heinrich AK (1958) On the nutrition of marine copepods in the tropical region. Dokl Akad Nauk SSSR 119: 1028-1034 [Transl NSF, USA]

Heinrich AK (1962) The life histories of plankton animals and seasonal cycles of plankton communities in the oceans. J Cons Perm Int Explor Mer 27: 15-24

Helland-Hansen B, Nansen F (1909) The Norwegian Sea. - Its physical oceanography based upon the Norwegian researches 1900-1904. Rep Nor Fish Mar Invest 2(2): 1-390

Hempel G (1985) On the biology of polar seas, particularly the Southern Ocean. In: Gray JS, Christiansen ME (eds) Marine biology of polar regions and effects of stress on marine organisms. Wiley, Chichester, pp 3-33

Hempel I, Hempel G (1985) Field observations on the developmental ascent of larval *Euphausia superba* (Crustacea). Polar Biol 6: 121-126

Heptner MV (1971) To the copepod fauna of the Kurile-Kamchatka Trench. The families Euchaetidae, Lucicutiidae, Heterorhabdidae. Tr Shirshov Inst Oceanology 92: 73-161

Herman Y, Andersen OGN (1989) Foraminifera and Pteropoda beneath the Arctic sea ice: New distributions. In: Herman Y (ed) The Arctic seas. - Climatology, oceanography, geology and biology. Van Nostrand Reinhold, New York, pp 223-234

Hirche H-J (1991) Distribution of dominant calanoid copepod species in the Greenland Sea during late fall. Polar Biol 11: 351-362

Hirche H-J, Baumann MEM, Kattner G, Gradinger R (1991) Plankton distribution and the impact of copepod grazing on primary production in Fram Strait, Greenland Sea. J Mar Syst 2: 477-494

Hirche H-J, Hagen W, Mumm N, Richter C (1994) The Northeast Water Polynya, Greenland Sea. III. Meso- and macrozooplankton distribution and production of dominant herbivorous copepods during spring. Polar Biol (in press)

Honjo S (1990) Particle fluxes and modern sedimentation in the polar oceans. In: Smith Jr WO (ed) Polar Oceanography, Part B: Chemistry, biology and geology. Academic Press, London, pp 687-739

Hopkins TL (1969) Zooplankton standing crop in the Arctic Basin. Limnol Oceanogr 14: 80-85

Hopkins TL (1985) Food web of an Antarctic midwater ecosystem. Mar Biol 89: 197-212

Hopkins TL (1987) Midwater food web in McMurdo Sound, Ross Sea, Antarctica. Mar Biol 96: 93-106

Hopkins TL, Lancraft TM, Torres JJ, Donnelly (1993) Community structure and trophic ecology of zooplankton in the Scotia Sea marginal ice zone in winter (1988). Deep-Sea Res 40: 81-105

Huntley M, Strong KW, Dengler AT (1983) Dynamics and community structure of zooplankton in the Davis Strait and northern Labrador Sea. Arctic 36(2): 143-161

Hurlbert SH (1971) The nonconcept of species diversity: a critique and alternative parameters. Ecology 52: 577-586

Ikeda T, Skjoldal HR (1989) Metabolism and elemental composition of zooplankton from the Barents Sea during early Arctic summer. Mar Biol 100: 173-183

Jashnov VA (1970) Distribution of *Calanus* species in the seas of the northern hemisphere. Int Rev ges Hydrobiol 55(2): 197-212

Jespersen P (1934) The „Godthåb" expedition. Copepoda. Medd Grønland 79(10): 1-166

Johannessen OM (1986) Brief overview of the physical oceanography. In: Hurdle BG (ed) The Nordic seas. Springer, Berlin, pp 103-127

Johannessen JA, Johannessen OM, Svendsen E, Shuchman R, Manley T, Campbell WJ, Josberger EG, Sandven S, Gascard JC, Olaussen T, Davidson K, Van Leer J (1987) Mesoscale eddies in the Fram Strait marginal ice zone during the 1983 and 1984 marginal ice zone experiments. J Geophys Res 92(C7): 6754-6772

Johnson MW (1963) Zooplankton collections from the high Polar Basin with special reference to the Copepoda. Limnol Oceanogr 8(1): 89-102

Kattner G, Hirche H-J, Krause M (1989) Spatial variability in lipid composition of calanoid copepods from Fram Strait, the Arctic. Mar Biol 102: 473-480

Kock R (1992) Ostracoden im Epipelagial vor der Antarktischen Halbinsel - ein Beitrag zur Systematik sowie zur Verbreitung und Populationsstruktur unter Berücksichtigung der Saisonalität. Ber Polarforsch 106, 205 pp

Kosobokova KN (1978) Diurnal vertical distribution of *Calanus hyperboreus* Krøyer and *Calanus glacialis* Jashnov in the central Polar Basin. Oceanology 18(4): 476-480

Kosobokova KN (1980) Caloric value of some zooplankton representatives from the central Arctic Basin and the White Sea. Oceanology 20(1): 84-89

Kosobokova KN (1982) Composition and distribution of the biomass of zooplankton in the central Arctic Basin. Oceanology 22(6): 744-750

Koszteyn J, Kwasniewski S (1991) Copepoda (Calanoida and Cyclopoida). In: Klekowski RZ, Weslawski JM (eds) Atlas of the marine fauna of southern Spitsbergen, 2(1), pp 8-117

Kruskal JB, Wish M (1978) Multidimensional scaling. Sage Publications, Beverly Hills, California, 93 pp

Kurbjeweit F (1993) Reproduktion und Lebenszyklen dominanter Copepodenarten aus dem Weddellmeer, Antarktis. Ber Polarforsch 129, 237 pp

Legendre L, Gosselin M, Hirche H-J, Kattner G, Rosenberg G (1993) Environmental control and potential fate of size-fractionated phytoplankton production in the Greenland Sea (75°N). Mar Ecol Progr Ser 98: 297-313

Longhurst AR (1976) Vertical migration. In: Cushing DH, Walsh JJ (eds) The ecology of the seas. Blackwell, Oxford, pp 116-137

Longhurst AR (1985) The structure and evolution of plankton communities. Progr Oceanogr 15: 1-35

Longhurst AR, Sameoto D, Herman AW (1984) Vertical distribution of Arctic zooplankton in summer: eastern Canadian Archipelago. J Plankton Res 6(1): 137-168

Longhurst AR, Platt T, Harrison WG, Head EJH, Herman AW, Horne E, Conover RJ, Li WKW, Subba Rao DV, Sameoto D, Smith JC, Smith REH (1989) Biological oceanography in the Canadian High Arctic. Rapp P-v Réun Cons int Explor Mer 188: 80-89

Lysholm B, Nordgaard O (1945) Copepoda from the „Michael Sars" North Atlantic deep-sea expedition 1910. Rep Sci Res „Michael Sars"N Atl Deep-Sea Exp 5(7): 1-60

Margalef R (1989) Le plancton: survivre et s'organiser dans un fluide mobile. In: Denis MM (ed) Océanologie - actualité et prospective. Centre d' Océanologie de Marseille, pp 169-185

Marr JWS (1962) The natural history and geography of the Antarctic krill (*Euphausia superba* Dana). Discovery Rep 32: 33-464

Marshall SM, Orr AP (1972) The biology of a marine copepod. - *Calanus finmarchicus*. Springer, Berlin, 195 pp

Matthews JBL (1964) On the biology of some bottom-living copepods (Aetideidae and Phaennidae) from western Norway. Sarsia 16: 1-46

Mauchline J (1992) Taxonomy, distribution and biology of *Euchaeta barbata* (= *E. farrani*) (Copepoda: Calanoida). Sarsia 77: 131-142

McAllister CD (1961) Zooplankton studies at ocean weather station „P" in the northeast Pacific Ocean. J Fish Res Bd Can 18(1): 1-29

McLaren IA (1969) Population and production ecology of zooplankton in Ogac Lake, a landlocked fjord on Baffin Island. J Fish Res Bd Can 26: 1485-1559

McLaren IA, Laberge E, Corkett CJ, Sevigny JM (1989) Life cycles of four species of *Pseudo-calanus* in Nova Scotia. Can J Zool 67(3): 552-558

Mel'nikov IA (1989) Ecology of Arctic Ocean cryopelagic fauna. In: Herman Y (ed) The Arctic seas. - Climatology, oceanography, geology and biology. Van Nostrand Reinhold, New York, pp 235-255

Metcalf WG (1955) On the formation of bottom water in the Norwegian Basin. Trans Am Geophys Union 36(4): 595-600

Metz C (1993) Verbreitung von Cyclopoida (Copepoda, Crustacea) im Weddellmeer. Diploma thesis, Kiel University, 80 pp

Minoda T (1967) Seasonal distribution of Copepoda in the Arctic Ocean from June to December, 1964. Rec Oceanogr Wks Jap 9(1): 161-172

Mizdalski E (1988) Weight and length data of zooplankton in the Weddell Sea in austral spring 1986 (ANT V/3). Ber Polarforsch 55, 72 pp

Morales A (1993) Vertikale und regionale Verteilung des Mesozooplanktons im Nordostatlantik unter der besonderen Berücksichtigung von Copepoden. Ber Inst Meeresk Kiel 239, 191 pp

Mumm N (1991) Zur sommerlichen Verteilung des Mesozooplanktons im Nansen-Becken, Nordpolarmeer. Ber Polarforsch 92, 146 pp

Nansen F (1906) Northern waters: Captain Roald Amundsen's oceanographic observations in the Arctic seas in 1901. - Vid Selskabets Skrifter. I. Math- naturv Kl 1(3). Dybwad, Christiania, 145 pp

Nemoto T, Harrison G (1981) High latitude ecosystems. In: Longhurst AR (ed) Analysis of marine ecosystems. Academic Press, London, pp 95-126

Nishida S (1985) Taxonomy and distribution of the family Oithonidae (Copepoda, Cyclopoida) in the Pacific and Indian Oceans. Bull Ocean Res Inst, Tokyo University, 20: 1-167

Norrbin MF (1991) Gonad maturation as an indication of seasonal cycles for several species of small copepods in the Barents Sea. In: Sakshaug E, Hopkins CCE, Øritsland NA (eds) Proc Pro Mare Symp 1990. Polar Res 10(1): 421-432

Norrbin MF, Båmstedt U (1984) Energy contents in benthic and planktonic invertebrates of Kosterfjorden, Sweden.- A comparison of energetic strategies in marine organism groups. Ophelia 23(1): 47-64

Omori M, Ikeda T (1984) Methods in marine zooplankton ecology. Wiley, New York, 332 pp

Øresland V (1990) Feeding and predation impact of the chaetognath *Eukrohnia hamata* in Gerlache Strait, Antarctic Peninsula. Mar Ecol Progr Ser 63: 201-209

Østvedt OJ (1955) Zooplankton investigations from weather ship „M" in the Norwegian Sea, 1948-49. Hvalradets Skr 40: 1-93

Paquette RG, Bourke RH, Newton JF, Perdue WF (1985) The East Greenland Polar Front in autumn. J Geophys Res 90(C3): 4866-4882

Park T (1978) Calanoid copepods (Aetideidae and Euchaetidae) from Antarctic and Subantarctic waters. In: Pawson DL (ed) Biology of the Antarctic Seas VII. Antarctic Res Ser 27(4): 91-290

Pavshtiks EA (1968) The influence of currents upon seasonal fluctuations in the plankton of Davis Strait. Sarsia 34: 383-392

Pavshtiks EA (1983) Some patterns in the life of the plankton of the central Arctic Basin. Can Transl Fish Aquat Sci 4917, 24 pp

Perry RK (1986) Bathymetry. In: Hurdle BG (ed) The Nordic seas. Springer, Berlin, pp 211-234

Pielou EC (1969) An introduction to mathematical ecology. Wiley-Interscience, New York, 286 pp

Poulsen EM (1973) Ostracoda - Myodocopa. IIIb. Halocypriformes - Halocypridae Conchoeciinae. Dana Rep 84: 1-224

Quadfasel D, Meincke J (1987) Note on the thermal structure of the Greenland Sea gyres. Deep-Sea Res 34: 1883-1888

Quadfasel D, Gascard J-C, Koltermann K-P (1987) Large-scale oceanography in Fram Strait during the 1984 Marginal Ice Zone Experiment. J Geophys Res 92(C7): 6719-6728

Raymont JEG (1983) Plankton and productivity in the oceans, 2. Zooplankton. Pergamon Press, Oxford, 824 pp

Razouls C (1993) Bilan taxonomique actuel des copépodes planctoniques marins et des eaux saumâtres. Proc I Europ Crust Conf 1992, 64(3): 300-313

Richter C (1990) Untersuchungen an küstennahem Plankton in Nordchile: Das Buchtplankton der Coquimbo-Region (30°S) unter besonderer Berücksichtigung des Phytoplanktons. Diploma thesis, Kiel University, 103 pp

Rodríguez J, Mullin MM (1986) Relation between biomass and body weight of plankton in a steady state oceanic system. Limnol Oceanogr 31: 361-370

Rudels B (1993) High latitude ocean convection. In: Stone DB, Runcorn SK (eds) Flow and creep in the solar system: observations, modeling and theory. Kluwer Academic Publ, pp 323-356

Rudels B, Quadfasel D (1991) Convection and deep water formation in the Arctic Ocean - Greenland Sea system. J Mar Syst 2: 435-450

Rudels B, Quadfasel D, Friedrich H, Houssais M-N (1989) Greenland Sea convection in the winter of 1987-1988. J Geophys Res 94(C3): 3223-3227

Rudyakov YA (1983) Vertical distribution of *Calanus hyperboreus* (Copepoda) in the central Arctic Basin. Oceanology 23(2): 249-253

Sameoto DD (1984) Vertical distribution of zooplankton biomass and species in northeastern Baffin Bay related to temperature and salinity. Polar Biol 2: 213-224

Sands NJ (1980) Ecological studies on the deep-water pelagic community of Korsfjorden, western Norway. - Population dynamics of the chaetognaths from 1971-1974. Sarsia 65(1): 1-12

Sars GO (1900) Crustacea. In: Nansen F (ed) The Norwegian North Polar Expedition 1893-1896.- Scient Res 1(5): 1-137

Sars GO (1903) An account of the Crustacea of Norway, 4. Copepoda Calanoida.- With short descriptions and figures of all the species. Bergen Museum, 171 pp

Scherzinger T (1994) Der Lebenszyklus des calanoiden Copepoden *Metridia longa* (Lubbock) in der zentralen Grönlandsee. Diploma thesis, TU Berlin (in prep)

Schott F, Visbeck M, Fischer J (1993) Observations of vertical currents and convection in the central Greenland Sea during the winter of 1988-1989. J Geophys Res 98(C8): 14401- 14421

Shannon CE, Weaver W (1963) The mathematical theory of communication. Univ Illinois Press, 117 pp

Skogsberg T (1920) Studies on marine ostracods, 1.- Cyprinids, halocyprids, and polycopids. Zool Bidr Upps (Suppl 1): 1-784

Smetacek V (1988) Plankton characteristics. In: Postma H, Zijlstra JJ (eds) Continental shelves. Ecosystems of the world, 27. Elsevier, Amsterdam, pp 93-130

Smethie WM, Chipman DW, Swift JH, Koltermann KP (1988) Chloroflouromethanes in the Arctic Mediterranean seas: Evidence for formation of bottom water in the Eurasian Basin and deep-water exchange through Fram Strait. Deep-Sea Res 35: 347-369

Smith SL (1988) Copepods in Fram Strait in summer: distribution, feeding and metabolism. J Mar Res 46: 145-181

Smith SL, Schnack-Schiel SB (1990) Polar zooplankton. In: Smith Jr WO (ed) Polar oceanography, Part B: Chemistry, biology and geology. Academic Press, London, pp 527-598

Smith SL, Brink KH, Santander H, Cowles TJ, Huyer A (1981) The effect of advection on variations in zooplankton at a single location near Cabo Nazca, Peru. In: Richards, FA (ed) Coastal upwelling. Coastal and estuarine sciences, 1. American Geophysical Union, Washington, pp 400-410

Smith Jr WO, Sakshaug E (1990) Polar phytoplankton. In: Smith Jr WO (ed) Polar oceanography, Part B: Chemistry, biology and geology. Academic Press, London, pp 477-525

Sømme JD (1934) Animal plankton of the Norwegian coast waters and the open sea. I. Production of *Calanus finmarchicus* (Gunner) and *Calanus hyperboreus* (Krøyer) in the Lofoten area. Rep Nor Fish Invest 4(9): 1-163

Steele JH (ed) (1978) Spatial pattern in plankton communities. Plenum Press, New York, 470 pp

Sullivan BK (1980) In situ feeding behavior of *Sagitta elegans* and *Eukrohnia hamata* (Chaetognatha) in relation to the vertical distribution and abundance of prey at ocean station „P". Limnol Oceanogr 25(2): 317-326

Swift JH (1986) The arctic waters. In: Hurdle BG (ed) The Nordic seas. Springer, Berlin, pp 129-153

Swift JH, Aagard K (1981) Seasonal transitions and water mass formation in the Iceland and Greenland seas. Deep-Sea Res 28: 1107-1130

Swift JH, Aagard K, Malmberg S-A (1980) The contribution of the Denmark Strait overflow to the deep North Atlantic. Deep-Sea Res 27: 29-42

UNESCO (1979) Zooplankton sampling. Tranter DJ, Fraser HJ (eds). UNESCO press, Paris, 174 pp

Ussing HH (1938) The biology of some important plankton animals in the fjords of East Greenland. Medd Grønland 100: 1-108

van Aken HM (1989) A phenomenological study of the Arctic Front in the West Spitsbergen Current. ICES Council meeting 1989, Int Council Explor Sea, Copenhagen, 9 pp

van Aken HM, Quadfasel D, Warpakowski A (1991) The Arctic Front in the Greenland Sea during February 1989: Hydrographic and biological observations. J Geophys Res 96(C3): 4739-4750

van der Spoel S (1967) Euthecosomata, a group with remarkable developmental stages (Gastropoda, Pteropoda). Noorduyn en Zoon, Gorinchem, 375 pp

Vervoort W (1957) Copepods from Antarctic and Subantarctic plankton samples. BANZ Antarctic Res Exped Rep Ser B (Zoology and Botany) 3: 1-160.

Vinje TE (1977) Sea ice conditions in the European sector of the marginal seas of the Arctic, 1966-75. Norsk Polarinst Årbok 1975, pp 163-174

Vinogradov (1970) Vertical distribution of the oceanic zooplankton. Israel Progr Sci Transl, Jerusalem, 339 pp

Virketis MA (1957) Some data on the zooplankton of the central part of the Arctic Basin. Materials on the observations of the scientific research drifting stations NP-3 and NP-4 in 1954-1955, 1: 238-342 [in Russian]

Visbeck M (1993) Konvektion im offenen Ozean. Interpretation von Beobachtungen aus der Grönlandsee und dem westlichen Mittelmeer. Ber Inst Meeresk 237, 187 pp

Wadhams P (1986) The ice cover. In: Hurdle BG (ed) The Nordic seas. Springer, Berlin, pp 21-84

Wassmann P, Peinert R, Smetacek V (1991) Patterns of production and sedimentation in the boreal and polar northeast Atlantic. In: Sakshaug E, Hopkins CCE, Øritsland NA (eds) Proc Pro Mare Symp 1990. Polar Res 10(1): 209-228

Weslawski JM (1991) Malacostraca. In: Klekowski RZ, Weslawski JM (eds) Atlas of the marine fauna of southern Spitsbergen, 2(1), pp 118-357

Wiborg KF (1954) Investigations on zooplankton in coastal and offshore waters off western and northwestern Norway. Rep Nor Fish Invest 11(1): 1-246

Wolfenden RN (1904) Notes on the Copepoda of the North Atlantic Sea and the Faroe Channel. J Mar Biol Ass UK 7: 110-146

Acknowledgements

I would like to thank Prof. G. Hempel for supervising this dissertation, for valuable suggestions and for the swift and critical revision of the thesis.
This work would not be possible without the initiative and encouragement of Dr. H.-J. Hirche and the excellent cooperation with him and other co-workers of the Greenland Sea Project, namely Dr. R. Weigmann-Haass, T. Scherzinger, Dr. W. Hagen, J. Wegner and Dr. D. Quadfasel, who made available their samples and data to this study.
Special thanks to Dr. W. Hagen for competent advice throughout this investigation and painstaking revision of the manuscript. Dr. R. Gradinger reviewed an earlier, and Prof. M. Spindler the final draft of the thesis.
Dr. N. Mumm introduced me to Arctic zooplankton, Drs. F. Pagès, K. Hülsemann and S. Kwasniewski helped in solving taxonomic problems.
Dr. D. Piepenburg gave statistical advice and Dr. K.R. Clarke provided the ANOSIM program.
Thanks to all members of the Institut für Polarökologie for a truly exceptional working environment.
Finally, I would like to thank my family for their loving support and patience.

This work was financed by a fellowship from the State of Schleswig-Holstein and by the Deutsche Forschungsgemeinschaft (DFG) through the Sonderforschungsbereich (SFB) 313 of Kiel University.

APPENDIX 1.1

Mean individual dry weights (DW_i) used in the biomass calculations with references to source of data

Taxon	Stage	DW_i [mg]	s.d.	Pres.	Season	Region	Reference
Calanus finmarchicus	CVI m	†0.28	-	-	-	-	-
	CVI f	0.327	0.076	1,2	4,5	2,3,4,5,6	2,5,7,8
	CV	0.274	0.098	1,2	4,5	2,3,4,6	2,5,8,
	CIV	*0.128	-	-	2	5	3
	CIII	*0.046	-	-	2	5	3
Calanus glacialis	CVI m	0.752	0.179	3	2,3,4	1	4,9
	CVI f	0.890	0.235	2,3	2,3,4,5	1,2,5	4,5,6,7,9
	CV	0.778	0.307	2,3	2,3,4,5	1,2,3	4,5,9
	CIV	0.169	0.064	2,3	2,3,4,5	1,3	4,5,9
	CIII	0.043	0.014	3	2,3,4,5	1	4,9
Calanus hyperboreus	CVI m	1.254	0.250	3	2	1	4,9
	CVI f	2.350	0.689	2	2,3,4	3	5,6
	CV	1.021	0.452	2	2,3,4	3	5,6
	CIV	0.206	0.017	2	2,4	3	5,6
	CIII	0.056	0.005	2	4	3	5
Metridia longa	CVI m	0.137	0.037	1,2,3	2,3,4,5	1,3,6	2,4,5,9
	CVI f	0.287	0.045	2	3,4	3	5
	CV	0.120	0.036	2,3	2,3,4,5	1,3	4,5,9
	CIV	0.034	0.006	2,3	2,3,4,5	1,4	4,5,9
Euchaeta barbata	CVI m	†2.973	-	2	4	4	5
	CVI f	9.056	0.255	2	4	3,4	5
Euchaeta glacialis	CVI m	3.348	-	2	4	1	5
	CVI f	5.907	1.129	2	3,4	1,2,3	5
Euchaeta norvegica	CVI m	1.789	0.185	1,2	1-5	1,6	1,5,12
	CVI f	4.672	0.756	1,2	1-5	2,6	1,5,12
Euchaeta spp.	CV	1.681	0.882	2	4	1,4	5
	CIV	0.377	0.009	2	4	4	5
	CIII	*0.121	0.017	2	5	3	13
	CII	*0.048	0.011	2	5	3	13
	CI	*0.038	0.010	2	5	3	13
Scaphocalanus magnus	CVI m	†0.635	0.062	2	4	1	5
	CVI f	0.722	0.023	2	4	1	5
Scaphocalanus spp.	-	0.035	0.004	2	2	7	10
Scolecithricella minor	-	0.024	0.004	2	2	7	10
Pseudocalanus minutus	-	*0.023	0.009	2	5	3	13
Microcalanus spp.	-	*0.007	0.004	2	5	3	13
Spinocalanus spp.	-	0.013	0.004	2	2	7	10
Oithona spp.	-	0.003	0	1,3	4,5	1,6	2,11
Oncaea spp.	-	*0.002	<0.001	2	5	3	13
nauplii	-	†0.001	-	-	-	-	-
Bopyridae	-	*0.030	-	2	5	3	13
Meganyctiphanes norvegica	-	65	35	2	3,4	1,2,4	5
Thysanoessa inermis	-	33	17	2	3,4	1,4	5
Thysanoessa longicaudata	-	4	1	2	3,4	1,3,4	5
Hymenodora glacialis	-	41	32	2	4	1,3,4	5
Polychaeta	-	*0.062	-	2	5	3	13
Limacina spp.	-	0.343	-	2	4	4	5
Oikopleura vanhoeffeni	-	‡0.2	-	3	4	1	11

APPENDIX 1.1 (continued)

Taxon	Stage	DW_i [mg]	s.d.	Pres.	Season	Region	Reference
Crystallophyes amygdalina	-	†0.8	-	-	-	-	-
Dimophyes arctica	-	‡0.8	-	3	4	1	11
Muggiaea bargmannae	-	†0.8	-	-	-	-	-
Aegina citrea	-	1.9	1.0	3	1,3	3	13
Aglantha digitale	-	2.9	1.2	3	1,3	3	13
Botrynema spp.	-	6	4	3	1,3	3	13

Abbreviations: s.d.= standard deviation (or range), Pres.= Preservation method

Number codes:
•Pres. [1= fresh, 2= frozen, 3= formaline]
•Season [1= winter, 2= spring, 3=early summer, 4= summer, 5= fall]
•Region [1= Arctic/East Greenland shelf, 2= Fram Strait, 3= Greenland Sea Gyre, 4= West Spitsbergen Current/Norwegian Sea, 5= Barents Sea, 6= Kosterfjorden, 7= Southern Ocean]
•Reference [1= Båmstedt 1981, 2= Båmstedt et al. 1990, 3= Båmstedt et al. 1991, 4= Conover and Huntley 1991, 5= Hagen (unpubl.), 6= Hirche et al. 1994, 7= Ikeda and Skjoldal 1989, 8= Kattner et al. 1989, 9= Kosobokova 1980, 10= Mizdalski 1988, 11= Mumm 1991, 12= Norrbin and Båmstedt 1984, 13= Richter (unpubl.)]

Symbols: *= converted from carbon (C), ‡= converted from ash free dry weight (AFDW), assuming C:DW=0.5 and AFDW:DW= 0.9 (Båmstedt 1986). AFDW:DW= 0.4 was used for Siphonophora (Clarke et al. 1992). †= inferred from length

APPENDIX 1.2

Dry weight-length relationships used in biomass calculations and references to source of data

Taxon	a	b	r^2	c	Pres.	Season	Region	Reference
Aetideopsis spp.	*0.005	4.659	0.79	p	frozen	fall	GSG	3
Chiridius/Gaidius spp.	†0.010	3.412	0.90	"	formaline	summer	AO	2
Heterorhabdus norvegicus	†0.003	4.716	0.99	"	"	"	"	2
Boroecia/Discoconchoecia sp.	‡0.033	2.370	0.95	"	formaline	summer	AO	2
Themisto spp.	¥0.009	2.407	0.94	"	"	"	"	2
Eukrohnia spp.	0.041	0.165	0.95	e	"	fall	GSG	1
Crossota norvegica	0.322	0.191	0.97	"	"	winter, summer	"	3

Dry weight (DW) in mg, length (L) in mm of cephalothorax (Copepoda) or longest dimension of animal. Coefficients [a, b] and coefficient of determination [r^2] are given for power ($DW= aL^b$) or exponential regression ($DW= ae^{bL}$). Curve fit [c] is indicated (e= exponential, p= power fit), as is the preservation method [Pres.]

Abbreviations: AO= Arctic Ocean, GSG= Greenland Sea Gyre

References: 1= Hirche (unpubl.), 2= Mumm 1991, 3= Richter (unpubl.)

Symbols: *= converted from carbon (C), †= converted from ash-free dry weight (AFDW), assuming C:DW=0.5 and AFDW:DW=0.9 (Båmstedt 1986), ‡= converted from AFDW, assuming AFDW:DW=0.7 [cf. Mizdalski (1988) for *Conchoecia*], ¥= converted from AFDW, assuming AFDW:DW=0.8 [cf. Båmstedt (1981) for *Parathemisto*]